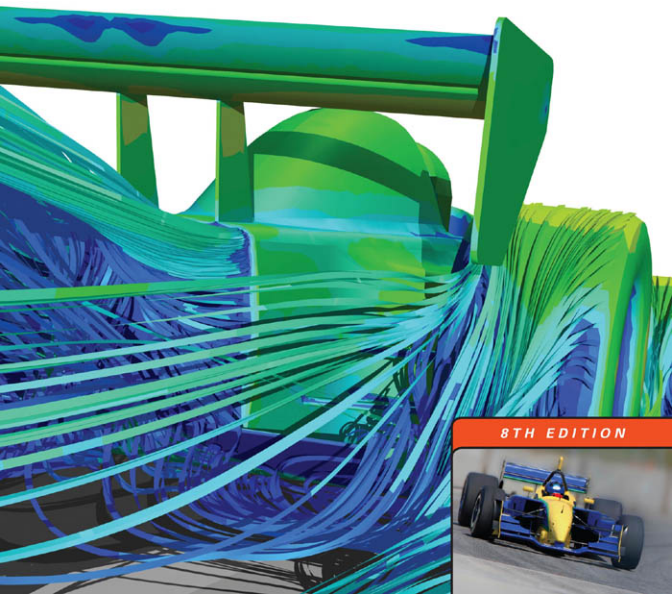


PHILIP J. PRITCHARD

*Fox AND McDonald's*  
INTRODUCTION TO  
*Fluid Mechanics*



8TH EDITION



# 8

## *Internal Incompressible Viscous Flow*

### 8.1 Introduction

#### Part A Fully Developed Laminar Flow

### 8.2 Fully Developed Laminar Flow Between Infinite Parallel Plates

### 8.3 Fully Developed Laminar Flow in a Pipe

#### Part B Flow in Pipes and Ducts

### 8.4 Shear Stress Distribution in Fully Developed Pipe Flow

### 8.5 Turbulent Velocity Profiles in Fully Developed Pipe Flow

### 8.6 Energy Considerations in Pipe Flow

### 8.7 Calculation of Head Loss

### 8.8 Solution of Pipe Flow Problems

#### Part C Flow Measurement

### 8.9 Direct Methods

### 8.10 Restriction Flow Meters for Internal Flows

### 8.11 Linear Flow Meters

## 8.12 Traversing Methods

## 8.13 Summary and Useful Equations



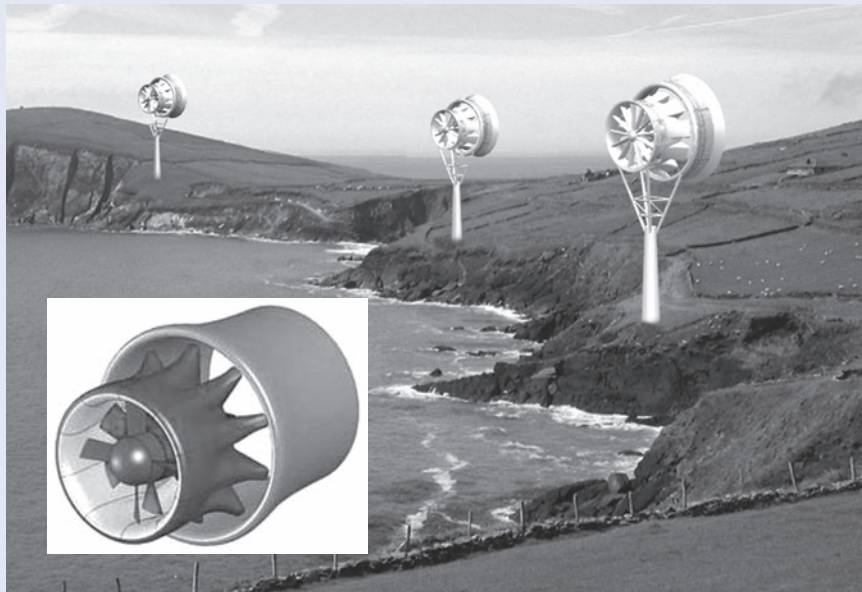
## Case Study in Energy and the Environment

**Wind Power: The FloDesign Wind Turbine**

We are all now familiar with the ubiquitous three-bladed wind turbines that are being used to generate increasing amounts of power. The technology is already quite mature, so new developments will be incremental: improved blade designs, better controls, and composite materials to allow larger turbines. The largest in the world, being built by a Norwegian team, will be 533 ft tall with a rotor diameter of 475 ft, and it will generate about 10 MW, sufficient for more than 2000 homes. Bearing in mind that the Empire State Building is 1250 ft tall, this wind turbine will be huge—so big it must be installed offshore.

Engineers are still investigating alternatives to these designs. *FloDesign Wind Turbine*, a spin-off from the aerospace company *FloDesign* based in Wilbraham, Massachusetts, is developing a prototype that, according to CEO Stanley Kowalski III, will be up to three times more efficient than conventional wind

turbines. From the front, the wind turbine looks something like the air intake of a jet engine (not surprisingly, considering *FloDesign*'s history). The shaped cowlings shown in the figure guide the air into spinning vortices as it exits the device, accelerating the flow and causing a significant pressure drop. The incoming wind first meets a set of fixed stator blades, which direct it onto the rotor blades to extract power from the flow. The exiting air hence has lower energy and velocity than the air flowing around the turbine, but the device's shroud is so shaped that the relatively fast-moving outside air is blended with the exiting air in the area just behind the rotors, creating a low-pressure region behind the turbine blades. This is where the device has an advantage over conventional turbines; the induced low-pressure region actually draws air into the device at an increased rate, generating more power. This idea is not new, but past attempts to build similar turbines were limited by the fact that such a turbine had to be very precisely aligned with the wind's direction (within



Two views of the FloDesign Wind Turbine (Pictures courtesy of FloDesign Wind Turbine)

about  $4^\circ$ ); this device will work at angles of up to  $20^\circ$  off the wind.

Theoretically (as we'll learn in Chapter 10), conventional wind turbines capture a maximum of 59.3 percent of the wind energy. The new design generates as much power as a conventional wind turbine with blades twice as big. The smaller blade size of the new design means the *FloDesign Wind Turbine* could be packed closer together than conventional turbines, increasing the amount of power that can be generated per acre of land. Because its blades are lighter and smaller, the design starts spinning and generating power at lower wind speeds, and it is more tolerant of unstable wind patterns, making it

excellent for windy regions where large turbines cannot be used, such as in cities. Smaller blades can also be allowed to spin faster, reducing the need for expensive gearboxes that conventional wind turbines must use to connect slow-moving rotors to a high-speed generator. With fewer gears and other moving parts, the company claims it can reduce the number of components by up to 75 percent, reducing costs and making maintenance easier.

*FloDesign* has already built a small prototype for wind-tunnel tests. Their next step is to build a 12-ft-diameter, 10-kW system for field tests. The prototype will be finished in 2010, with commercial wind turbines to follow.

#### VIDEO

*The Reynolds Transition Experiment.*

Flows completely bounded by solid surfaces are called internal flows. Thus internal flows include many important and practical flows such as those through pipes, ducts, nozzles, diffusers, sudden contractions and expansions, valves, and fittings.

Internal flows may be laminar or turbulent. Some laminar flow cases may be solved analytically. In the case of turbulent flow, analytical solutions are not possible, and we must rely heavily on semi-empirical theories and on experimental data. The nature of laminar and turbulent flows was discussed in Section 2.6. For internal flows, the flow regime (laminar or turbulent) is primarily a function of the Reynolds number.

In this chapter we will only consider incompressible flows; hence we will study the flow of liquids as well as gases that have negligible heat transfer and for which the Mach number  $M < 0.3$ ; a value of  $M = 0.3$  in air corresponds to a speed of approximately 100 m/s. Following a brief introduction, this chapter is divided into the following parts:

**Part A:** Part A discusses fully developed laminar flow of a Newtonian fluid between parallel plates and in a pipe. These two cases can be studied analytically.

**Part B:** Part B is about laminar and turbulent flows in pipes and ducts. The laminar flow analysis follows from Part A; the turbulent flow (which is the most common) is too complex to be analyzed, so experimental data will be used to develop solution techniques.

**Part C:** Part C is a discussion of methods of flow measurement.

#### VIDEO

*Variable Viscosity Experiment (Animation).*

## 8.1 Introduction

### Laminar versus Turbulent Flow

#### VIDEO

*Variable Viscosity Experiment: Pressure Drop.*

As discussed previously in Section 2.6, the pipe flow regime (laminar or turbulent) is determined by the Reynolds number,  $Re = \rho \bar{V} D / \mu$ . One can demonstrate, by the classic Reynolds experiment, the qualitative difference between laminar and turbulent flows. In this experiment water flows from a large reservoir through a clear tube. A thin filament of dye injected at the entrance to the tube allows visual observation of the flow. At low flow rates (low Reynolds numbers) the dye injected into the flow remains in a single filament along the tube; there is little dispersion of dye because the flow is laminar. A laminar flow is one in which the fluid flows in laminae, or layers; there is no macroscopic mixing of adjacent fluid layers.

As the flow rate through the tube is increased, the dye filament eventually becomes unstable and breaks up into a random motion throughout the tube; the line of dye is stretched and twisted into myriad entangled threads, and it quickly disperses throughout the entire flow field. This behavior of turbulent flow is caused by small, high-frequency velocity fluctuations superimposed on the mean motion of a turbulent flow, as illustrated earlier in Fig. 2.15; the mixing of fluid particles from adjacent layers of fluid results in rapid dispersion of the dye. We mentioned in Chapter 2 an everyday example of the difference between laminar and turbulent flow—when you gently turn on the kitchen faucet (not aerated). For very low flow rates, the water exits smoothly (indicating laminar flow in the pipe); for higher flow rates, the flow is churned up (turbulent flow).

Under normal conditions, transition to turbulence occurs at  $Re \approx 2300$  for flow in pipes: For water flow in a 1-in. diameter pipe, this corresponds to an average speed of 0.3 ft/s. With great care to maintain the flow free from disturbances, and with smooth surfaces, experiments have been able to maintain laminar flow in a pipe to a Reynolds number of about 100,000! However, most engineering flow situations are not so carefully controlled, so we will take  $Re \approx 2300$  as our benchmark for transition to turbulence. Transition Reynolds numbers for some other flow situations are given in the Examples. Turbulence occurs when the viscous forces in the fluid are unable to damp out random fluctuations in the fluid motion (generated, for example, by roughness of a pipe wall), and the flow becomes chaotic. For example, a high-viscosity fluid such as motor oil is able to damp out fluctuations more effectively than a low viscosity fluid such as water and therefore remains laminar even at relatively high flow rates. On the other hand, a high-density fluid will generate significant inertia forces due to the random fluctuations in the motion, and this fluid will transition to turbulence at a relatively low flow rate.

## The Entrance Region

Figure 8.1 illustrates laminar flow in the entrance region of a circular pipe. The flow has uniform velocity  $U_0$  at the pipe entrance. Because of the no-slip condition at the wall, we know that the velocity at the wall must be zero along the entire length of the pipe. A boundary layer (Section 2.6) develops along the walls of the channel. The solid surface exerts a retarding shear force on the flow; thus the speed of the fluid in the neighborhood of the surface is reduced. At successive sections along the pipe in this entry region, the effect of the solid surface is felt farther out into the flow.

For incompressible flow, mass conservation requires that, as the speed close to the wall is reduced, the speed in the central frictionless region of the pipe must increase slightly to compensate; for this inviscid central region, then, the pressure (as indicated by the Bernoulli equation) must also drop somewhat.

Sufficiently far from the pipe entrance, the boundary layer developing on the pipe wall reaches the pipe centerline and the flow becomes entirely viscous. The velocity profile shape then changes slightly after the inviscid core disappears. When the profile shape no longer changes with increasing distance  $x$ , the flow is called *fully developed*. The distance

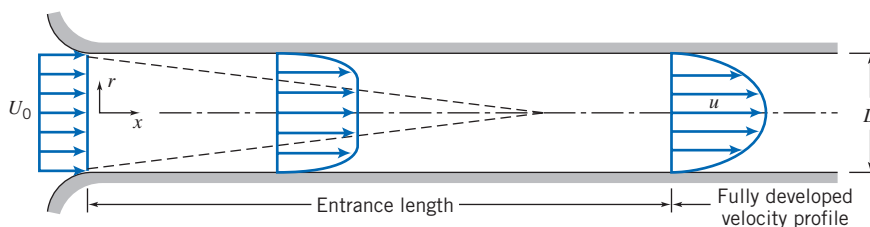


Fig. 8.1 Flow in the entrance region of a pipe.



CLASSIC VIDEO

Turbulence.

VIDEO

Laminar Pipe Flow: Velocity Profile.

VIDEO

Pipe Flow: Laminar.

VIDEO

Pipe Flow: Transitional.

VIDEO

Pipe Flow: Turbulent.



downstream from the entrance to the location at which fully developed flow begins is called the *entrance length*. The actual shape of the fully developed velocity profile depends on whether the flow is laminar or turbulent. In Fig. 8.1 the profile is shown qualitatively for a laminar flow. Although the velocity profiles for some fully developed laminar flows can be obtained by simplifying the complete equations of motion from Chapter 5, turbulent flows cannot be so treated.

For laminar flow, it turns out that entrance length,  $L$ , is a function of Reynolds number,

$$\frac{L}{D} \simeq 0.06 \frac{\rho \bar{V} D}{\mu} \quad (8.1)$$

where  $\bar{V} \equiv Q/A$  is the average velocity (because flow rate  $Q = A\bar{V} = AU_0$ , we have  $\bar{V} = U_0$ ). Laminar flow in a pipe may be expected only for Reynolds numbers less than 2300. Thus the entrance length for laminar pipe flow may be as long as

$$L \simeq 0.06 ReD \leq (0.06)(2300) D = 138D$$

or nearly 140 pipe diameters. If the flow is turbulent, enhanced mixing among fluid layers causes more rapid growth of the boundary layer. Experiments show that the mean velocity profile becomes fully developed within 25 to 40 pipe diameters from the entrance. However, the details of the turbulent motion may not be fully developed for 80 or more pipe diameters. We are now ready to study laminar internal flows (Part A), as well as laminar and turbulent flows in pipes and ducts (Part B). For these we will be focusing on what happens after the entrance region, i.e., fully developed flows.

## Part A Fully Developed Laminar Flow

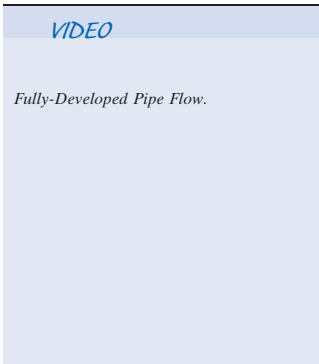
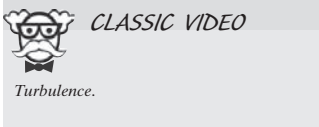
In this section we consider a few classic examples of fully developed laminar flows. Our intent is to obtain detailed information about the velocity field because knowledge of the velocity field permits calculation of shear stress, pressure drop, and flow rate.

### 8.2 Fully Developed Laminar Flow Between Infinite Parallel Plates

The flow between parallel plates is appealing because the geometry is the simplest possible, but why *would* there be a flow at all? The answer is that flow could be generated by applying a pressure gradient parallel to the plates, or by moving one plate parallel with respect to the other, or by having a body force (e.g., gravity) parallel to the plates, or by a combination of these driving mechanisms. We will consider all of these possibilities.

#### Both Plates Stationary

Fluid in high-pressure hydraulic systems (such as the brake system of an automobile) often leaks through the annular gap between a piston and cylinder. For very small gaps (typically 0.005 mm or less), this flow field may be modeled as flow between infinite parallel plates, as indicated in the sketch of Fig. 8.2. To calculate the leakage flow rate, we must first determine the velocity field.



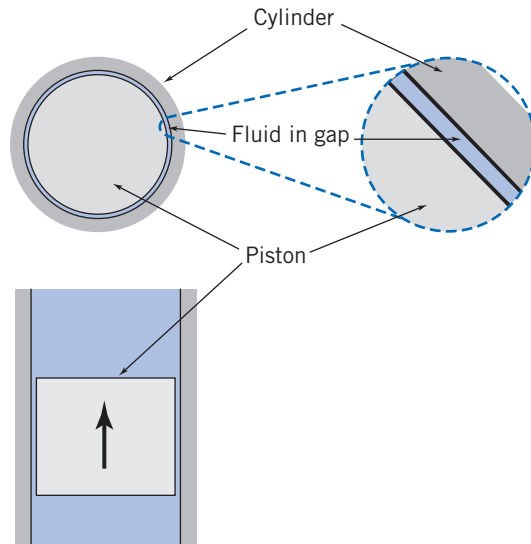


**Fig. 8.2** Piston-cylinder approximated as parallel plates.

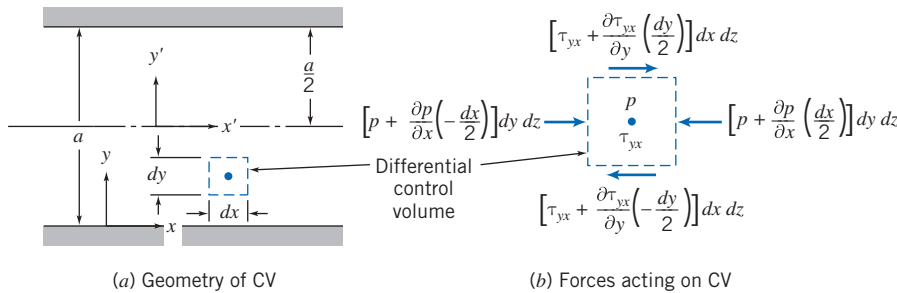


**Fig. 8.3** Control volume for analysis of laminar flow between stationary infinite parallel plates.

Let us consider the fully developed laminar flow between horizontal infinite parallel plates. The plates are separated by distance  $a$ , as shown in Fig. 8.3. The plates are considered infinite in the  $z$  direction, with no variation of any fluid property in this direction. The flow is also assumed to be steady and incompressible. Before starting our analysis, what do we know about the flow field? For one thing we know that the  $x$  component of velocity must be zero at both the upper and lower plates as a result of the no-slip condition at the wall. The boundary conditions are then

$$\begin{aligned} \text{at } y = 0 & \quad u = 0 \\ \text{at } y = a & \quad u = 0 \end{aligned}$$

Since the flow is fully developed, the velocity cannot vary with  $x$  and, hence, depends on  $y$  only, so that  $u = u(y)$ . Furthermore, there is no component of velocity in either the  $y$  or  $z$  direction ( $v = w = 0$ ). In fact, for fully developed flow only the pressure can and will change (in a manner to be determined from the analysis) in the  $x$  direction.

This is an obvious case for using the Navier–Stokes equations in rectangular coordinates (Eqs. 5.27). Using the above assumptions, these equations can be greatly simplified and then solved using the boundary conditions (see Problem 8.17). In this section we will instead take a longer route—using a differential control volume—to bring out some important features of the fluid mechanics.

For our analysis we select a differential control volume of size  $dV = dx dy dz$ , and apply the  $x$  component of the momentum equation.

Basic equation:

$$= 0(3) = 0(1)$$

$$F_{S_x} + F_{B_x} = \frac{\partial}{\partial t} \int_{CV} u \rho dV + \int_{CS} u \rho \vec{V} \cdot d\vec{A} \quad (4.18a)$$

Assumptions: (1) Steady flow (given)  
 (2) Fully developed flow (given)  
 (3)  $F_{B_x} = 0$  (given)

The very nature of fully developed flow is that the velocity profile is the same at all locations along the flow; hence there is no change in momentum. Equation 4.18a then reduces to the simple result that the sum of the surface forces on the control volume is zero,

$$F_{S_x} = 0 \quad (8.2)$$

The next step is to sum the forces acting on the control volume in the  $x$  direction. We recognize that normal forces (pressure forces) act on the left and right faces and tangential forces (shear forces) act on the top and bottom faces.

If the pressure at the center of the element is  $p$ , then the pressure force on the left face is

$$dF_L = \left( p - \frac{\partial p}{\partial x} \frac{dx}{2} \right) dy dz$$

and the pressure force on the right face is

$$dF_R = - \left( p + \frac{\partial p}{\partial x} \frac{dx}{2} \right) dy dz$$

If the shear stress at the center of the element is  $\tau_{yx}$ , then the shear force on the bottom face is

$$dF_B = - \left( \tau_{yx} - \frac{d\tau_{yx}}{dy} \frac{dy}{2} \right) dx dz$$

and the shear force on the top face is

$$dF_T = \left( \tau_{yx} + \frac{d\tau_{yx}}{dy} \frac{dy}{2} \right) dx dz$$

Note that in expanding the shear stress,  $\tau_{yx}$ , in a Taylor series about the center of the element, we have used the total derivative rather than a partial derivative. We did this because we recognized that  $\tau_{yx}$  is only a function of  $y$ , since  $u = u(y)$ .

Using the four surface forces  $dF_L$ ,  $dF_R$ ,  $dF_B$ , and  $dF_T$  in Eq. 8.2, this equation simplifies to

$$\frac{\partial p}{\partial x} = \frac{d\tau_{yx}}{dy} \quad (8.3)$$

This equation states that because there is no change in momentum, the net pressure force (which is actually  $-\partial p/\partial x$ ) balances the net friction force (which is actually  $-d\tau_{yx}/dy$ ). Equation 8.3 has an interesting feature: The left side is at most a function of  $x$  only (this follows immediately from writing the  $y$  component of the momentum equation); the right side is at most a function of  $y$  only (the flow is fully developed, so



it does not change with  $x$ ). Hence, the only way the equation can be valid for all  $x$  and  $y$  is for each side to in fact be constant:

$$\frac{d\tau_{yx}}{dy} = \frac{\partial p}{\partial x} = \text{constant}$$

Integrating this equation, we obtain

$$\tau_{yx} = \left( \frac{\partial p}{\partial x} \right) y + c_1$$

which indicates that the shear stress varies linearly with  $y$ . We wish to find the velocity distribution. To do so, we need to relate the shear stress to the velocity field. For a Newtonian fluid we can use Eq. 2.15 because we have a one-dimensional flow [or we could have started with the full stress equation (Eq. 5.25a) and simplified],

$$\tau_{yx} = \mu \frac{du}{dy} \quad (2.15)$$

so we get

$$\mu \frac{du}{dy} = \left( \frac{\partial p}{\partial x} \right) y + c_1$$

Integrating again

$$u = \frac{1}{2\mu} \left( \frac{\partial p}{\partial x} \right) y^2 + \frac{c_1}{\mu} y + c_2 \quad (8.4)$$

It is interesting to note that if we had started with the Navier–Stokes equations (Eqs. 5.27) instead of using a differential control volume, after only a few steps (i.e., simplifying and integrating twice) we would have obtained Eq. 8.4 (see Problem 8.17). To evaluate the constants,  $c_1$  and  $c_2$ , we must apply the boundary conditions. At  $y = 0$ ,  $u = 0$ . Consequently,  $c_2 = 0$ . At  $y = a$ ,  $u = 0$ . Hence

$$0 = \frac{1}{2\mu} \left( \frac{\partial p}{\partial x} \right) a^2 + \frac{c_1}{\mu} a$$

This gives

$$c_1 = -\frac{1}{2} \left( \frac{\partial p}{\partial x} \right) a$$

and hence,

$$u = \frac{1}{2\mu} \left( \frac{\partial p}{\partial x} \right) y^2 - \frac{1}{2\mu} \left( \frac{\partial p}{\partial x} \right) ay = \frac{a^2}{2\mu} \left( \frac{\partial p}{\partial x} \right) \left[ \left( \frac{y}{a} \right)^2 - \left( \frac{y}{a} \right) \right] \quad (8.5)$$

At this point we have the velocity profile. This is key to finding other flow properties, as we next discuss.

### Shear Stress Distribution

The shear stress distribution is given by

$$\tau_{yx} = \left( \frac{\partial p}{\partial x} \right) y + c_1 = \left( \frac{\partial p}{\partial x} \right) y - \frac{1}{2} \left( \frac{\partial p}{\partial x} \right) a = a \left( \frac{\partial p}{\partial x} \right) \left[ \frac{y}{a} - \frac{1}{2} \right] \quad (8.6a)$$

### Volume Flow Rate

The volume flow rate is given by

$$Q = \int_A \vec{V} \cdot d\vec{A}$$

For a depth  $l$  in the  $z$  direction,

$$Q = \int_0^a ul \, dy \quad \text{or} \quad \frac{Q}{l} = \int_0^a \frac{1}{2\mu} \left( \frac{\partial p}{\partial x} \right) (y^2 - ay) \, dy$$

Thus the volume flow rate per unit depth is given by

$$\frac{Q}{l} = -\frac{1}{12\mu} \left( \frac{\partial p}{\partial x} \right) a^3 \quad (8.6b)$$

### Flow Rate as a Function of Pressure Drop

Since  $\partial p/\partial x$  is constant, the pressure varies linearly with  $x$  and

$$\frac{\partial p}{\partial x} = \frac{p_2 - p_1}{L} = \frac{-\Delta p}{L}$$

Substituting into the expression for volume flow rate gives

$$\frac{Q}{l} = -\frac{1}{12\mu} \left[ \frac{-\Delta p}{L} \right] a^3 = \frac{a^3 \Delta p}{12\mu L} \quad (8.6c)$$

### Average Velocity

The average velocity magnitude,  $\bar{V}$ , is given by

$$\bar{V} = \frac{Q}{A} = -\frac{1}{12\mu} \left( \frac{\partial p}{\partial x} \right) \frac{a^3 l}{la} = -\frac{1}{12\mu} \left( \frac{\partial p}{\partial x} \right) a^2 \quad (8.6d)$$

### Point of Maximum Velocity

To find the point of maximum velocity, we set  $du/dy$  equal to zero and solve for the corresponding  $y$ . From Eq. 8.5

$$\frac{du}{dy} = \frac{a^2}{2\mu} \left( \frac{\partial p}{\partial x} \right) \left[ \frac{2y}{a^2} - \frac{1}{a} \right]$$

Thus,

$$\frac{du}{dy} = 0 \quad \text{at} \quad y = \frac{a}{2}$$

At

$$y = \frac{a}{2}, \quad u = u_{\max} = -\frac{1}{8\mu} \left( \frac{\partial p}{\partial x} \right) a^2 = \frac{3}{2} \bar{V} \quad (8.6e)$$

### Transformation of Coordinates

In deriving the above relations, the origin of coordinates,  $y = 0$ , was taken at the bottom plate. We could just as easily have taken the origin at the centerline of the channel. If we

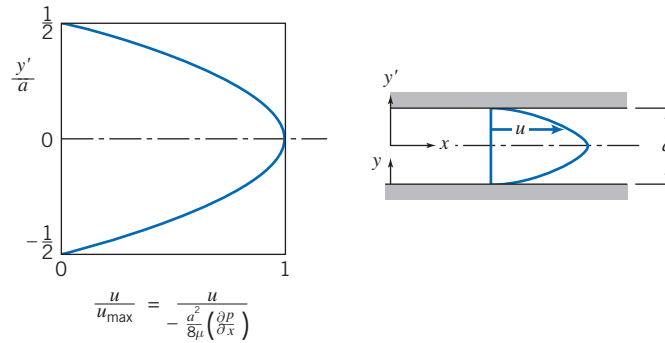


**Fig. 8.4** Dimensionless velocity profile for fully developed laminar flow between infinite parallel plates.

denote the coordinates with origin at the channel centerline as  $x, y'$ , the boundary conditions are  $u = 0$  at  $y' = \pm a/2$ .

To obtain the velocity profile in terms of  $x, y'$ , we substitute  $y = y' + a/2$  into Eq. 8.5. The result is

$$u = \frac{a^2}{2\mu} \left( \frac{\partial p}{\partial x} \right) \left[ \left( \frac{y'}{a} \right)^2 - \frac{1}{4} \right] \quad (8.7)$$

Equation 8.7 shows that the velocity profile for laminar flow between stationary parallel plates is parabolic, as shown in Fig. 8.4.

Since all stresses were related to velocity gradients through Newton's law of viscosity, and the additional stresses that arise as a result of turbulent fluctuations have not been accounted for, *all of the results in this section are valid for laminar flow only*. Experiments show that laminar flow between stationary parallel plates becomes turbulent for Reynolds numbers (defined as  $Re = \rho \bar{V} a / \mu$ ) greater than approximately 1400. Consequently, the Reynolds number should be checked after using Eqs. 8.6 to ensure a valid solution.

### Example 8.7 LEAKAGE FLOW PAST A PISTON

A hydraulic system operates at a gage pressure of 20 MPa and 55°C. The hydraulic fluid is SAE 10W oil. A control valve consists of a piston 25 mm in diameter, fitted to a cylinder with a mean radial clearance of 0.005 mm. Determine the leakage flow rate if the gage pressure on the low-pressure side of the piston is 1.0 MPa. (The piston is 15 mm long.)

**Given:** Flow of hydraulic oil between piston and cylinder, as shown. Fluid is SAE 10W oil at 55°C.

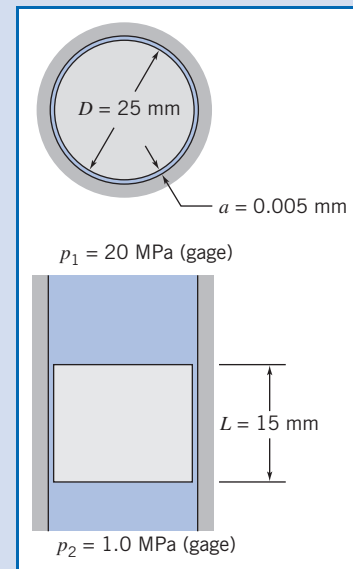
**Find:** Leakage flow rate,  $Q$ .

**Solution:**

The gap width is very small, so the flow may be modeled as flow between parallel plates. Equation 8.6c may be applied.

**Governing equation:**

$$\frac{Q}{l} = \frac{a^3 \Delta p}{12\mu L} \quad (8.6c)$$



**Assumptions:** (1) Laminar flow.  
 (2) Steady flow.  
 (3) Incompressible flow.  
 (4) Fully developed flow.  
 (Note  $L/a = 15/0.005 = 3000!$ )

The plate width,  $l$ , is approximated as  $l = \pi D$ . Thus

$$Q = \frac{\pi D a^3 \Delta p}{12 \mu L}$$

For SAE 10W oil at 55°C,  $\mu = 0.018 \text{ kg}/(\text{m} \cdot \text{s})$ , from Fig. A.2, Appendix A. Thus

$$Q = \frac{\pi}{12} \times 25 \text{ mm} \times (0.005)^3 \text{ mm}^3 \times (20 - 1) 10^6 \frac{\text{N}}{\text{m}^2} \times \frac{\text{m} \cdot \text{s}}{0.018 \text{ kg}} \times \frac{1}{15 \text{ mm}} \times \frac{\text{kg} \cdot \text{m}}{\text{N} \cdot \text{s}^2}$$

$$Q = 57.6 \text{ mm}^3/\text{s} \quad \leftarrow \frac{Q}{A}$$

To ensure that flow is laminar, we also should check the Reynolds number.

$$\bar{V} = \frac{Q}{A} = \frac{Q}{\pi D a} = 57.6 \frac{\text{mm}^3}{\text{s}} \times \frac{1}{\pi} \times \frac{1}{25 \text{ mm}} \times \frac{1}{0.005 \text{ mm}} \times \frac{\text{m}}{10^3 \text{ mm}} = 0.147 \text{ m/s}$$

and

$$Re = \frac{\rho \bar{V} a}{\mu} = \frac{SG \rho_{\text{H}_2\text{O}} \bar{V} a}{\mu}$$

For SAE 10W oil,  $SG = 0.92$ , from Table A.2, Appendix A. Thus

$$Re = 0.92 \times 1000 \frac{\text{kg}}{\text{m}^3} \times 0.147 \frac{\text{m}}{\text{s}} \times 0.005 \text{ mm} \times \frac{\text{m} \cdot \text{s}}{0.018 \text{ kg}} \times \frac{\text{m}}{10^3 \text{ mm}} = 0.0375$$

Thus flow is surely laminar, since  $Re \ll 1400$ .

## Upper Plate Moving with Constant Speed, $U$

The second basic way to generate flow between infinite parallel plates is to have one plate move parallel to the other, either with or without an applied pressure gradient. We will next analyze this problem for the case of laminar flow.

Such a flow commonly occurs, for example, in a journal bearing (a commonly used type of bearing, e.g., the main crankshaft bearings in the engine of an automobile). In such a bearing, an inner cylinder, the journal, rotates inside a stationary member. At light loads, the centers of the two members essentially coincide, and the small clearance gap is symmetric. Since the gap is small, it is reasonable to “unfold” the bearing and to model the flow field as flow between infinite parallel plates, as indicated in the sketch of Fig. 8.5.

Let us now consider a case where the upper plate is moving to the right with constant speed,  $U$ . All we have done in going from a stationary upper plate to a moving upper plate is to change one of the boundary conditions. The boundary conditions for the moving plate case are

$$\begin{array}{lll} u = 0 & \text{at} & y = 0 \\ u = U & \text{at} & y = a \end{array}$$

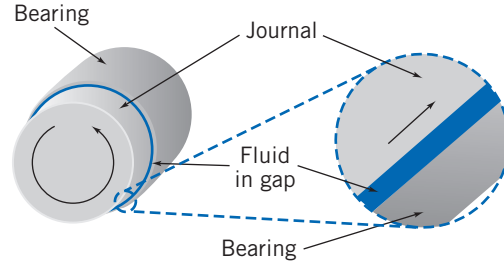


**Fig. 8.5** Journal bearing approximated as parallel plates.

Since only the boundary conditions have changed, there is no need to repeat the entire analysis of the previous section. The analysis leading to Eq. 8.4 is equally valid for the moving plate case. Thus the velocity distribution is given by

$$u = \frac{1}{2\mu} \left( \frac{\partial p}{\partial x} \right) y^2 + \frac{c_1}{\mu} y + c_2 \quad (8.4)$$

and our only task is to evaluate constants  $c_1$  and  $c_2$  by using the appropriate boundary conditions. [Note once again that using the full Navier–Stokes equations (Eqs. 5.27) would have led very quickly to Eq. 8.4.]

At  $y = 0$ ,  $u = 0$ . Consequently,  $c_2 = 0$ .

At  $y = a$ ,  $u = U$ . Consequently,

$$U = \frac{1}{2\mu} \left( \frac{\partial p}{\partial x} \right) a^2 + \frac{c_1}{\mu} a \quad \text{and thus} \quad c_1 = \frac{U\mu}{a} - \frac{1}{2} \left( \frac{\partial p}{\partial x} \right) a$$

Hence,

$$u = \frac{1}{2\mu} \left( \frac{\partial p}{\partial x} \right) y^2 + \frac{Uy}{a} - \frac{1}{2\mu} \left( \frac{\partial p}{\partial x} \right) ay = \frac{Uy}{a} + \frac{1}{2\mu} \left( \frac{\partial p}{\partial x} \right) (y^2 - ay)$$

$$u = \frac{Uy}{a} + \frac{a^2}{2\mu} \left( \frac{\partial p}{\partial x} \right) \left[ \left( \frac{y}{a} \right)^2 - \left( \frac{y}{a} \right) \right] \quad (8.8)$$

It is reassuring to note that Eq. 8.8 reduces to Eq. 8.5 for a stationary upper plate (set  $U = 0$ ). From Eq. 8.8, for zero pressure gradient (for  $\partial p/\partial x = 0$ ) the velocity varies linearly with  $y$ . This was the case treated earlier in Chapter 2; this linear profile is called a *Couette* flow, after a 19th-century physicist.

We can obtain additional information about the flow from the velocity distribution of Eq. 8.8.

### Shear Stress Distribution

The shear stress distribution is given by  $\tau_{yx} = \mu(du/dy)$ ,

$$\tau_{yx} = \mu \frac{U}{a} + \frac{a^2}{2} \left( \frac{\partial p}{\partial x} \right) \left[ \frac{2y}{a^2} - \frac{1}{a} \right] = \mu \frac{U}{a} + a \left( \frac{\partial p}{\partial x} \right) \left[ \frac{y}{a} - \frac{1}{2} \right] \quad (8.9a)$$

### Volume Flow Rate

The volume flow rate is given by  $Q = \int_A \vec{V} \cdot d\vec{A}$ . For depth  $l$  in the  $z$  direction

$$Q = \int_0^a ul \, dy \quad \text{or} \quad \frac{Q}{l} = \int_0^a \left[ \frac{Uy}{a} + \frac{1}{2\mu} \left( \frac{\partial p}{\partial x} \right) (y^2 - ay) \right] dy$$

Thus the volume flow rate per unit depth is given by

$$\frac{Q}{l} = \frac{Ua}{2} - \frac{1}{12\mu} \left( \frac{\partial p}{\partial x} \right) a^3 \quad (8.9b)$$

### Average Velocity

The average velocity magnitude,  $\bar{V}$ , is given by

$$\bar{V} = \frac{Q}{A} = l \left[ \frac{Ua}{2} - \frac{1}{12\mu} \left( \frac{\partial p}{\partial x} \right) a^3 \right] / la = \frac{U}{2} - \frac{1}{12\mu} \left( \frac{\partial p}{\partial x} \right) a^2 \quad (8.9c)$$

### Point of Maximum Velocity

To find the point of maximum velocity, we set  $du/dy$  equal to zero and solve for the corresponding  $y$ . From Eq. 8.8

$$\frac{du}{dy} = \frac{U}{a} + \frac{a^2}{2\mu} \left( \frac{\partial p}{\partial x} \right) \left[ \frac{2y}{a^2} - \frac{1}{a} \right] = \frac{U}{a} + \frac{a}{2\mu} \left( \frac{\partial p}{\partial x} \right) \left[ 2\left(\frac{y}{a}\right) - 1 \right]$$

Thus,

$$\frac{du}{dy} = 0 \quad \text{at} \quad y = \frac{a}{2} - \frac{U/a}{(1/\mu)(\partial p/\partial x)}$$

There is no simple relation between the maximum velocity,  $u_{\max}$ , and the mean velocity,  $\bar{V}$ , for this flow case.

Equation 8.8 suggests that the velocity profile may be treated as a combination of a linear and a parabolic velocity profile; the last term in Eq. 8.8 is identical to that in Eq. 8.5. The result is a family of velocity profiles, depending on  $U$  and  $(1/\mu)(\partial p/\partial x)$ ; three profiles are sketched in Fig. 8.6. (As shown in Fig. 8.6, some reverse flow—flow in the negative  $x$  direction—can occur when  $\partial p/\partial x > 0$ .)

Again, all of the results developed in this section are valid for laminar flow only. Experiments show that this flow becomes turbulent (for  $\partial p/\partial x = 0$ ) at a Reynolds number of approximately 1500, where  $Re = \rho Ua/\mu$  for this flow case. Not much information is available for the case where the pressure gradient is not zero.

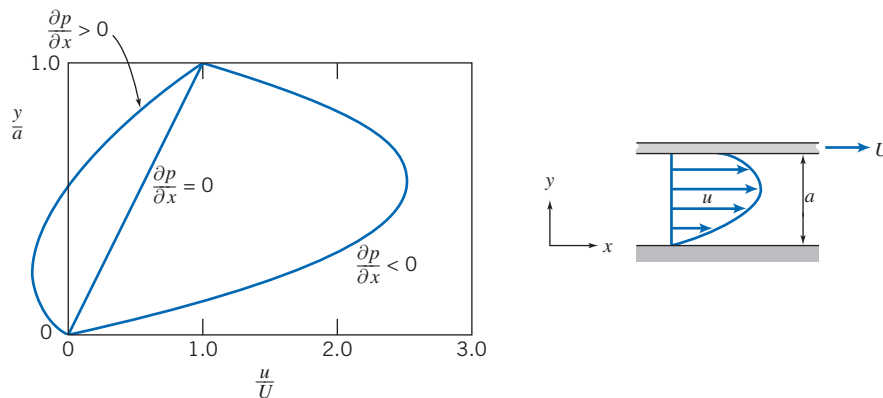


**Fig. 8.6** Dimensionless velocity profile for fully developed laminar flow between infinite parallel plates: upper plate moving with constant speed,  $U$ .



### Example 8.2 TORQUE AND POWER IN A JOURNAL BEARING

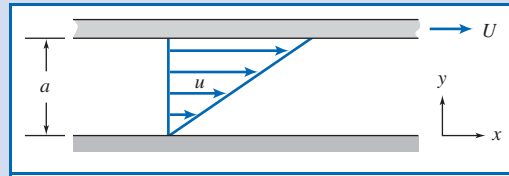
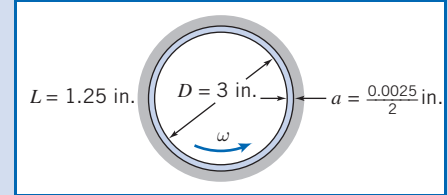
A crankshaft journal bearing in an automobile engine is lubricated by SAE 30 oil at 210°F. The bearing diameter is 3 in., the diametral clearance is 0.0025 in., and the shaft rotates at 3600 rpm; it is 1.25 in. long. The bearing is under no load, so the clearance is symmetric. Determine the torque required to turn the journal and the power dissipated.

**Given:** Journal bearing, as shown. Note that the gap width,  $a$ , is *half* the diametral clearance. Lubricant is SAE 30 oil at 210°F. Speed is 3600 rpm.

**Find:** (a) Torque,  $T$ .  
(b) Power dissipated.

**Solution:**

Torque on the journal is caused by viscous shear in the oil film. The gap width is small, so the flow may be modeled as flow between infinite parallel plates:



**Governing equation:**

$$\tau_{yx} = \mu \frac{U}{a} + a \left( \frac{\partial p}{\partial x} \right) \left[ \frac{y}{a} - \frac{1}{2} \right] \quad (8.9a)$$

- Assumptions:**
- (1) Laminar flow.
  - (2) Steady flow.
  - (3) Incompressible flow.
  - (4) Fully developed flow.
  - (5) Infinite width ( $L/a = 1.25/0.00125 = 1000$ , so this is a reasonable assumption).
  - (6)  $\partial p/\partial x = 0$  (flow is symmetric in the actual bearing at no load).

Then

$$\tau_{yx} = \mu \frac{U}{a} = \mu \frac{\omega R}{a} = \mu \frac{\omega D}{2a}$$

For SAE 30 oil at 210°F (99°C),  $\mu = 9.6 \times 10^{-3} \text{ N} \cdot \text{s/m}^2$  ( $2.01 \times 10^{-4} \text{ lbf} \cdot \text{s/ft}^2$ ), from Fig. A.2, Appendix A. Thus,

$$\begin{aligned} \tau_{yx} &= 2.01 \times 10^{-4} \frac{\text{lbf} \cdot \text{s}}{\text{ft}^2} \times 3600 \frac{\text{rev}}{\text{min}} \times 2\pi \frac{\text{rad}}{\text{rev}} \times \frac{\text{min}}{60 \text{ s}} \times 3 \text{ in.} \times \frac{1}{2} \times \frac{1}{0.00125 \text{ in.}} \\ \tau_{yx} &= 90.9 \text{ lbf/ft}^2 \end{aligned}$$

The total shear force is given by the shear stress times the area. It is applied to the journal surface. Therefore, for the torque

$$\begin{aligned} T &= FR = \tau_{yx} \pi D L R = \frac{\pi}{2} \tau_{yx} D^2 L \\ &= \frac{\pi}{2} \times 90.9 \frac{\text{lbf}}{\text{ft}^2} \times (3)^2 \text{ in.}^2 \times \frac{\text{ft}^2}{144 \text{ in.}^2} \times 1.25 \text{ in.} \\ T &= 11.2 \text{ in.} \cdot \text{lbf} \end{aligned}$$

The power dissipated in the bearing is

$$\begin{aligned}\dot{W} &= FU = FR\omega = T\omega \\ &= 11.2 \text{ in.} \cdot \text{lbf} \times 3600 \frac{\text{rev}}{\text{min}} \times \frac{\text{min}}{60 \text{ s}} \times 2\pi \frac{\text{rad}}{\text{rev}} \times \frac{\text{ft}}{12 \text{ in.}} \times \frac{\text{hp} \cdot \text{s}}{550 \text{ ft} \cdot \text{lbf}} \\ \dot{W} &= 0.640 \text{ hp} \leftarrow \dot{W}\end{aligned}$$

To ensure laminar flow, check the Reynolds number.

$$Re = \frac{\rho Ua}{\mu} = \frac{SG\rho_{\text{H}_2\text{O}}Ua}{\mu} = \frac{SG\rho_{\text{H}_2\text{O}}\omega Ra}{\mu}$$

Assume, as an approximation, the specific gravity of SAE 30 oil is the same as that of SAE 10W oil. From Table A.2, Appendix A,  $SG = 0.92$ . Thus

$$\begin{aligned}Re &= 0.92 \times 1.94 \frac{\text{slug}}{\text{ft}^3} \times \frac{(3600)2\pi}{60} \frac{\text{rad}}{\text{s}} \times 1.5 \text{ in.} \times 0.00125 \text{ in.} \\ &\quad \times \frac{\text{ft}^2}{2.01 \times 10^{-4} \text{ lbf} \cdot \text{s}} \times \frac{\text{ft}^2}{144 \text{ in.}^2} \times \frac{\text{lbf} \cdot \text{s}^2}{\text{slug} \cdot \text{ft}} \\ Re &= 43.6\end{aligned}$$

Therefore, the flow is laminar, since  $Re \ll 1500$ .

In this problem we approximated the circular-streamline flow in a small annular gap as a linear flow between infinite parallel plates. As we saw in Example 5.10, for the small value of the gap width  $a$  to radius  $R$  ratio  $a/R$  (in this problem  $<1\%$ ), the error in shear stress is about  $\frac{1}{2}$  of this ratio. Hence, the error introduced is insignificant—much less than the uncertainty associated with obtaining a viscosity for the oil.

We have seen how steady, one-dimensional laminar flows between two plates can be generated by applying a pressure gradient, by moving one plate with respect to the other, or by having both driving mechanisms present. To finish our discussion of this type of flow, Example 8.3 examines a *gravity-driven* steady, one-dimensional laminar flow down a vertical wall. Once again, the direct approach would be to start with the two-dimensional rectangular coordinate form of the Navier–Stokes equations (Eqs. 5.27; see Problem 8.44); instead we will use a differential control volume.

### Example 8.3 LAMINAR FILM ON A VERTICAL WALL

A viscous, incompressible, Newtonian liquid flows in steady, laminar flow down a vertical wall. The thickness,  $\delta$ , of the liquid film is constant. Since the liquid free surface is exposed to atmospheric pressure, there is no pressure gradient. For this gravity-driven flow, apply the momentum equation to differential control volume  $dx \, dy \, dz$  to derive the velocity distribution in the liquid film.

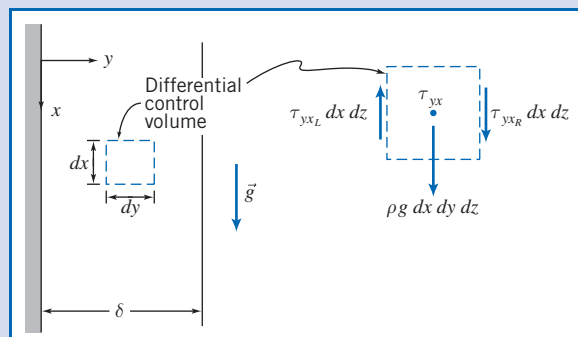
**Given:** Fully developed laminar flow of incompressible, Newtonian liquid down a vertical wall; thickness,  $\delta$ , of the liquid film is constant and  $\partial p / \partial x = 0$ .

**Find:** Expression for the velocity distribution in the film.

**Solution:**

The  $x$  component of the momentum equation for a control volume is

$$F_{S_x} + F_{B_x} = \frac{\partial}{\partial t} \int_{CV} u \rho \, dV + \int_{CS} u \rho \vec{V} \cdot d\vec{A} \quad (4.18a)$$



Under the conditions given we are dealing with a steady, incompressible, fully developed laminar flow.

For steady flow,  $\frac{\partial}{\partial t} \int_{CV} u \rho dV = 0$

For fully developed flow,  $\int_{CS} u \rho \vec{V} \cdot d\vec{A} = 0$

Thus the momentum equation for the present case reduces to

$$F_{S_x} + F_{B_x} = 0$$

The body force,  $F_{B_x}$ , is given by  $F_{B_x} = \rho g dV = \rho g dx dy dz$ . The only surface forces acting on the differential control volume are shear forces on the vertical surfaces. (Since we have a free-surface flow, with straight streamlines, the pressure is atmospheric throughout; no net pressure forces act on the control volume.)

If the shear stress at the center of the differential control volume is  $\tau_{yx}$ , then,

$$\text{shear stress on left face is } \tau_{yx_L} = \left( \tau_{yx} - \frac{d\tau_{yx}}{dy} \frac{dy}{2} \right)$$

and

$$\text{shear stress on right face is } \tau_{yx_R} = \left( \tau_{yx} + \frac{d\tau_{yx}}{dy} \frac{dy}{2} \right)$$

The direction of the shear stress vectors is taken consistent with the sign convention of Section 2.3. Thus on the left face, a minus  $y$  surface,  $\tau_{yx_L}$  acts upward, and on the right face, a plus  $y$  surface,  $\tau_{yx_R}$  acts downward.

The surface forces are obtained by multiplying each shear stress by the area over which it acts. Substituting into  $F_{S_x} + F_{B_x} = 0$ , we obtain

$$-\tau_{yx_L} dx dz + \tau_{yx_R} dx dz + \rho g dx dy dz = 0$$

or

$$-\left( \tau_{yx} - \frac{d\tau_{yx}}{dy} \frac{dy}{2} \right) dx dz + \left( \tau_{yx} + \frac{d\tau_{yx}}{dy} \frac{dy}{2} \right) dx dz + \rho g dx dy dz = 0$$

Simplifying gives

$$\frac{d\tau_{yx}}{dy} + \rho g = 0 \quad \text{or} \quad \frac{d\tau_{yx}}{dy} = -\rho g$$

Since

$$\tau_{yx} = \mu \frac{du}{dy} \quad \text{then} \quad \mu \frac{d^2 u}{dy^2} = -\rho g \quad \text{and} \quad \frac{d^2 u}{dy^2} = -\frac{\rho g}{\mu}$$

Integrating with respect to  $y$  gives

$$\frac{du}{dy} = -\frac{\rho g}{\mu} y + c_1$$

Integrating again, we obtain

$$u = -\frac{\rho g}{\mu} \frac{y^2}{2} + c_1 y + c_2$$

To evaluate constants  $c_1$  and  $c_2$ , we apply appropriate boundary conditions:

- (i)  $y = 0, \quad u = 0$  (no-slip)
- (ii)  $y = \delta, \quad \frac{du}{dy} = 0$  (neglect air resistance, i.e., assume zero shear stress at free surface)

From boundary condition (i),  $c_2 = 0$

From boundary condition (ii),  $0 = -\frac{\rho g}{\mu} \delta + c_1$  or  $c_1 = \frac{\rho g}{\mu} \delta$

Hence,

$$u = -\frac{\rho g}{\mu} \frac{y^2}{2} + \frac{\rho g}{\mu} \delta y \quad \text{or} \quad u = \frac{\rho g}{\mu} \delta^2 \left[ \left( \frac{y}{\delta} \right) - \frac{1}{2} \left( \frac{y}{\delta} \right)^2 \right] \quad \leftarrow u(y)$$

Using the velocity profile it can be shown that:

$$\text{the volume flow rate is } Q/l = \frac{\rho g}{3\mu} \delta^3$$

$$\text{the maximum velocity is } U_{\max} = \frac{\rho g}{2\mu} \delta^2$$

$$\text{the average velocity is } \bar{V} = \frac{\rho g}{3\mu} \delta^2$$

Flow in the liquid film is laminar for  $Re = \bar{V}\delta/\nu \leq 1000$  [1].

#### Notes:

- ✓ This problem is a special case ( $\theta = 90^\circ$ ) of the inclined plate flow analyzed in Example 5.9 that we solved using the Navier–Stokes equations.
- ✓ This problem and Example 5.9 demonstrate that use of the differential control volume approach or the Navier–Stokes equations leads to the same result.

## 8.3 Fully Developed Laminar Flow in a Pipe

### VIDEO

Laminar Flow Exiting from a Tube.

As a final example of fully developed laminar flow, let us consider fully developed laminar flow in a pipe. Here the flow is axisymmetric. Consequently it is most convenient to work in cylindrical coordinates. This is yet another case where we could use the Navier–Stokes equations, this time in cylindrical coordinates (Eqs. B.3). Instead we will again take the longer route—using a differential control volume—to bring out some important features of the fluid mechanics. The development will be very similar to that for parallel plates in the previous section; cylindrical coordinates just make the analysis a little trickier mathematically. Since the flow is axisymmetric, the control volume will be a differential annulus, as shown in Fig. 8.7. The control volume length is  $dx$  and its thickness is  $dr$ .

For a fully developed steady flow, the  $x$  component of the momentum equation (Eq. 4.18a), when applied to the differential control volume, once again reduces to

$$F_{S_x} = 0$$

The next step is to sum the forces acting on the control volume in the  $x$  direction. We know that normal forces (pressure forces) act on the left and right ends of the control volume, and that tangential forces (shear forces) act on the inner and outer cylindrical surfaces.

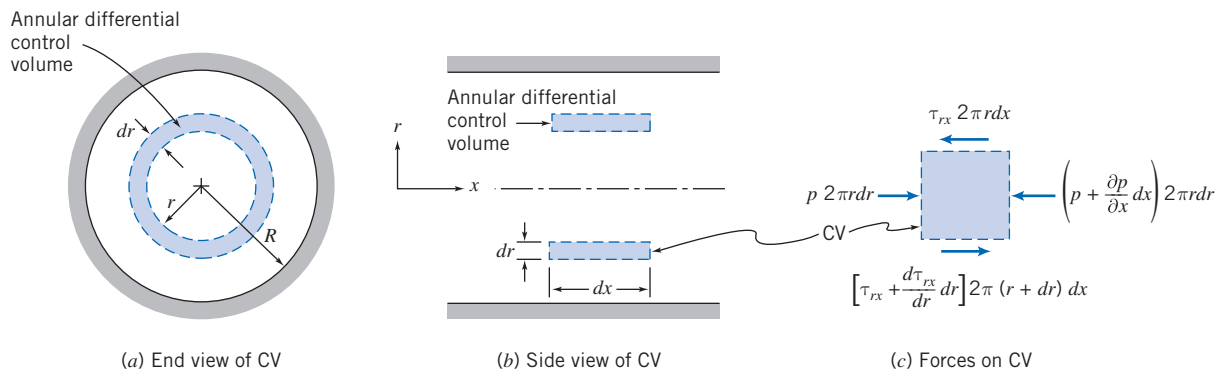


Fig. 8.7 Differential control volume for analysis of fully developed laminar flow in a pipe.

If the pressure at the left face of the control volume is  $p$ , then the pressure force on the left end is

$$dF_L = p 2\pi r dr$$

The pressure force on the right end is

$$dF_R = -\left(p + \frac{\partial p}{\partial x} dx\right) 2\pi r dr$$

If the shear stress at the inner surface of the annular control volume is  $\tau_{rx}$ , then the shear force on the inner cylindrical surface is

$$dF_I = -\tau_{rx} 2\pi r dx$$

The shear force on the outer cylindrical surface is

$$dF_O = \left(\tau_{rx} + \frac{d\tau_{rx}}{dr} dr\right) 2\pi (r + dr) dx$$

The sum of the  $x$  components of force,  $dF_L$ ,  $dF_R$ ,  $dF_I$ , and  $dF_O$ , acting on the control volume must be zero. This leads to the condition that

$$-\frac{\partial p}{\partial x} 2\pi r dr dx + \tau_{rx} 2\pi dr dx + \frac{d\tau_{rx}}{dr} 2\pi r dr dx = 0$$

Dividing this equation by  $2\pi r dr dx$  and solving for  $\partial p/\partial x$  gives

$$\frac{\partial p}{\partial x} = \frac{\tau_{rx}}{r} + \frac{d\tau_{rx}}{dr} = \frac{1}{r} \frac{d(r\tau_{rx})}{dr}$$

Comparing this to the corresponding equation for parallel plates (Eq. 8.3) shows the mathematical complexity introduced because we have cylindrical coordinates. The left side of the equation is at most a function of  $x$  only (the pressure is uniform at each section); the right side is at most a function of  $r$  only (because the flow is fully developed). Hence, the only way the equation can be valid for all  $x$  and  $r$  is for both sides to in fact be constant:

$$\frac{1}{r} \frac{d(r\tau_{rx})}{dr} = \frac{\partial p}{\partial x} = \text{constant} \quad \text{or} \quad \frac{d(r\tau_{rx})}{dr} = r \frac{\partial p}{\partial x}$$

We are not quite finished, but already we have an important result: *In a constant diameter pipe, the pressure drops uniformly along the pipe length* (except for the entrance region).

Integrating this equation, we obtain

$$r\tau_{rx} = \frac{r^2}{2} \left(\frac{\partial p}{\partial x}\right) + c_1$$

or

$$\tau_{rx} = \frac{r}{2} \left(\frac{\partial p}{\partial x}\right) + \frac{c_1}{r} \quad (8.10)$$

Since  $\tau_{rx} = \mu du/dr$ , we have

$$\mu \frac{du}{dr} = \frac{r}{2} \left(\frac{\partial p}{\partial x}\right) + \frac{c_1}{r}$$

and

$$u = \frac{r^2}{4\mu} \left( \frac{\partial p}{\partial x} \right) + \frac{c_1}{\mu} \ln r + c_2 \quad (8.11)$$

We need to evaluate constants  $c_1$  and  $c_2$ . However, we have only the one boundary condition that  $u = 0$  at  $r = R$ . What do we do? Before throwing in the towel, let us look at the solution for the velocity profile given by Eq. 8.11. Although we do not know the velocity at the pipe centerline, we do know from physical considerations that the velocity must be finite at  $r = 0$ . The only way that this can be true is for  $c_1$  to be zero. (We could have also concluded that  $c_1 = 0$  from Eq. 8.10—which would otherwise yield an infinite stress at  $r = 0$ .) Thus, from physical considerations, we conclude that  $c_1 = 0$ , and hence

$$u = \frac{r^2}{4\mu} \left( \frac{\partial p}{\partial x} \right) + c_2$$

The constant,  $c_2$ , is evaluated by using the available boundary condition at the pipe wall: at  $r = R$ ,  $u = 0$ . Consequently,

$$0 = \frac{R^2}{4\mu} \left( \frac{\partial p}{\partial x} \right) + c_2$$

This gives

$$c_2 = -\frac{R^2}{4\mu} \left( \frac{\partial p}{\partial x} \right)$$

and hence

$$u = \frac{r^2}{4\mu} \left( \frac{\partial p}{\partial x} \right) - \frac{R^2}{4\mu} \left( \frac{\partial p}{\partial x} \right) = \frac{1}{4\mu} \left( \frac{\partial p}{\partial x} \right) (r^2 - R^2)$$

or

$$u = -\frac{R^2}{4\mu} \left( \frac{\partial p}{\partial x} \right) \left[ 1 - \left( \frac{r}{R} \right)^2 \right] \quad (8.12)$$

Since we have the velocity profile, we can obtain a number of additional features of the flow.

### Shear Stress Distribution

The shear stress is

$$\tau_{rx} = \mu \frac{du}{dr} = \frac{r}{2} \left( \frac{\partial p}{\partial x} \right) \quad (8.13a)$$

### Volume Flow Rate

The volume flow rate is

$$\begin{aligned} Q &= \int_A \vec{V} \cdot d\vec{A} = \int_0^R u 2\pi r dr = \int_0^R \frac{1}{4\mu} \left( \frac{\partial p}{\partial x} \right) (r^2 - R^2) 2\pi r dr \\ Q &= -\frac{\pi R^4}{8\mu} \left( \frac{\partial p}{\partial x} \right) \end{aligned} \quad (8.13b)$$



### Flow Rate as a Function of Pressure Drop

We proved that in fully developed flow the pressure gradient,  $\partial p/\partial x$ , is constant. Therefore,  $\partial p/\partial x = (p_2 - p_1)/L = -\Delta p/L$ . Substituting into Eq. 8.13b for the volume flow rate gives

$$Q = -\frac{\pi R^4}{8\mu} \left[ \frac{-\Delta p}{L} \right] = \frac{\pi \Delta p R^4}{8\mu L} = \frac{\pi \Delta p D^4}{128\mu L} \quad (8.13c)$$

for laminar flow in a horizontal pipe. Note that  $Q$  is a sensitive function of  $D$ ;  $Q \sim D^4$ , so, for example, doubling the diameter  $D$  increases the flow rate  $Q$  by a factor of 16.

### Average Velocity

The average velocity magnitude,  $\bar{V}$ , is given by

$$\bar{V} = \frac{Q}{A} = \frac{Q}{\pi R^2} = -\frac{R^2}{8\mu} \left( \frac{\partial p}{\partial x} \right) \quad (8.13d)$$

### Point of Maximum Velocity

To find the point of maximum velocity, we set  $du/dr$  equal to zero and solve for the corresponding  $r$ . From Eq. 8.12

$$\frac{du}{dr} = \frac{1}{2\mu} \left( \frac{\partial p}{\partial x} \right) r$$

Thus,

$$\frac{du}{dr} = 0 \quad \text{at} \quad r = 0$$

At  $r = 0$ ,

$$u = u_{\max} = U = -\frac{R^2}{4\mu} \left( \frac{\partial p}{\partial x} \right) = 2\bar{V} \quad (8.13e)$$

The velocity profile (Eq. 8.12) may be written in terms of the maximum (centerline) velocity as

$$\frac{u}{U} = 1 - \left( \frac{r}{R} \right)^2 \quad (8.14)$$

The parabolic velocity profile, given by Eq. 8.14 for fully developed laminar pipe flow, was sketched in Fig. 8.1.

## Example 8.4 CAPILLARY VISCOMETER

A simple and accurate viscometer can be made from a length of capillary tubing. If the flow rate and pressure drop are measured, and the tube geometry is known, the viscosity of a Newtonian liquid can be computed from Eq. 8.13c. A test of a certain liquid in a capillary viscometer gave the following data:

Flow rate:	880 mm <sup>3</sup> /s	Tube length:	1 m
Tube diameter:	0.50 mm	Pressure drop:	1.0 MPa

Determine the viscosity of the liquid.

**Given:** Flow in a capillary viscometer.  
The flow rate is  $Q = 880 \text{ mm}^3/\text{s}$ .

**Find:** The fluid viscosity.

**Solution:**

Equation 8.13c may be applied.

**Governing equation:**  $Q = \frac{\pi \Delta p D^4}{128 \mu L} \quad (8.13c)$

**Assumptions:** (1) Laminar flow.  
(2) Steady flow.  
(3) Incompressible flow.  
(4) Fully developed flow.  
(5) Horizontal tube.

Then

$$\mu = \frac{\pi \Delta p D^4}{128 L Q} = \frac{\pi}{128} \times 1.0 \times 10^6 \frac{\text{N}}{\text{m}^2} \times (0.50)^4 \text{ mm}^4 \times \frac{\text{s}}{880 \text{ mm}^3} \times \frac{1}{1 \text{ m}} \times \frac{\text{m}}{10^3 \text{ mm}}$$

$$\mu = 1.74 \times 10^{-3} \text{ N} \cdot \text{s} / \text{m}^2 \leftarrow \mu$$

Check the Reynolds number. Assume the fluid density is similar to that of water,  $999 \text{ kg/m}^3$ . Then

$$\bar{V} = \frac{Q}{A} = \frac{4Q}{\pi D^2} = \frac{4}{\pi} \times 880 \frac{\text{mm}^3}{\text{s}} \times \frac{1}{(0.50)^2 \text{ mm}^2} \times \frac{\text{m}}{10^3 \text{ mm}} = 4.48 \text{ m/s}$$

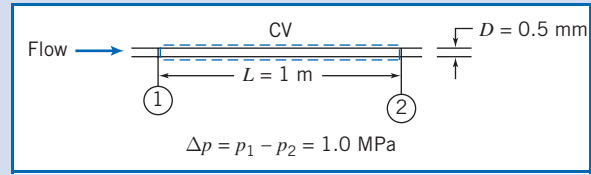
and

$$Re = \frac{\rho \bar{V} D}{\mu} = 999 \frac{\text{kg}}{\text{m}^3} \times 4.48 \frac{\text{m}}{\text{s}} \times 0.50 \text{ mm}$$

$$\times \frac{\text{m}^2}{1.74 \times 10^{-3} \text{ N} \cdot \text{s}} \times \frac{\text{m}}{10^3 \text{ mm}} \times \frac{\text{N} \cdot \text{s}^2}{\text{kg} \cdot \text{m}}$$

$$Re = 1290$$

Consequently, since  $Re < 2300$ , the flow is laminar.



This problem is a little oversimplified. To design a capillary viscometer the entrance length, liquid temperature, and kinetic energy of the flowing liquid would all need to be considered.

## Part B Flow in Pipes and Ducts

In this section we will be interested in determining the factors that affect the pressure in an incompressible fluid as it flows in a pipe or duct (we will refer to “pipe” but imply “duct,” too). If we ignore friction for a moment (and assume steady flow and consider a streamline in the flow), the Bernoulli equation from Chapter 6 applies,

$$\frac{p}{\rho} + \frac{V^2}{2} + gz = \text{constant} \quad (6.8)$$

From this equation we can see what *tends* to lead to a *pressure decrease* along the streamline in this frictionless flow: a *reduction of area* at some point in the pipe (causing an increase in the velocity  $V$ ), or the pipe having a *positive incline* (so  $z$  increases). Conversely, the pressure will tend to increase if the flow area is increased or the pipe slopes downward. We say “tends to” because one factor may counteract another; for example, we may have a downward sloping pipe (tending to increase pressure) with a reduction in diameter (tending to decrease pressure).

In reality, flows in pipes and ducts experience significant friction and are often turbulent, so the Bernoulli equation does not apply (it doesn't even make sense to use  $V$ ; instead we will use  $\bar{V}$ , to represent the average velocity at a section along the pipe). We will learn that, in effect, friction effects lead to a continual reduction in the value of the Bernoulli constant of Eq. 6.8 (this represents a “loss” of mechanical energy). We have already seen that, in contrast to the Bernoulli equation, for laminar flow there is a pressure drop even for a horizontal, constant diameter pipe; in this section we will see that turbulent flows experience an even larger pressure drop. We will need to replace the Bernoulli equation with an energy equation that incorporates the effects of friction.

In summary, we can state that *three* factors tend to reduce the pressure in a pipe flow: a decrease in pipe area, an upward slope, and friction. For now we will focus on pressure loss due to friction and so will analyze pipes that are of constant area and that are horizontal.

We have already seen in the previous section that for laminar flow we can theoretically deduce the pressure drop. Rearranging Eq. 8.13c to solve for the pressure drop  $\Delta p$ ,

$$\Delta p = \frac{128\mu L Q}{\pi D^4}$$

We would like to develop a similar expression that applies for turbulent flows, but we will see that this is not possible analytically; instead, we will develop expressions based on a combination of theoretical and experimental approaches. Before proceeding, we note that it is conventional to break losses due to friction into two categories: *major losses*, which are losses due to friction in the constant-area sections of the pipe; and *minor losses* (sometimes larger than “major” losses), which are losses due to valves, elbows, and so on (and we will treat the pressure drop at the entrance region as a minor loss term).

Since circular pipes are most common in engineering applications, the basic analysis will be performed for circular geometries. The results can be extended to other geometries by introducing the hydraulic diameter, which is treated in Section 8.7. (Open channel flows will be treated in Chapter 11, and compressible flow in ducts will be treated in Chapter 13.)

## Shear Stress Distribution in Fully Developed Pipe Flow 8.4

We consider again fully developed flow in a horizontal circular pipe, except now we may have laminar or turbulent flow. In Section 8.3 we showed that a force balance between friction and pressure forces leads to Eq. 8.10:

$$\tau_{rx} = \frac{r}{2} \left( \frac{\partial p}{\partial x} \right) + \frac{c_1}{r} \quad (8.10)$$

Because we cannot have infinite stress at the centerline, the constant of integration  $c_1$  must be zero, so

$$\tau_{rx} = \frac{r}{2} \frac{\partial p}{\partial x} \quad (8.15)$$

Equation 8.15 indicates that *for both laminar and turbulent fully developed flows the shear stress varies linearly across the pipe*, from zero at the centerline to a maximum at

the pipe wall. The stress on the wall,  $\tau_w$  (equal and opposite to the stress in the fluid at the wall), is given by

$$\tau_w = -[\tau_{rx}]_{r=R} = -\frac{R}{2} \frac{\partial p}{\partial x} \quad (8.16)$$

For *laminar* flow we used our familiar stress equation  $\tau_{rx} = \mu \, du/dr$  in Eq. 8.15 to eventually obtain the laminar velocity distribution. This led to a set of usable equations, Eqs. 8.13, for obtaining various flow characteristics; e.g., Eq. 8.13c gave a relationship for the flow rate  $Q$ , a result first obtained experimentally by Jean Louis Poiseuille, a French physician, and independently by Gotthilf H. L. Hagen, a German engineer, in the 1850s [2].

Unfortunately there is no equivalent stress equation for *turbulent* flow, so we cannot replicate the laminar flow analysis to derive turbulent equivalents of Eqs. 8.13. All we can do in this section is indicate some classic semi-empirical results [3].

As we discussed in Section 2.6, and illustrated in Fig. 2.17, turbulent flow is represented at each point by the time-mean velocity  $\bar{u}$  plus (for a two-dimensional flow) randomly fluctuating velocity components  $u'$  and  $v'$  in the  $x$  and  $y$  directions (in this context  $y$  is the distance inwards from the pipe wall). These components continuously transfer momentum between adjacent fluid layers, tending to reduce any velocity gradient present. This effect shows up as an apparent stress, first introduced by Osborne Reynolds, and called the *Reynolds stress*.<sup>1</sup> This stress is given by  $-\rho \overline{u'v'}$ , where the overbar indicates a time average. Hence, we find

$$\tau = \tau_{\text{lam}} + \tau_{\text{turb}} = \mu \frac{d\bar{u}}{dy} - \rho \overline{u'v'} \quad (8.17)$$

Do not misunderstand the minus sign in Eq. 8.17—it turns out that  $u'$  and  $v'$  are negatively correlated, so that  $\tau_{\text{turb}} = -\rho \overline{u'v'}$  is positive. In Fig. 8.8, experimental measurements of the Reynolds stress for fully developed turbulent pipe flow at two Reynolds numbers are presented;  $Re_U = UD/\nu$ , where  $U$  is the centerline velocity. The turbulent shear stress has been nondimensionalized with the wall shear stress. Recall that Eq. 8.15 showed that the shear stress in the fluid varies linearly from  $\tau_w$  at the pipe wall ( $y/R \rightarrow 0$ ) to zero at the centerline ( $y/R = 1$ ); from Fig. 8.8 we see that the Reynolds stress has almost the same trend, so that the friction is almost all due to Reynolds stress. What Fig. 8.8 *doesn't* show is that close to the wall ( $y/R \rightarrow 0$ ) the Reynolds stress drops to zero. This is because the no-slip condition holds, so not

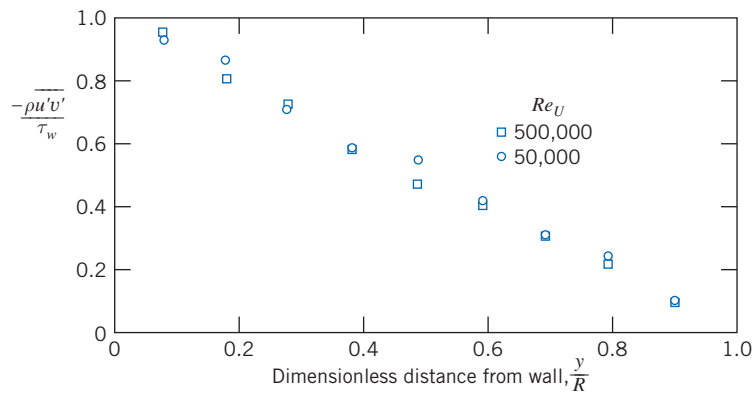


**Fig. 8.8** Turbulent shear stress (Reynolds stress) for fully developed turbulent flow in a pipe. (Data from Laufer [5].)

<sup>1</sup>The Reynolds stress terms arise from consideration of the complete equations of motion for turbulent flow [4].

only does the mean velocity  $\bar{u} \rightarrow 0$ , but also the fluctuating velocity components  $u'$  and  $v' \rightarrow 0$  (the wall tends to suppress the fluctuations). Hence, the turbulent stress,  $\tau_{\text{turb}} = -\rho \overline{u'v'} \rightarrow 0$ , as we approach the wall, and is zero at the wall. Since the Reynolds stress is zero at the wall, Eq. 8.17 shows that the wall shear is given by  $\tau_w = \mu(d\bar{u}/dy)_{y=0}$ . In the region very close to the wall, called the *wall layer*, viscous shear is dominant. In the region between the wall layer and the central portion of the pipe both viscous and turbulent shear are important.

## Turbulent Velocity Profiles in Fully Developed Pipe Flow 8.5

Except for flows of very viscous fluids in small diameter ducts, internal flows generally are turbulent. As noted in the discussion of shear stress distribution in fully developed pipe flow (Section 8.4), in turbulent flow there is no universal relationship between the stress field and the mean velocity field. Thus, for turbulent flows we are forced to rely on experimental data.

Dividing Eq. 8.17 by  $\rho$  gives

$$\frac{\tau}{\rho} = \nu \frac{d\bar{u}}{dy} - \overline{u'v'} \quad (8.18)$$

The term  $\tau/\rho$  arises frequently in the consideration of turbulent flows; it has dimensions of velocity squared. In particular, the quantity  $(\tau_w/\rho)^{1/2}$  is called the *friction velocity* and is denoted by the symbol  $u_*$ . It is a constant for a given flow.

The velocity profile for fully developed turbulent flow through a smooth pipe is shown in Fig. 8.9. The plot is semilogarithmic;  $\bar{u}/u_*$  is plotted against  $\log(yu_*/\nu)$ . The nondimensional parameters  $\bar{u}/u_*$  and  $yu_*/\nu$  arise from dimensional analysis if one reasons that the velocity in the neighborhood of the wall is determined by the conditions at the wall, the fluid properties, and the distance from the wall. It is simply fortuitous that the dimensionless plot of Fig. 8.9 gives a fairly accurate representation of the velocity profile in a pipe away from the wall; note the small deviations in the region of the pipe centerline.

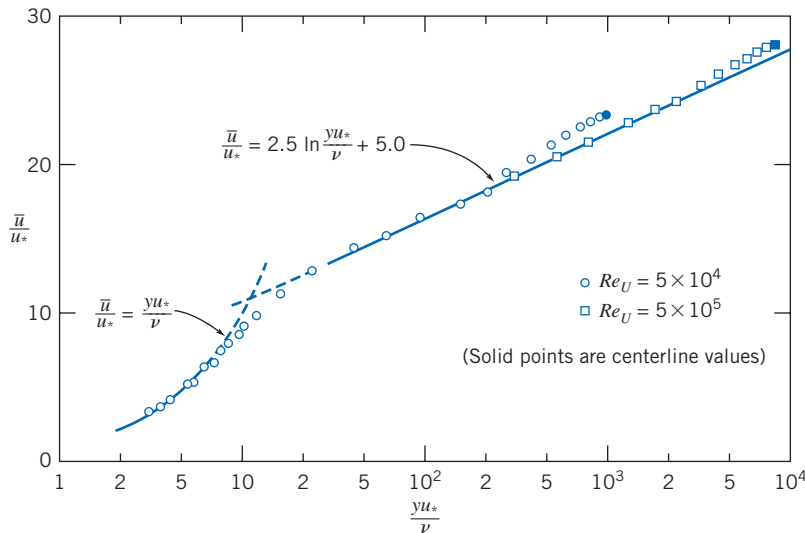


**Fig. 8.9** Turbulent velocity profile for fully developed flow in a smooth pipe. (Data from Laufer [5].)

### VIDEO

*The Glen Canyon Dam: A Turbulent Pipe Flow.*

In the region very close to the wall where viscous shear is dominant, the mean velocity profile follows the linear viscous relation

$$u^+ = \frac{\bar{u}}{u_*} = \frac{yu_*}{\nu} = y^+ \quad (8.19)$$

where  $y$  is distance measured from the wall ( $y = R - r$ ;  $R$  is the pipe radius), and  $\bar{u}$  is mean velocity. Equation 8.19 is valid for  $0 \leq y^+ \leq 5-7$ ; this region is called the *viscous sublayer*.

For values of  $yu_*/\nu > 30$ , the data are quite well represented by the semilogarithmic curve-fit equation

$$\frac{\bar{u}}{u_*} = 2.5 \ln \frac{yu_*}{\nu} + 5.0 \quad (8.20)$$

In this region both viscous and turbulent shear are important (although turbulent shear is expected to be significantly larger). There is considerable scatter in the numerical constants of Eq. 8.20; the values given represent averages over many experiments [6]. The region between  $y^+ = 5-7$  and  $y^+ = 30$  is referred to as the *transition region*, or *buffer layer*.

If Eq. 8.20 is evaluated at the centerline ( $y = R$  and  $u = U$ ) and the general expression of Eq. 8.20 is subtracted from the equation evaluated at the centerline, we obtain

$$\frac{U - \bar{u}}{u_*} = 2.5 \ln \frac{R}{y} \quad (8.21)$$

where  $U$  is the centerline velocity. Equation 8.21, referred to as the *defect law*, shows that the velocity defect (and hence the general shape of the velocity profile in the neighborhood of the centerline) is a function of the distance ratio only and does not depend on the viscosity of the fluid.

The velocity profile for turbulent flow through a smooth pipe may also be approximated by the empirical *power-law* equation

$$\frac{\bar{u}}{U} = \left(\frac{y}{R}\right)^{1/n} = \left(1 - \frac{r}{R}\right)^{1/n} \quad (8.22)$$

where the exponent,  $n$ , varies with the Reynolds number. In Fig. 8.10 the data of Laufer [5] are shown on a plot of  $\ln y/R$  versus  $\ln \bar{u}/U$ . If the power-law profile were an accurate representation of the data, all data points would fall on a straight line of slope  $n$ . Clearly the data for  $Re_U = 5 \times 10^4$  deviate from the best-fit straight line in the neighborhood of the wall.

Hence the power-law profile is not applicable close to the wall ( $y/R < 0.04$ ). Since the velocity is low in this region, the error in calculating integral quantities such as mass, momentum, and energy fluxes at a section is relatively small. The power-law profile gives an infinite velocity gradient at the wall and hence cannot be used in calculations of wall shear stress. Although the profile fits the data close to the centerline, it fails to give zero slope there. Despite these shortcomings, the power-law profile is found to give adequate results in many calculations.

Data from Hinze [7] suggest that the variation of power-law exponent  $n$  with Reynolds number (based on pipe diameter,  $D$ , and centerline velocity,  $U$ ) for fully developed flow in smooth pipes is given by

$$n = -1.7 + 1.8 \log Re_U \quad (8.23)$$

for  $Re_U > 2 \times 10^4$ .

#### VIDEO

Computer Simulation: Turbulent Channel Flow 1.

#### VIDEO

Computer Simulation: Turbulent Channel Flow 2.

#### VIDEO

Computer Simulation: Turbulent Channel Flow 3.



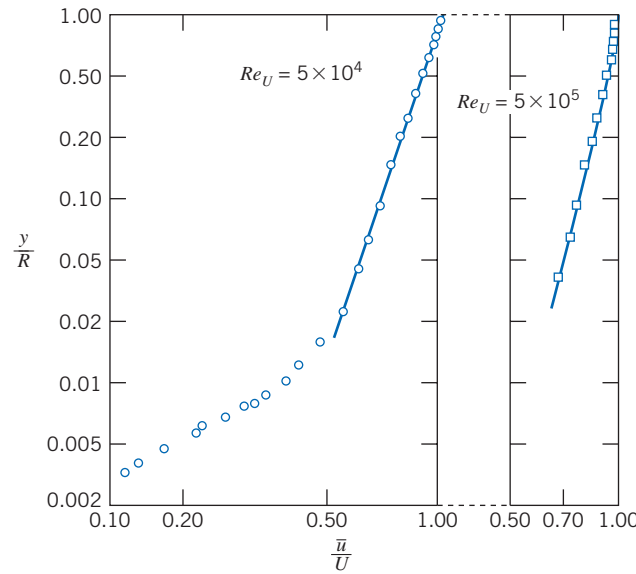


**Fig. 8.10** Power-law velocity profiles for fully developed turbulent flow in a smooth pipe. (Data from Laufer [5].)

Since the average velocity is  $\bar{V} = Q/A$ , and

$$Q = \int_A \vec{V} \cdot d\vec{A}$$

the ratio of the average velocity to the centerline velocity may be calculated for the power-law profiles of Eq. 8.22 assuming the profiles to be valid from wall to centerline. The result is

$$\frac{\bar{V}}{U} = \frac{2n^2}{(n+1)(2n+1)} \quad (8.24)$$

From Eq. 8.24, we see that as  $n$  increases (with increasing Reynolds number) the ratio of the average velocity to the centerline velocity increases; with increasing Reynolds number the velocity profile becomes more blunt or “fuller” (for  $n = 6$ ,  $\bar{V}/U = 0.79$  and for  $n = 10$ ,  $\bar{V}/U = 0.87$ ). As a representative value, 7 often is used for the exponent; this gives rise to the term “a one-seventh power profile” for fully developed turbulent flow:

$$\frac{\bar{u}}{U} = \left(\frac{y}{R}\right)^{1/7} = \left(1 - \frac{r}{R}\right)^{1/7}$$

Velocity profiles for  $n = 6$  and  $n = 10$  are shown in Fig. 8.11. The parabolic profile for fully developed laminar flow is included for comparison. It is clear that the turbulent profile has a much steeper slope near the wall. This is consistent with our discussion leading to Eq. 8.17—the fluctuating velocity components  $u'$  and  $v'$  continuously transfer momentum between adjacent fluid layers, tending to reduce the velocity gradient.

## Energy Considerations in Pipe Flow 8.6

We have so far used the momentum and conservation of mass equations, in control volume form, to discuss viscous flow. It is obvious that viscous effects will have an

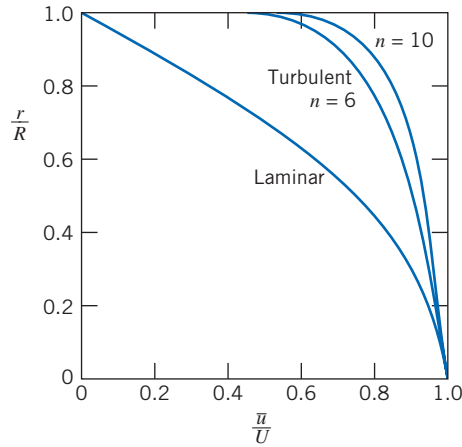


**Fig. 8.11** Velocity profiles for fully developed pipe flow.

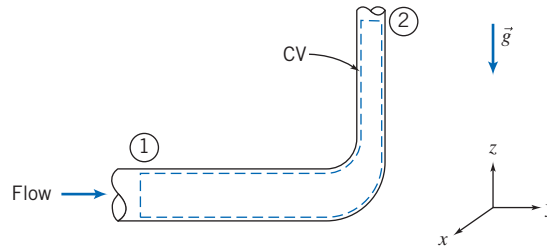


**Fig. 8.12** Control volume and coordinates for energy analysis of flow through a 90° reducing elbow.

important effect on energy considerations. In Section 6.5 we discussed the Energy Grade Line (EGL),

$$EGL = \frac{p}{\rho g} + \frac{V^2}{2g} + z \quad (6.16b)$$

and saw that this is a measure of the total mechanical energy (“pressure,” kinetic and potential, per unit mass) in a flow. We can expect that instead of being constant (which it was for inviscid flow), the EGL will continuously decrease in the direction of flow as friction “eats” the mechanical energy (Examples 8.9 and 8.10 have sketches of such EGL—and HGL—curves; you may wish to preview them). We can now consider the energy equation (the first law of thermodynamics) to obtain information on the effects of friction.

Consider, for example, steady flow through the piping system, including a reducing elbow, shown in Fig. 8.12. The control volume boundaries are shown as dashed lines. They are normal to the flow at sections ① and ② and coincide with the inside surface of the pipe wall elsewhere.

Basic equation:

$$\dot{Q} - \dot{W}_s - \dot{W}_{\text{shear}} - \dot{W}_{\text{other}} = \frac{\partial}{\partial t} \int_{CV} e \rho dV + \int_{CS} (e + pv) \rho \vec{V} \cdot d\vec{A} \quad (4.56)$$

$$e = u + \frac{V^2}{2} + gz$$

- Assumptions: (1)  $\dot{W}_s = 0$ ,  $\dot{W}_{\text{other}} = 0$ .  
 (2)  $\dot{W}_{\text{shear}} = 0$  (although shear stresses are present at the walls of the elbow, the velocities are zero there, so there is no possibility of work).  
 (3) Steady flow.  
 (4) Incompressible flow.  
 (5) Internal energy and pressure uniform across sections ① and ②.

Under these assumptions the energy equation reduces to

$$\begin{aligned} \dot{Q} = \dot{m}(u_2 - u_1) + \dot{m} \left( \frac{p_2}{\rho} - \frac{p_1}{\rho} \right) + \dot{m}g(z_2 - z_1) \\ + \int_{A_2} \frac{V_2^2}{2} \rho V_2 dA_2 - \int_{A_1} \frac{V_1^2}{2} \rho V_1 dA_1 \end{aligned} \quad (8.25)$$

Note that we have *not* assumed the velocity to be uniform at sections ① and ②, since we know that for viscous flows the velocity at a cross-section cannot be uniform. However, it is convenient to introduce the average velocity into Eq. 8.25 so that we can eliminate the integrals. To do this, we define a kinetic energy coefficient.

### Kinetic Energy Coefficient

The *kinetic energy coefficient*,  $\alpha$ , is defined such that

$$\int_A \frac{V^2}{2} \rho V dA = \alpha \int_A \frac{\bar{V}^2}{2} \rho V dA = \alpha \dot{m} \frac{\bar{V}^2}{2} \quad (8.26a)$$

or

$$\alpha = \frac{\int_A \rho V^3 dA}{\dot{m} \bar{V}^2} \quad (8.26b)$$

We can think of  $\alpha$  as a correction factor that allows us to use the average velocity  $\bar{V}$  in the energy equation to compute the kinetic energy at a cross section.

For laminar flow in a pipe (velocity profile given by Eq. 8.12),  $\alpha = 2.0$ .

In turbulent pipe flow, the velocity profile is quite flat, as shown in Fig. 8.11. We can use Eq. 8.26b together with Eqs. 8.22 and 8.24 to determine  $\alpha$ . Substituting the power-law velocity profile of Eq. 8.22 into Eq. 8.26b, we obtain

$$\alpha = \left( \frac{U}{\bar{V}} \right)^3 \frac{2n^2}{(3+n)(3+2n)} \quad (8.27)$$

Equation 8.24 gives  $\bar{V}/U$  as a function of the power-law exponent  $n$ ; combining this with Eq. 8.27 leads to a fairly complicated expression in  $n$ . The overall result is that in the realistic range of  $n$ , from  $n = 6$  to  $n = 10$  for high Reynolds numbers,  $\alpha$  varies from 1.08 to 1.03; for the one-seventh power profile ( $n = 7$ ),  $\alpha = 1.06$ . Because  $\alpha$  is reasonably close to unity for high Reynolds numbers, and because the change in kinetic energy is usually small compared with the dominant terms in the energy equation, we shall almost always use the approximation  $\alpha = 1$  in our pipe flow calculations.

### Head Loss

Using the definition of  $\alpha$ , the energy equation (Eq. 8.25) can be written

$$\dot{Q} = \dot{m}(u_2 - u_1) + \dot{m} \left( \frac{p_2}{\rho} - \frac{p_1}{\rho} \right) + \dot{m}g(z_2 - z_1) + \dot{m} \left( \frac{\alpha_2 \bar{V}_2^2}{2} - \frac{\alpha_1 \bar{V}_1^2}{2} \right)$$

Dividing by the mass flow rate gives

$$\frac{\delta Q}{dm} = u_2 - u_1 + \frac{p_2}{\rho} - \frac{p_1}{\rho} + gz_2 - gz_1 + \frac{\alpha_2 \bar{V}_2^2}{2} - \frac{\alpha_1 \bar{V}_1^2}{2}$$

Rearranging this equation, we write

$$\left( \frac{p_1}{\rho} + \alpha_1 \frac{\bar{V}_1^2}{2} + gz_1 \right) - \left( \frac{p_2}{\rho} + \alpha_2 \frac{\bar{V}_2^2}{2} + gz_2 \right) = (u_2 - u_1) - \frac{\delta Q}{dm} \quad (8.28)$$

In Eq. 8.28, the term

$$\left( \frac{p}{\rho} + \alpha \frac{\bar{V}^2}{2} + gz \right)$$

represents the mechanical energy per unit mass at a cross section. (Compare it to the EGL expression, Eq. 6.16b, for computing “mechanical” energy, which we discussed at the beginning of this section. The differences are that in the EGL we divide by  $g$  to obtain the EGL in units of feet or meters, and here  $\alpha \bar{V}^2$  allows for the fact that in a pipe flow we have a velocity profile, not a uniform flow.) The term  $u_2 - u_1 - \delta Q/dm$  is equal to the difference in mechanical energy per unit mass between sections ① and ②. It represents the (irreversible) conversion of mechanical energy at section ① to unwanted thermal energy ( $u_2 - u_1$ ) and loss of energy via heat transfer ( $-\delta Q/dm$ ). We identify this group of terms as the total energy loss per unit mass and designate it by the symbol  $h_{lr}$ . Then

$$\left( \frac{p_1}{\rho} + \alpha_1 \frac{\bar{V}_1^2}{2} + gz_1 \right) - \left( \frac{p_2}{\rho} + \alpha_2 \frac{\bar{V}_2^2}{2} + gz_2 \right) = h_{lr} \quad (8.29)$$

The dimensions of energy per unit mass  $FL/M$  are equivalent to dimensions of  $L^2/t^2$ . Equation 8.29 is one of the most important and useful equations in fluid mechanics. It enables us to compute the loss of mechanical energy caused by friction between two sections of a pipe. We recall our discussion at the beginning of Part B, where we discussed what would cause the pressure to change. We hypothesized a frictionless flow (i.e., described by the Bernoulli equation, or Eq. 8.29 with  $\alpha = 1$  and  $h_{lr} = 0$ ) so that the pressure could only change if the velocity changed (if the pipe had a change in diameter), or if the potential changed (if the pipe was not horizontal). Now, with friction, Eq. 8.29 indicates that the pressure will change even for a constant-area horizontal pipe—mechanical energy will be continuously changed into thermal energy.

As the empirical science of hydraulics developed during the 19th century, it was common practice to express the energy balance in terms of energy per unit *weight* of flowing liquid (e.g., water) rather than energy per unit *mass*, as in Eq. 8.29. When Eq. 8.29 is divided by the acceleration of gravity,  $g$ , we obtain

$$\left( \frac{p_1}{\rho g} + \alpha_1 \frac{\bar{V}_1^2}{2g} + z_1 \right) - \left( \frac{p_2}{\rho g} + \alpha_2 \frac{\bar{V}_2^2}{2g} + z_2 \right) = \frac{h_{lr}}{g} = H_{lr} \quad (8.30)$$

Each term in Eq. 8.30 has dimensions of energy per unit weight of flowing fluid. Then the net dimensions of  $H_{lr} = h_{lr}/g$  are  $(L^2/t^2)(t^2/L) = L$ , or feet of flowing liquid. Since the term head loss is in common use, we shall use it when referring to either  $H_{lr}$  (with dimensions of energy per unit weight or length) or  $h_{lr} = gH_{lr}$  (with dimensions of energy per unit mass).

Equation 8.29 (or Eq. 8.30) can be used to calculate the pressure difference between any two points in a piping system, provided the head loss,  $h_{lr}$  (or  $H_{lr}$ ), can be determined. We shall consider calculation of head loss in the next section.

## Calculation of Head Loss 8.7

Total head loss,  $h_{lt}$ , is regarded as the sum of major losses,  $h_l$ , due to frictional effects in fully developed flow in constant-area tubes, and minor losses,  $h_{lm}$ , resulting from entrances, fittings, area changes, and so on. Consequently, we consider the major and minor losses separately.

### Major Losses: Friction Factor

The energy balance, expressed by Eq. 8.29, can be used to evaluate the major head loss. For fully developed flow through a constant-area pipe,  $h_{lm} = 0$ , and  $\alpha_1 (\bar{V}_1^2/2) = \alpha_2 (\bar{V}_2^2/2)$ ; Eq. 8.29 reduces to

$$\frac{p_1 - p_2}{\rho} = g(z_2 - z_1) + h_l \quad (8.31)$$

If the pipe is horizontal, then  $z_2 = z_1$  and

$$\frac{p_1 - p_2}{\rho} = \frac{\Delta p}{\rho} = h_l \quad (8.32)$$

Thus the major head loss can be expressed as the pressure loss for fully developed flow through a horizontal pipe of constant area.

Since head loss represents the energy converted by frictional effects from mechanical to thermal energy, head loss for fully developed flow in a constant-area duct depends only on the details of the flow through the duct. Head loss is independent of pipe orientation.

#### a. Laminar Flow

In laminar flow, we saw in Section 8.3 that the pressure drop may be computed analytically for fully developed flow in a horizontal pipe. Thus, from Eq. 8.13c,

$$\Delta p = \frac{128\mu L Q}{\pi D^4} = \frac{128\mu L \bar{V}(\pi D^2/4)}{\pi D^4} = 32 \frac{L}{D} \frac{\mu \bar{V}}{D}$$

Substituting in Eq. 8.32 gives

$$h_l = 32 \frac{L}{D} \frac{\mu \bar{V}}{\rho D} = \frac{L}{D} \frac{\bar{V}^2}{2} \left( 64 \frac{\mu}{\rho \bar{V} D} \right) = \left( \frac{64}{Re} \right) \frac{L}{D} \frac{\bar{V}^2}{2} \quad (8.33)$$

(We shall see the reason for writing  $h_l$  in this form shortly.)

#### b. Turbulent Flow

In turbulent flow we cannot evaluate the pressure drop analytically; we must resort to experimental results and use dimensional analysis to correlate the experimental data. In fully developed turbulent flow, the pressure drop,  $\Delta p$ , caused by friction in a horizontal constant-area pipe is known to depend on pipe diameter,  $D$ , pipe length,  $L$ , pipe roughness,  $e$ , average flow velocity,  $\bar{V}$ , fluid density,  $\rho$ , and fluid viscosity,  $\mu$ . In functional form

$$\Delta p = \Delta p(D, L, e, \bar{V}, \rho, \mu)$$

We applied dimensional analysis to this problem in Example 7.2. The results were a correlation of the form

$$\frac{\Delta p}{\rho \bar{V}^2} = f\left(\frac{\mu}{\rho \bar{V} D}, \frac{L}{D}, \frac{e}{D}\right)$$

We recognize that  $\mu/\rho \bar{V} D = 1/Re$ , so we could just as well write

$$\frac{\Delta p}{\rho \bar{V}^2} = \phi\left(Re, \frac{L}{D}, \frac{e}{D}\right)$$

Substituting from Eq. 8.32, we see that

$$\frac{h_l}{\bar{V}^2} = \phi\left(Re, \frac{L}{D}, \frac{e}{D}\right)$$

Although dimensional analysis predicts the functional relationship, we must obtain actual values experimentally.

Experiments show that the nondimensional head loss is directly proportional to  $L/D$ . Hence we can write

$$\frac{h_l}{\bar{V}^2} = \frac{L}{D} \phi_1\left(Re, \frac{e}{D}\right)$$

Since the function,  $\phi_1$ , is still undetermined, it is permissible to introduce a constant into the left side of the above equation. By convention the number  $\frac{1}{2}$  is introduced into the denominator so that the left side of the equation is the ratio of the head loss to the kinetic energy per unit mass of flow. Then

$$\frac{h_l}{\frac{1}{2} \bar{V}^2} = \frac{L}{D} \phi_2\left(Re, \frac{e}{D}\right)$$

The unknown function,  $\phi_2(Re, e/D)$ , is defined as the *friction factor*,  $f$ ,

$$f \equiv \phi_2\left(Re, \frac{e}{D}\right)$$

and

$$h_l = f \frac{L}{D} \frac{\bar{V}^2}{2} \quad (8.34)$$

or

$$H_l = f \frac{L}{D} \frac{\bar{V}^2}{2g} \quad (8.35)$$

The friction factor<sup>2</sup> is determined experimentally. The results, published by L. F. Moody [8], are shown in Fig. 8.13.

To determine head loss for fully developed flow with known conditions, the Reynolds number is evaluated first. Roughness,  $e$ , is obtained from Table 8.1. Then the friction factor,  $f$ , can be read from the appropriate curve in Fig. 8.13, at the known values of  $Re$  and  $e/D$ . Finally, head loss can be found using Eq. 8.34 or Eq. 8.35.

<sup>2</sup>The friction factor defined by Eq. 8.34 is the *Darcy friction factor*. The *Fanning friction factor*, less frequently used, is defined in Problem 8.95.



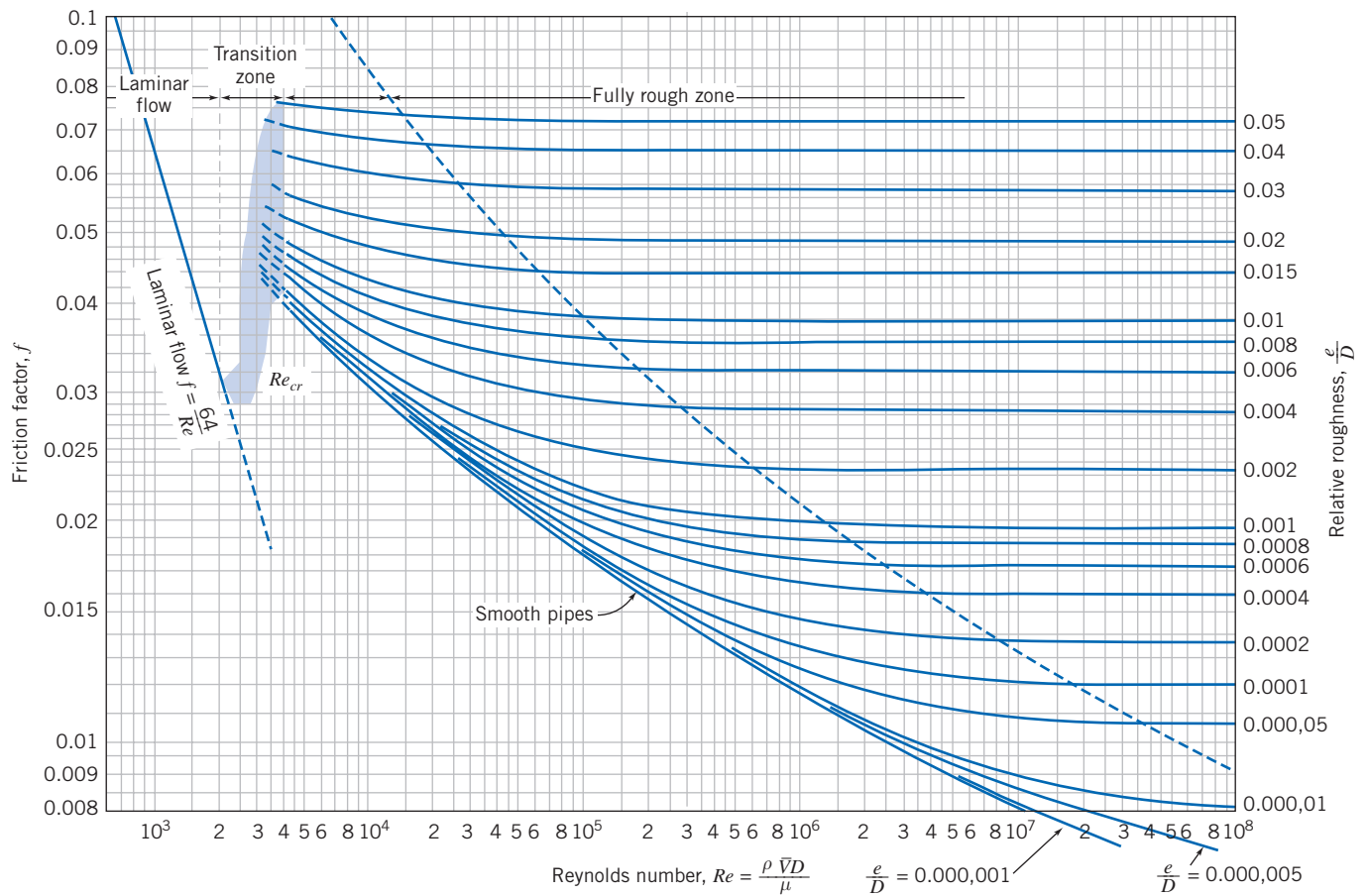


**Fig. 8.13** Friction factor for fully developed flow in circular pipes. (Data from Moody [8], used by permission.)

**Table 8.1**

**Roughness for Pipes of Common Engineering Materials**

Pipe	Roughness, $e$	
	Feet	Millimeters
Riveted steel	0.003–0.03	0.9–9
Concrete	0.001–0.01	0.3–3
Wood stave	0.0006–0.003	0.2–0.9
Cast iron	0.00085	0.26
Galvanized iron	0.0005	0.15
Asphalted cast iron	0.0004	0.12
Commercial steel or wrought iron	0.00015	0.046
Drawn tubing	0.000005	0.0015

Source: Data from Moody [8].

Several features of Fig. 8.13 require some discussion. The friction factor for laminar flow may be obtained by comparing Eqs. 8.33 and 8.34:

$$h_f = \left( \frac{64}{Re} \right) \frac{L}{D} \frac{\bar{V}^2}{2} = f \frac{L}{D} \frac{\bar{V}^2}{2}$$

Consequently, for laminar flow

$$f_{\text{laminar}} = \frac{64}{Re} \quad (8.36)$$

Thus, in laminar flow, the friction factor is a function of Reynolds number only; it is independent of roughness. Although we took no notice of roughness in deriving Eq. 8.33, experimental results verify that the friction factor is a function only of Reynolds number in laminar flow.

The Reynolds number in a pipe may be changed most easily by varying the average flow velocity. If the flow in a pipe is originally laminar, increasing the velocity until the critical Reynolds number is reached causes transition to occur; the laminar flow gives way to turbulent flow. The effect of transition on the velocity profile was discussed in Section 8.5. Figure 8.11 shows that the velocity gradient at the tube wall is much larger for turbulent flow than for laminar flow. This change in velocity profile causes the wall shear stress to increase sharply, with the same effect on the friction factor.

As the Reynolds number is increased above the transition value, the velocity profile continues to become fuller, as noted in Section 8.5. For values of relative roughness  $e/D \leq 0.001$ , the friction factor at first tends to follow the smooth pipe curve, along which friction factor is a function of Reynolds number only. However, as the Reynolds number increases, the velocity profile becomes still fuller. The size of the thin viscous sublayer near the tube wall decreases. As roughness elements begin to poke through this layer, the effect of roughness becomes important, and the friction factor becomes a function of both the Reynolds number *and* the relative roughness.

At very large Reynolds number, most of the roughness elements on the tube wall protrude through the viscous sublayer; the drag and, hence, the pressure loss, depend only on the size of the roughness elements. This is termed the “fully rough” flow regime; the friction factor depends only on  $e/D$  in this regime.

For values of relative roughness  $e/D \geq 0.001$ , as the Reynolds number is increased above the transition value, the friction factor is greater than the smooth pipe value. As was the case for lower values of  $e/D$ , the value of Reynolds number at which the flow regime becomes fully rough decreases with increasing relative roughness.

To summarize the preceding discussion, we see that as Reynolds number is increased, the friction factor decreases as long as the flow remains laminar. At transition,  $f$  increases sharply. In the turbulent flow regime, the friction factor decreases gradually and finally levels out at a constant value for large Reynolds number.

Bear in mind that the actual loss of energy is  $h_l$  (Eq. 8.34), which is proportional to  $f$  and  $\bar{V}^2$ . Hence, for laminar flow  $h_l \propto \bar{V}$  (because  $f = 64/Re$ , and  $Re \propto \bar{V}$ ); for the transition region there is a sudden increase in  $h_l$ ; for the fully rough zone  $h_l \propto \bar{V}^2$  (because  $f \approx \text{const.}$ ), and for the rest of the turbulent region  $h_l$  increases at a rate somewhere between  $\bar{V}$  and  $\bar{V}^2$ . We conclude that the head loss *always* increases with flow rate, and more rapidly when the flow is turbulent.

To avoid having to use a graphical method for obtaining  $f$  for turbulent flows, various mathematical expressions have been fitted to the data. The most widely used formula for friction factor is from Colebrook [9],

$$\frac{1}{\sqrt{f}} = -2.0 \log \left( \frac{e/D}{3.7} + \frac{2.51}{Re\sqrt{f}} \right) \quad (8.37)$$

Equation 8.37 is implicit in  $f$ , but these days most scientific calculators have an equation-solving feature that can be easily used to find  $f$  for a given roughness ratio  $e/D$  and Reynolds number  $Re$  (and some calculators have the Colebrook equation itself built in!). Certainly a spreadsheet such as *Excel*, or other mathematical computer

applications, can also be used (there is an *Excel* add-in for computing  $f$  for laminar and turbulent flows available on the Web site). Even without using these automated approaches, Eq. 8.37 is not difficult to solve for  $f$ —all we need to do is iterate. Equation 8.37 is quite stable—almost any initial guess value for  $f$  in the right side will, after very few iterations, lead to a converged value for  $f$  to three significant figures. From Fig. 8.13, we can see that for turbulent flows  $f < 0.1$ ; hence  $f = 0.1$  would make a good initial value. Another strategy is to use Fig. 8.13 to obtain a good first estimate; then usually one iteration using Eq. 8.37 yields a good value for  $f$ . As an alternative, Haaland [10] developed the following equation,

$$\frac{1}{\sqrt{f}} = -1.8 \log \left[ \left( \frac{e/D}{3.7} \right)^{1.11} + \frac{6.9}{Re} \right]$$

as an approximation to the Colebrook equation; for  $Re > 3000$ , it gives results within about 2 percent of the Colebrook equation, without the need to iterate.

For turbulent flow in smooth pipes, the Blasius correlation, valid for  $Re \leq 10^5$ , is

$$f = \frac{0.316}{Re^{0.25}} \quad (8.38)$$

When this relation is combined with the expression for wall shear stress (Eq. 8.16), the expression for head loss (Eq. 8.32), and the definition of friction factor (Eq. 8.34), a useful expression for the wall shear stress is obtained as

$$\tau_w = 0.0332 \rho \bar{V}^2 \left( \frac{\nu}{R\bar{V}} \right)^{0.25} \quad (8.39)$$

This equation will be used later in our study of turbulent boundary-layer flow over a flat plate (Chapter 9).

All of the  $e$  values given in Table 8.1 are for new pipes, in relatively good condition. Over long periods of service, corrosion takes place and, particularly in hard water areas, lime deposits and rust scale form on pipe walls. Corrosion can weaken pipes, eventually leading to failure. Deposit formation increases wall roughness appreciably, and also decreases the effective diameter. These factors combine to cause  $e/D$  to increase by factors of 5 to 10 for old pipes (see Problem 10.63). An example is shown in Fig. 8.14.

Curves presented in Fig. 8.13 represent average values for data obtained from numerous experiments. The curves should be considered accurate within approximately  $\pm 10$  percent, which is sufficient for many engineering analyses. If more accuracy is needed, actual test data should be used.

## Minor Losses

The flow in a piping system may be required to pass through a variety of fittings, bends, or abrupt changes in area. Additional head losses are encountered, primarily as a result of flow separation. (Energy eventually is dissipated by violent mixing in the separated zones.) These losses will be minor (hence the term *minor losses*) if the piping system includes long lengths of constant-area pipe. Depending on the device, minor losses traditionally are computed in one of two ways, either

$$h_{l_m} = K \frac{\bar{V}^2}{2} \quad (8.40a)$$

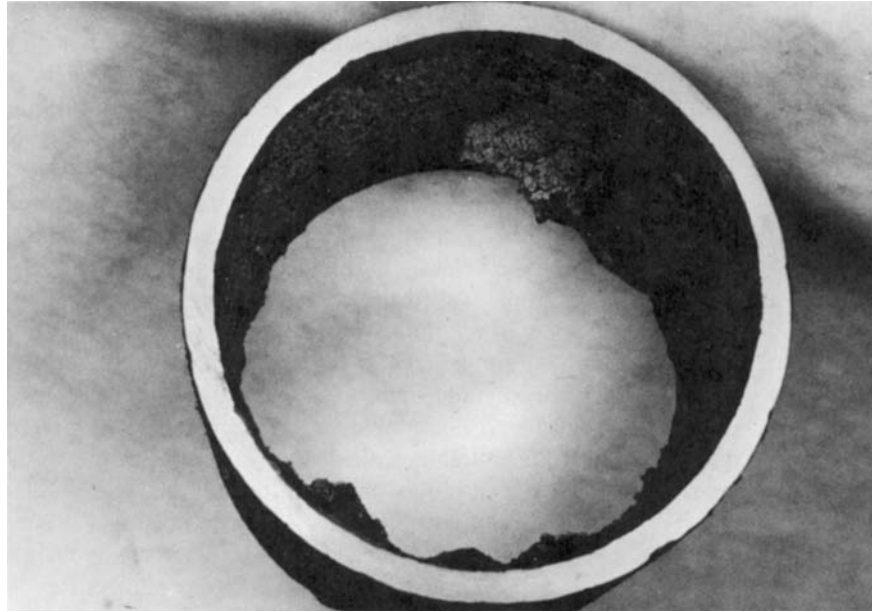


**Fig. 8.14** Pipe section removed after 40 years of service as a water line, showing formation of scale. (Photo courtesy of Alan T. McDonald.)

where the *loss coefficient*,  $K$ , must be determined experimentally for each situation, or

$$h_{lm} = f \frac{L_e}{D} \frac{\bar{V}^2}{2} \quad (8.40b)$$

where  $L_e$  is an *equivalent length* of straight pipe.

For flow through pipe bends and fittings, the loss coefficient,  $K$ , is found to vary with pipe size (diameter) in much the same manner as the friction factor,  $f$ , for flow through a straight pipe. Consequently, the equivalent length,  $L_e/D$ , tends toward a constant for different sizes of a given type of fitting.

Experimental data for minor losses are plentiful, but they are scattered among a variety of sources. Different sources may give different values for the same flow configuration. The data presented here should be considered as representative for some commonly encountered situations; in each case the source of the data is identified.




#### a. Inlets and Exits

A poorly designed inlet to a pipe can cause appreciable head loss. If the inlet has sharp corners, flow separation occurs at the corners, and a *vena contracta* is formed. The fluid must accelerate locally to pass through the reduced flow area at the vena contracta. Losses in mechanical energy result from the unconfined mixing as the flow stream decelerates again to fill the pipe. Three basic inlet geometries are shown in Table 8.2. From the table it is clear that the loss coefficient is reduced significantly when the inlet is rounded even slightly. For a well-rounded inlet ( $r/D \geq 0.15$ ) the entrance loss coefficient is almost negligible. Example 8.9 illustrates a procedure for experimentally determining the loss coefficient for a pipe inlet.

The kinetic energy per unit mass,  $\alpha \bar{V}^2/2$ , is completely dissipated by mixing when flow discharges from a duct into a large reservoir or plenum chamber. The situation corresponds to flow through an abrupt expansion with  $AR = 0$  (Fig. 8.15). The minor loss coefficient thus equals  $\alpha$ , which as we saw in the previous section we usually set

Table 8.2

Minor Loss Coefficients for Pipe Entrances

Entrance Type		Minor Loss Coefficient, $K^a$			
Reentrant		0.78			
Square-edged		0.5			
Rounded		$r/D$	0.02	0.06	$\geq 0.15$
		$K$	0.28	0.15	0.04

<sup>a</sup>Based on  $h_{lm} = K(\bar{V}^2/2)$ , where  $\bar{V}$  is the mean velocity in the pipe.

Source: Data from Reference [11].

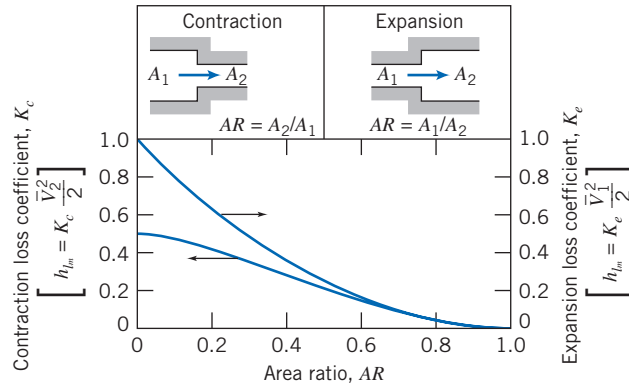


**Fig. 8.15** Loss coefficients for flow through sudden area changes. (Data from Streeter [1].)

to 1 for turbulent flow. No improvement in minor loss coefficient for an exit is possible; however, addition of a diffuser can reduce  $\bar{V}_1^2/2$  and therefore  $h_{lm}$  considerably (see Example 8.10).

### b. Enlargements and Contractions

Minor loss coefficients for sudden expansions and contractions in circular ducts are given in Fig. 8.15. Note that both loss coefficients are based on the *larger*  $\bar{V}^2/2$ . Thus losses for a sudden expansion are based on  $\bar{V}_1^2/2$ , and those for a contraction are based on  $\bar{V}_2^2/2$ .

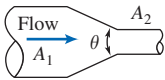
Losses caused by area change can be reduced somewhat by installing a nozzle or diffuser between the two sections of straight pipe. Data for nozzles are given in Table 8.3. Note that the final column (data for the included angle  $\theta = 180^\circ$ ) agrees with the data of Fig. 8.15.

Losses in diffusers depend on a number of geometric and flow variables. Diffuser data most commonly are presented in terms of a pressure recovery coefficient,  $C_p$ , defined as the ratio of static pressure rise to inlet dynamic pressure,

$$C_p \equiv \frac{p_2 - p_1}{\frac{1}{2} \rho \bar{V}_1^2} \quad (8.41)$$

Table 8.3

Loss Coefficients ( $K$ ) for Gradual Contractions: Round and Rectangular Ducts

Included Angle, $\theta$ , Degrees								
	$A_2/A_1$	10	15–40	50–60	90	120	150	180
	0.50	0.05	0.05	0.06	0.12	0.18	0.24	0.26
	0.25	0.05	0.04	0.07	0.17	0.27	0.35	0.41
	0.10	0.05	0.05	0.08	0.19	0.29	0.37	0.43

Note: Coefficients are based on  $h_{l_m} = K(\bar{V}_2^2/2)$ .

Source: Data from ASHRAE [12].

This shows what fraction of the inlet kinetic energy shows up as a pressure rise. It is not difficult to show (using the Bernoulli and continuity equations; see Problem 8.201) that the ideal (frictionless) pressure recovery coefficient is given by

$$C_{p_i} = 1 - \frac{1}{AR^2} \quad (8.42)$$

where  $AR$  is the area ratio. Hence, the ideal pressure recovery coefficient is a function only of the area ratio. In reality a diffuser typically has turbulent flow, and the static pressure rise in the direction of flow may cause flow separation from the walls if the diffuser is poorly designed; flow pulsations can even occur. For these reasons the actual  $C_p$  will be somewhat less than indicated by Eq. 8.42. For example, data for conical diffusers with fully developed turbulent pipe flow at the inlet are presented in Fig. 8.16 as a function of geometry. Note that more tapered diffusers (small divergence angle  $\phi$  or large dimensionless length  $N/R_1$ ) are more likely to approach the ideal constant value for  $C_p$ . As we make the cone shorter, for a given fixed area ratio we start to see a drop in  $C_p$ —we can consider the cone length at which this starts to happen the optimum length (it is the shortest length for which we obtain the maximum coefficient for a given area ratio—closest to that predicted by Eq. 8.42). We can relate  $C_p$  to the head loss. If gravity is neglected, and  $\alpha_1 = \alpha_2 = 1.0$ , the head loss equation, Eq. 8.29, reduces to

$$\left[ \frac{p_1}{\rho} + \frac{\bar{V}_1^2}{2} \right] - \left[ \frac{p_2}{\rho} + \frac{\bar{V}_2^2}{2} \right] = h_{l_r} = h_{l_m}$$

Thus,

$$\begin{aligned} h_{l_m} &= \frac{\bar{V}_1^2}{2} - \frac{\bar{V}_2^2}{2} - \frac{p_2 - p_1}{\rho} \\ h_{l_m} &= \frac{\bar{V}_1^2}{2} \left[ \left( 1 - \frac{\bar{V}_2^2}{\bar{V}_1^2} \right) - \frac{p_2 - p_1}{\frac{1}{2}\rho\bar{V}_1^2} \right] = \frac{\bar{V}_1^2}{2} \left[ \left( 1 - \frac{\bar{V}_2^2}{\bar{V}_1^2} \right) - C_p \right] \end{aligned}$$

From continuity,  $A_1\bar{V}_1 = A_2\bar{V}_2$ , so

$$h_{l_m} = \frac{\bar{V}_1^2}{2} \left[ 1 - \left( \frac{A_1}{A_2} \right)^2 - C_p \right]$$

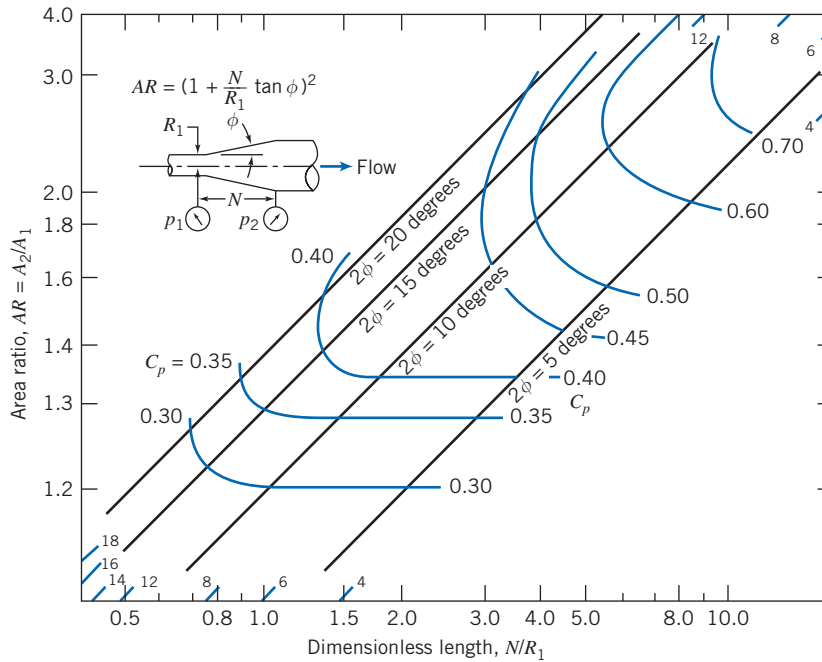


**Fig. 8.16** Pressure recovery for conical diffusers with fully developed turbulent pipe flow at inlet. (Data from Cockrell and Bradley [13].)

OR

$$h_{lm} = \frac{\bar{V}_1^2}{2} \left[ \left( 1 - \frac{1}{(AR)^2} \right) - C_p \right] \quad (8.43)$$

The frictionless result (Eq. 8.42) is obtained from Eq. 8.43 if  $h_{lm} = 0$ . We can combine Eqs. 8.42 and 8.43 to obtain an expression for the head loss in terms of the actual and ideal  $C_p$  values:

$$h_{lm} = (C_{pi} - C_p) \frac{\bar{V}_1^2}{2} \quad (8.44)$$

Performance maps for plane wall and annular diffusers [14] and for radial diffusers [15] are available in the literature.

Diffuser pressure recovery is essentially independent of Reynolds number for inlet Reynolds numbers greater than  $7.5 \times 10^4$  [16]. Diffuser pressure recovery with uniform inlet flow is somewhat better than that for fully developed inlet flow. Performance maps for plane wall, conical, and annular diffusers for a variety of inlet flow conditions are presented in [17].

Since static pressure rises in the direction of flow in a diffuser, flow may separate from the walls. For some geometries, the outlet flow is distorted. For wide angle diffusers, vanes or splitters can be used to suppress stall and improve pressure recovery [18].

### c. Pipe Bends

The head loss of a bend is larger than for fully developed flow through a straight section of equal length. The additional loss is primarily the result of secondary flow, and is represented most conveniently by an equivalent length of straight pipe. The equivalent length depends on the relative radius of curvature of the bend, as shown in



CLASSIC VIDEO

Flow Visualization.



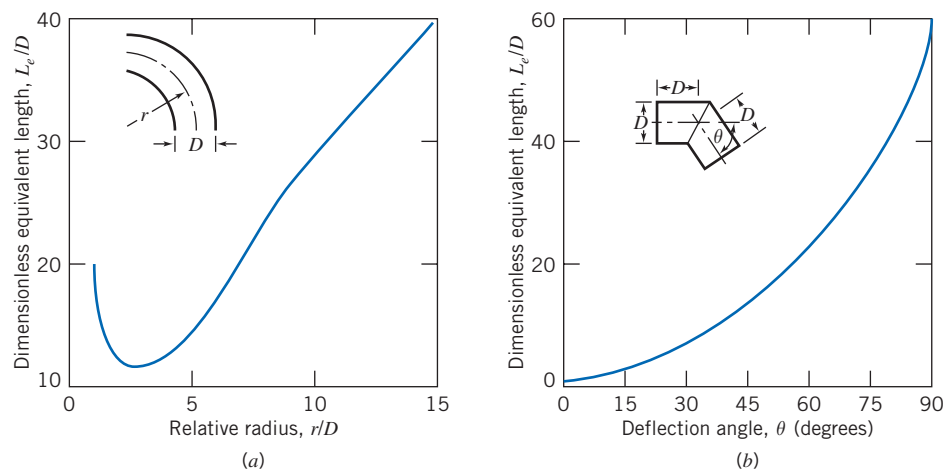


**Fig. 8.17** Representative total resistance ( $L_e/D$ ) for (a) 90° pipe bends and flanged elbows, and (b) miter bends. (Data from Reference [11].)

*Table 8.4*

**Representative Dimensionless Equivalent Lengths ( $L_e/D$ ) for Valves and Fittings**

Fitting Type	Equivalent Length, <sup>a</sup> $L_e/D$
Valves (fully open)	
Gate valve	8
Globe valve	340
Angle valve	150
Ball valve	3
Lift check valve: globe lift	600
angle lift	55
Foot valve with strainer: poppet disk	420
hinged disk	75
Standard elbow: 90°	30
45°	16
Return bend, close pattern	50
Standard tee: flow through run	20
flow through branch	60

<sup>a</sup>Based on  $h_{L_m} = f(L_e/D)(\bar{V}^2/2)$ .  
Source: Data from Reference [11].

Fig. 8.17*a* for 90° bends. An approximate procedure for computing the resistance of bends with other turning angles is given in [11].

Because they are simple and inexpensive to construct in the field, miter bends often are used in large pipe systems. Design data for miter bends are given in Fig. 8.17*b*. Note that you get what you pay for: From Fig. 8.17*a* the equivalent length for pipe bends varies from about 10 to about 40 diameters; for the cheaper 90° miter bend of Fig. 8.17*b* we get a much larger equivalent length of 60 diameters.

*d. Valves and Fittings*

Losses for flow through valves and fittings also may be expressed in terms of an equivalent length of straight pipe. Some representative data are given in Table 8.4.

All resistances are given for fully open valves; losses increase markedly when valves are partially open. Valve design varies significantly among manufacturers.



Whenever possible, resistances furnished by the valve supplier should be used if accurate results are needed.

Fittings in a piping system may have threaded, flanged, or welded connections. For small diameters, threaded joints are most common; large pipe systems frequently have flanged or welded joints.

In practice, insertion losses for fittings and valves vary considerably, depending on the care used in fabricating the pipe system. If burrs from cutting pipe sections are allowed to remain, they cause local flow obstructions, which increase losses appreciably.

Although the losses discussed in this section were termed “minor losses,” they can be a large fraction of the overall system loss. Thus a system for which calculations are to be made must be checked carefully to make sure all losses have been identified and their magnitudes estimated. If calculations are made carefully, the results will be of satisfactory engineering accuracy. You may expect to predict actual losses within  $\pm 10$  percent.

We include here one more device that changes the energy of the fluid—except this time the energy of the fluid will be increased, so it creates a “negative energy loss.”

## Pumps, Fans, and Blowers in Fluid Systems

In many practical flow situations (e.g., the cooling system of an automobile engine, the HVAC system of a building), the driving force for maintaining the flow against friction is a pump (for liquids) or a fan or blower (for gases). Here we will consider pumps, although all the results apply equally to fans and blowers. We generally neglect heat transfer and internal energy changes of the fluid (we will incorporate them later into the definition of the pump efficiency), so the first law of thermodynamics applied across the pump is

$$\dot{W}_{\text{pump}} = \dot{m} \left[ \left( \frac{p}{\rho} + \frac{\bar{V}^2}{2} + gz \right)_{\text{discharge}} - \left( \frac{p}{\rho} + \frac{\bar{V}^2}{2} + gz \right)_{\text{suction}} \right]$$

We can also compute the head  $\Delta h_{\text{pump}}$  (energy/mass) produced by the pump,

$$\Delta h_{\text{pump}} = \frac{\dot{W}_{\text{pump}}}{\dot{m}} = \left( \frac{p}{\rho} + \frac{\bar{V}^2}{2} + gz \right)_{\text{discharge}} - \left( \frac{p}{\rho} + \frac{\bar{V}^2}{2} + gz \right)_{\text{suction}} \quad (8.45)$$

In many cases the inlet and outlet diameters (and therefore velocities) and elevations are the same or negligibly different, so Eq. 8.45 simplifies to

$$\Delta h_{\text{pump}} = \frac{\Delta p_{\text{pump}}}{\rho} \quad (8.46)$$

It is interesting to note that a pump adds energy to the fluid in the form of a gain in pressure—the everyday, invalid perception is that pumps add kinetic energy to the fluid. (It is true that when a pump-pipe system is first started up, the pump does work to accelerate the fluid to its steady speed; this is when a pump driven by an electric motor is most in danger of burning out the motor.)

The idea is that in a pump-pipe system the head produced by the pump (Eq. 8.45 or 8.46) is needed to overcome the head loss for the pipe system. Hence, the flow rate in such a system depends on the pump characteristics and the major and minor losses of the pipe system. We will learn in Chapter 10 that the head produced by a given pump is not constant, but varies with flow rate through the pump, leading to the notion of “matching” a pump to a given system to achieve the desired flow rate.

A useful relation is obtained from Eq. 8.46 if we multiply by  $\dot{m} = \rho Q$  ( $Q$  is the flow rate) and recall that  $\dot{m} \Delta h_{\text{pump}}$  is the power supplied to the fluid,

$$\dot{W}_{\text{pump}} = Q \Delta p_{\text{pump}} \quad (8.47)$$

We can also define the pump efficiency:

$$\eta = \frac{\dot{W}_{\text{pump}}}{\dot{W}_{\text{in}}} \quad (8.48)$$

where  $\dot{W}_{\text{pump}}$  is the power reaching the fluid, and  $\dot{W}_{\text{in}}$  is the power input (usually electrical) to the pump.

We note that, when applying the energy equation (Eq. 8.29) to a pipe system, we may sometimes choose points 1 and 2 so that a pump is included in the system. For these cases we can simply include the head of the pump as a “negative loss”:

$$\left( \frac{p_1}{\rho} + \alpha_1 \frac{\bar{V}_1^2}{2} + gz_1 \right) - \left( \frac{p_2}{\rho} + \alpha_2 \frac{\bar{V}_2^2}{2} + gz_2 \right) = h_{\text{tr}} - \Delta h_{\text{pump}} \quad (8.49)$$

## Noncircular Ducts

The empirical correlations for pipe flow also may be used for computations involving noncircular ducts, provided their cross sections are not too exaggerated. Thus ducts of square or rectangular cross section may be treated if the ratio of height to width is less than about 3 or 4.

The correlations for turbulent pipe flow are extended for use with noncircular geometries by introducing the *hydraulic diameter*, defined as

$$D_h \equiv \frac{4A}{P} \quad (8.50)$$

in place of the diameter,  $D$ . In Eq. 8.50,  $A$  is cross-sectional area, and  $P$  is *wetted perimeter*, the length of wall in contact with the flowing fluid at any cross-section. The factor 4 is introduced so that the hydraulic diameter will equal the duct diameter for a circular cross section. For a circular duct,  $A = \pi D^2/4$  and  $P = \pi D$ , so that

$$D_h = \frac{4A}{P} = \frac{4\left(\frac{\pi}{4}\right)D^2}{\pi D} = D$$

For a rectangular duct of width  $b$  and height  $h$ ,  $A = bh$  and  $P = 2(b + h)$ , so

$$D_h = \frac{4bh}{2(b + h)}$$

If the *aspect ratio*,  $ar$ , is defined as  $ar = h/b$ , then

$$D_h = \frac{2h}{1 + ar}$$

for rectangular ducts. For a square duct,  $ar = 1$  and  $D_h = h$ .

As noted, the hydraulic diameter concept can be applied in the approximate range  $\frac{1}{4} < ar < 4$ . Under these conditions, the correlations for pipe flow give acceptably accurate results for rectangular ducts. Since such ducts are easy and cheap to fabricate

from sheet metal, they are commonly used in air conditioning, heating, and ventilating applications. Extensive data on losses for air flow are available (e.g., see [12, 19]).

Losses caused by secondary flows increase rapidly for more extreme geometries, so the correlations are not applicable to wide, flat ducts, or to ducts of triangular or other irregular shapes. Experimental data must be used when precise design information is required for specific situations.

## Solution of Pipe Flow Problems 8.8

Section 8.7 provides us with a complete scheme for solving many different pipe flow problems. For convenience we collect together the relevant computing equations.

The *energy equation*, relating the conditions at any two points 1 and 2 for a single-path pipe system, is

$$\left( \frac{p_1}{\rho} + \alpha_1 \frac{\bar{V}_1^2}{2} + gz_1 \right) - \left( \frac{p_2}{\rho} + \alpha_2 \frac{\bar{V}_2^2}{2} + gz_2 \right) = h_{t_f} = \sum h_l + \sum h_{l_m} \quad (8.29)$$

This equation expresses the fact that there will be a loss of mechanical energy (“pressure,” kinetic and/or potential) in the pipe. Recall that for turbulent flows  $\alpha \approx 1$ . Note that by judicious choice of points 1 and 2 we can analyze not only the entire pipe system, but also just a certain section of it that we may be interested in. The *total head loss* is given by the sum of the major and minor losses. (Remember that we can also include “negative losses” for any pumps present between points 1 and 2. The relevant form of the energy equation is then Eq. 8.49.)

Each *major loss* is given by

$$h_l = f \frac{L}{D} \frac{\bar{V}^2}{2} \quad (8.34)$$

where the *friction factor* is obtained from

$$f = \frac{64}{Re} \quad \text{for laminar flow } (Re < 2300) \quad (8.36)$$

or

$$\frac{1}{\sqrt{f}} = -2.0 \log \left( \frac{e/D}{3.7} + \frac{2.51}{Re\sqrt{f}} \right) \quad \text{for turbulent flow } (Re \geq 2300) \quad (8.37)$$

and Eqs. 8.36 and 8.37 are presented graphically in the Moody chart (Fig. 8.13).

Each *minor loss* is given either by

$$h_{l_m} = K \frac{\bar{V}^2}{2} \quad (8.40a)$$

where  $K$  is the device *loss coefficient*, or

$$h_{l_m} = f \frac{L_e}{D} \frac{\bar{V}^2}{2} \quad (8.40b)$$

where  $L_e$  is the additional *equivalent length* of pipe.

We also note that the flow rate  $Q$  is related to the average velocity  $\bar{V}$  at each pipe cross section by

$$Q = \pi \frac{D^2}{4} \bar{V}$$

We will apply these equations first to single-path systems.

## Single-Path Systems

In single-path pipe problems we generally know the system configuration (type of pipe material and hence pipe roughness, the number and type of elbows, valves, and other fittings, etc., and changes of elevation), as well as the fluid ( $\rho$  and  $\mu$ ) we will be working with. Although not the only possibilities, usually the goal is to determine one of the following:

- (a) The pressure drop  $\Delta p$ , for a given pipe ( $L$  and  $D$ ), and flow rate  $Q$ .
- (b) The pipe length  $L$ , for a given pressure drop  $\Delta p$ , pipe diameter  $D$ , and flow rate  $Q$ .
- (c) The flow rate  $Q$ , for a given pipe ( $L$  and  $D$ ), and pressure drop  $\Delta p$ .
- (d) The pipe diameter  $D$ , for a given pipe length  $L$ , pressure drop  $\Delta p$ , and flow rate  $Q$ .

Each of these cases often arises in real-world situations. For example, case (a) is a necessary step in selecting the correct size pump to maintain the desired flow rate in a system—the pump must be able to produce the system  $\Delta p$  at the specified flow rate  $Q$ . (We will discuss this in more detail in Chapter 10.) Cases (a) and (b) are computationally straightforward; we will see that cases (c) and (d) can be a little tricky to evaluate. We will discuss each case, and present an Example for each. The Examples present solutions as you might do them using a calculator, but there is also an *Excel* workbook for each. (Remember that the Web site has an *Excel* add-in that once installed will automatically compute  $f$  from  $Re$  and  $e/D$ !) The advantage of using a computer application such as a spreadsheet is that we do not have to use either the Moody chart (Fig. 8.13) or solve the implicit Colebrook equation (Eq. 8.37) to obtain turbulent friction factors—the application can find them for us! In addition, as we'll see, cases (c) and (d) involve significant iterative calculations that can be avoided by use of a computer application. Finally, once we have a solution using a computer application, engineering “what-ifs” become easy, e.g., if we double the head produced by a pump, how much will the flow rate in a given system increase?

### a. Find $\Delta p$ for a Given $L$ , $D$ , and $Q$

These types of problems are quite straightforward—the energy equation (Eq. 8.29) can be solved directly for  $\Delta p = (p_1 - p_2)$  in terms of known or computable quantities. The flow rate leads to the Reynolds number (or numbers if there is a diameter change) and hence the friction factor (or factors) for the flow; tabulated data can be used for minor loss coefficients and equivalent lengths. The energy equation can then be used to directly obtain the pressure drop. Example 8.5 illustrates this type of problem.

### b. Find $L$ for a Given $\Delta p$ , $D$ , and $Q$

These types of problems are also straightforward—the energy equation (Eq. 8.29) can be solved directly for  $L$  in terms of known or computable quantities. The flow rate again leads to the Reynolds number and hence the friction factor for the flow. Tabulated data can be used for minor loss coefficients and equivalent lengths. The energy equation can then be rearranged and solved directly for the pipe length. Example 8.6 illustrates this type of problem.

### c. Find $Q$ for a Given $\Delta p$ , $L$ , and $D$

These types of problems require either manual iteration or use of a computer application such as *Excel*. The unknown flow rate or velocity is needed before the Reynolds

number and hence the friction factor can be found. To manually iterate we first solve the energy equation directly for  $\bar{V}$  in terms of known quantities and the unknown friction factor  $f$ . To start the iterative process we make a guess for  $f$  (a good choice is to take a value from the fully turbulent region of the Moody chart because many practical flows are in this region) and obtain a value for  $\bar{V}$ . Then we can compute a Reynolds number and hence obtain a new value for  $f$ . We repeat the iteration process  $f \rightarrow \bar{V} \rightarrow Re \rightarrow f$  until convergence (usually only two or three iterations are necessary). A much quicker procedure is to use a computer application. For example, spreadsheets (such as *Excel*) have built-in solving features for solving one or more algebraic equations for one or more unknowns. Example 8.7 illustrates this type of problem.

#### d. Find $D$ for a Given $\Delta p$ , $L$ , and $Q$

These types of problems arise, for example, when we have designed a pump-pipe system and wish to choose the best pipe diameter—the best being the minimum diameter (for minimum pipe cost) that will deliver the design flow rate. We need to manually iterate, or use a computer application such as *Excel*. The unknown diameter is needed before the Reynolds number and relative roughness, and hence the friction factor, can be found. To manually iterate we could first solve the energy equation directly for  $D$  in terms of known quantities and the unknown friction factor  $f$ , and then iterate from a starting guess for  $f$  in a way similar to case (c) above:  $f \rightarrow D \rightarrow Re$  and  $e/D \rightarrow f$ . In practice this is a little unwieldy, so instead to manually find a solution we make successive guesses for  $D$  until the corresponding pressure drop  $\Delta p$  (for the given flow rate  $Q$ ) computed from the energy equation matches the design  $\Delta p$ . As in case (c) a much quicker procedure is to use a computer application. For example, spreadsheets (such as *Excel*) have built-in solving features for solving one or more algebraic equations for one or more unknowns. Example 8.8 illustrates this type of problem.

In choosing a pipe size, it is logical to work with diameters that are available commercially. Pipe is manufactured in a limited number of standard sizes. Some data for standard pipe sizes are given in Table 8.5. For data on extra strong or double extra strong pipes, consult a handbook, e.g., [11]. Pipe larger than 12 in. nominal diameter is produced in multiples of 2 in. up to a nominal diameter of 36 in. and in multiples of 6 in. for still larger sizes.

Table 8.5

Standard Sizes for Carbon Steel, Alloy Steel, and Stainless Steel Pipe

Nominal Pipe Size (in.)	Inside Diameter (in.)	Nominal Pipe Size (in.)	Inside Diameter (in.)
$\frac{1}{8}$	0.269	$2\frac{1}{2}$	2.469
$\frac{1}{4}$	0.364	3	3.068
$\frac{3}{8}$	0.493	4	4.026
$\frac{1}{2}$	0.622	5	5.047
$\frac{3}{4}$	0.824	6	6.065
1	1.049	8	7.981
$1\frac{1}{2}$	1.610	10	10.020
2	2.067	12	12.000

Source: Data from Reference [11].

### Example 8.5 PIPE FLOW INTO A RESERVOIR: PRESSURE DROP UNKNOWN

A 100-m length of smooth horizontal pipe is attached to a large reservoir. A pump is attached to the end of the pipe to pump water into the reservoir at a volume flow rate of  $0.01 \text{ m}^3/\text{s}$ . What pressure (gage) must the pump produce at the pipe to generate this flow rate? The inside diameter of the smooth pipe is 75 mm.

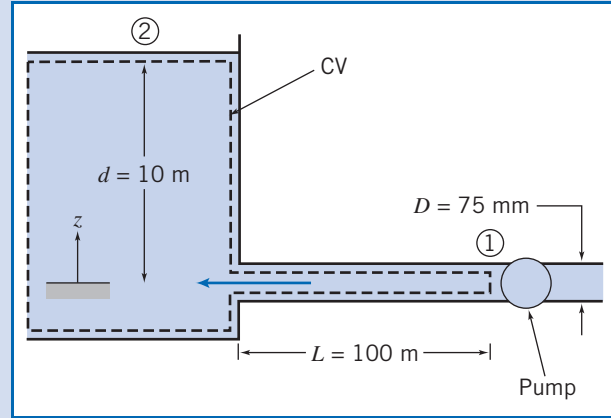
**Given:** Water is pumped at  $0.01 \text{ m}^3/\text{s}$  through a 75-mm-diameter smooth pipe, with  $L = 100 \text{ m}$ , into a constant-level reservoir of depth  $d = 10 \text{ m}$ .

**Find:** Pump pressure,  $p_1$ , required to maintain the flow.

**Solution:**

**Governing equations:**

$$\left( \frac{p_1}{\rho} + \alpha_1 \frac{\bar{V}_1^2}{2} + gz_1 \right) - \left( \frac{p_2}{\rho} + \alpha_2 \frac{\bar{V}_2^2}{2} + gz_2 \right) = h_{lr} = h_l + h_{lm} \quad (8.29)$$



where

$$h_l = f \frac{L}{D} \frac{\bar{V}^2}{2} \quad (8.34) \quad \text{and} \quad h_{lm} = K \frac{\bar{V}^2}{2} \quad (8.40a)$$

For the given problem,  $p_1 = p_{\text{pump}}$  and  $p_2 = 0$  (gage), so  $\Delta p = p_1 - p_2 = p_{\text{pump}}$ ,  $\bar{V}_1 = \bar{V}$ ,  $\bar{V}_2 \approx 0$ ,  $K$  (exit loss) = 1.0, and  $\alpha_1 \approx 1.0$ . If we set  $z_1 = 0$ , then  $z_2 = d$ . Simplifying Eq. 8.29 gives

$$\frac{\Delta p}{\rho} + \frac{\bar{V}^2}{2} - gd = f \frac{L}{D} \frac{\bar{V}^2}{2} + \frac{\bar{V}^2}{2} \quad (1)$$

The left side of the equation is the loss of mechanical energy between points ① and ②; the right side is the major and minor losses that contributed to the loss. Solving for the pressure drop,  $\Delta p = p_{\text{pump}}$ ,

$$p_{\text{pump}} = \Delta p = \rho \left( gd + f \frac{L}{D} \frac{\bar{V}^2}{2} \right)$$

Everything on the right side of the equation is known or can be readily computed. The flow rate  $Q$  leads to  $\bar{V}$ ,

$$\bar{V} = \frac{Q}{A} = \frac{4Q}{\pi D^2} = \frac{4}{\pi} \times 0.01 \frac{\text{m}^3}{\text{s}} \times \frac{1}{(0.075)^2 \text{ m}^2} = 2.26 \text{ m/s}$$

This in turn [assuming water at  $20^\circ\text{C}$ ,  $\rho = 999 \text{ kg/m}^3$ , and  $\mu = 1.0 \times 10^{-3} \text{ kg/(m} \cdot \text{s)}$ ] leads to the Reynolds number

$$Re = \frac{\rho \bar{V} D}{\mu} = 999 \frac{\text{kg}}{\text{m}^3} \times 2.26 \frac{\text{m}}{\text{s}} \times 0.075 \text{ m} \times \frac{\text{m} \cdot \text{s}}{1.0 \times 10^{-3} \text{ kg}} = 1.70 \times 10^5$$

For turbulent flow in a smooth pipe ( $e = 0$ ), from Eq. 8.37,  $f = 0.0162$ . Then

$$\begin{aligned}
 p_{\text{pump}} &= \Delta p = \rho \left( gd + f \frac{L}{D} \frac{\bar{V}^2}{2} \right) \\
 &= 999 \frac{\text{kg}}{\text{m}^3} \left( 9.81 \frac{\text{m}}{\text{s}^2} \times 10 \text{ m} + (0.0162) \times \frac{100 \text{ m}}{0.075 \text{ m}} \times \frac{(2.26)^2 \text{ m}^2}{2 \text{ s}^2} \right) \times \frac{\text{N} \cdot \text{s}^2}{\text{kg} \cdot \text{m}} \\
 p_{\text{pump}} &= 1.53 \times 10^5 \text{ N/m}^2 \text{ (gage)}
 \end{aligned}$$

Hence,

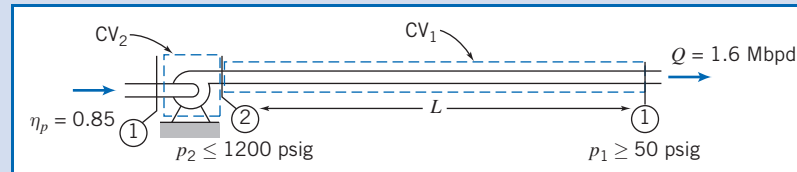
$$p_{\text{pump}} = 153 \text{ kPa (gage)} \longleftarrow p_{\text{pump}}$$

This problem illustrates the method for manually calculating pressure drop. The Excel workbook for this problem automatically computes  $Re$  and  $f$  from the given data. It then solves Eq. 1 directly for pressure  $p_{\text{pump}}$  without having to explicitly solve for it first. The workbook can be easily used to see, for example, how the pump pressure  $p_{\text{pump}}$  required to maintain flow  $Q$  is affected by changing the diameter  $D$ ; it is easily editable for other case (a) type problems.

### Example 8.6 FLOW IN A PIPELINE: LENGTH UNKNOWN

Crude oil flows through a level section of the Alaskan pipeline at a rate of 1.6 million barrels per day (1 barrel = 42 gal). The pipe inside diameter is 48 in.; its roughness is equivalent to galvanized iron. The maximum allowable pressure is 1200 psi; the minimum pressure required to keep dissolved gases in solution in the crude oil is 50 psi. The crude oil has  $SG = 0.93$ ; its viscosity at the pumping temperature of  $140^\circ\text{F}$  is  $\mu = 3.5 \times 10^{-4} \text{ lbf} \cdot \text{s/ft}^2$ . For these conditions, determine the maximum possible spacing between pumping stations. If the pump efficiency is 85 percent, determine the power that must be supplied at each pumping station.

**Given:** Flow of crude oil through horizontal section of Alaskan pipeline.



$$D = 48 \text{ in. (roughness of galvanized iron), } SG = 0.93, \mu = 3.5 \times 10^{-4} \text{ lbf} \cdot \text{s/ft}^2$$

- Find:** (a) Maximum spacing,  $L$ .  
(b) Power needed at each pump station.

**Solution:**

As shown in the figure, we assume that the Alaskan pipeline is made up of repeating pump-pipe sections. We can draw two control volumes:  $CV_1$ , for the pipe flow (state ② to state ①);  $CV_2$ , for the pump (state ① to state ②).

First we apply the energy equation for steady, incompressible pipe flow to  $CV_1$ .

**Governing equations:**

$$\left( \frac{p_2}{\rho} + \alpha_2 \frac{\bar{V}_2^2}{2} + g z_2 \right) - \left( \frac{p_1}{\rho} + \alpha_1 \frac{\bar{V}_1^2}{2} + g z_1 \right) = h_{iT} = h_i + h_{lm} \quad (8.29)$$

where

$$h_i = f \frac{L}{D} \frac{\bar{V}^2}{2} \quad (8.34) \quad \text{and} \quad h_{lm} = K \frac{\bar{V}^2}{2} \quad (8.40a)$$

- Assumptions:** (1)  $\alpha_1 \bar{V}_1^2 = \alpha_2 \bar{V}_2^2$ .  
 (2) Horizontal pipe,  $z_1 = z_2$ .  
 (3) Neglect minor losses.  
 (4) Constant viscosity.

Then, using CV<sub>1</sub>

$$\Delta p = p_2 - p_1 = f \frac{L}{D} \rho \frac{\bar{V}^2}{2} \quad (1)$$

or

$$L = \frac{2D}{f} \frac{\Delta p}{\rho \bar{V}^2} \text{ where } f = f(Re, e/D)$$

$$Q = 1.6 \times 10^6 \frac{\text{bbl}}{\text{day}} \times 42 \frac{\text{gal}}{\text{bbl}} \times \frac{\text{ft}^3}{7.48 \text{ gal}} \times \frac{\text{day}}{24 \text{ hr}} \times \frac{\text{hr}}{3600 \text{ s}} = 104 \text{ ft}^3/\text{s}$$

so

$$\bar{V} = \frac{Q}{A} = 104 \frac{\text{ft}^3}{\text{s}} \times \frac{4}{\pi(4)^2 \text{ ft}^2} = 8.27 \text{ ft/s}$$

$$Re = \frac{\rho \bar{V} D}{\mu} = (0.93) 1.94 \frac{\text{slug}}{\text{ft}^3} \times 8.27 \frac{\text{ft}}{\text{s}} \times 4 \text{ ft} \times \frac{\text{ft}^2}{3.5 \times 10^{-4} \text{ lbf} \cdot \text{s}} \times \frac{\text{lbf} \cdot \text{s}^2}{\text{slug} \cdot \text{ft}}$$

$$Re = 1.71 \times 10^5$$

From Table 8.1,  $e = 0.0005 \text{ ft}$  and hence  $e/D = 0.00012$ . Then from Eq. 8.37,  $f = 0.017$  and thus

$$L = \frac{2}{0.017} \times 4 \text{ ft} \times (1200 - 50) \frac{\text{lbf}}{\text{in}^2} \times \frac{\text{ft}^3}{(0.93) 1.94 \text{ slug}} \times \frac{\text{s}^2}{(8.27)^2 \text{ ft}^2} \\ \times 144 \frac{\text{in}^2}{\text{ft}^2} \times \frac{\text{slug} \cdot \text{ft}}{\text{lbf} \cdot \text{s}^2} = 6.32 \times 10^5 \text{ ft}$$

$$L = 632,000 \text{ ft (120 mi)} \longleftarrow L$$

To find the pumping power we can apply the first law of thermodynamics to CV<sub>2</sub>. This control volume consists only of the pump, and we saw in Section 8.7 that this law simplifies to

$$\dot{W}_{\text{pump}} = Q \Delta p_{\text{pump}} \quad (8.47)$$

and the pump efficiency is

$$\eta = \frac{\dot{W}_{\text{pump}}}{\dot{W}_{\text{in}}} \quad (8.48)$$

We recall that  $\dot{W}_{\text{pump}}$  is the power reaching the fluid, and  $\dot{W}_{\text{in}}$  is the power input. Because we have a repeating system the pressure rise through the pump (i.e., from state ① to state ②) equals the pressure drop in the pipe (i.e., from state ② to state ①),

$$\Delta p_{\text{pump}} = \Delta p$$



so that

$$\dot{W}_{\text{pump}} = Q \Delta p_{\text{pump}} = 104 \frac{\text{ft}^3}{\text{s}} \times \frac{(1200 - 50) \text{ lbf}}{\text{in}^2} \times \frac{144 \text{ in}^2}{\text{ft}^2} \times \frac{\text{hp} \cdot \text{s}}{550 \text{ ft} \cdot \text{lbf}} \approx 31,300 \text{ hp}$$

and the required power input is

$$\dot{W}_{\text{in.}} = \frac{\dot{W}_{\text{pump}}}{\eta} = \frac{31300 \text{ hp}}{0.85} = 36,800 \text{ hp} \leftarrow \dot{W}_{\text{needed}}$$

This problem illustrates the method for manually calculating pipe length  $L$ . The *Excel* workbook for this problem automatically computes  $Re$  and  $f$  from the given data. It then solves Eq. 1 directly for  $L$  without having to explicitly solve for it first. The workbook can be easily used to see, for example, how the flow rate  $Q$  depends on  $L$ ; it may be edited for other case (b) type problems.

### Example 8.7 FLOW FROM A WATER TOWER: FLOW RATE UNKNOWN

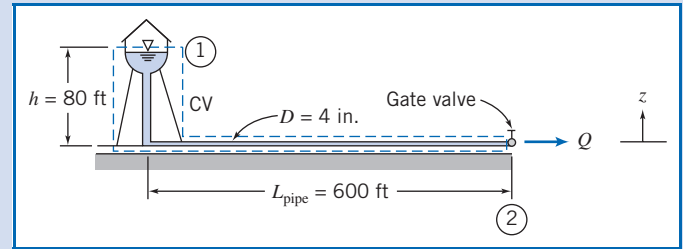
A fire protection system is supplied from a water tower and standpipe 80 ft tall. The longest pipe in the system is 600 ft and is made of cast iron about 20 years old. The pipe contains one gate valve; other minor losses may be neglected. The pipe diameter is 4 in. Determine the maximum rate of flow (gpm) through this pipe.

**Given:** Fire protection system, as shown.

**Find:**  $Q$ , gpm.

**Solution:**

**Governing equations:**



$$\left( \frac{p_1}{\rho} + \alpha_1 \frac{\bar{V}_1^2}{2} + gz_1 \right) - \left( \frac{p_2}{\rho} + \alpha_2 \frac{\bar{V}_2^2}{2} + gz_2 \right) = h_{lT} = h_l + h_{lm} \quad (8.29)$$

$\approx 0(2)$

where

$$h_l = f \frac{L}{D} \frac{\bar{V}^2}{2} \quad (8.34) \quad \text{and} \quad h_{lm} = f \frac{L_e}{D} \frac{\bar{V}^2}{2} \quad (8.40b)$$

**Assumptions:** (1)  $p_1 = p_2 = p_{\text{atm}}$   
(2)  $\bar{V}_1 = 0$ , and  $\alpha_2 \approx 1.0$ .

Then Eq. 8.29 can be written as

$$g(z_1 - z_2) - \frac{\bar{V}_2^2}{2} = h_{lT} = f \left( \frac{L}{D} + \frac{L_e}{D} \right) \frac{\bar{V}_2^2}{2} \quad (1)$$

For a fully open gate valve, from Table 8.4,  $L_e/D = 8$ . Thus

$$g(z_1 - z_2) = \frac{\bar{V}_2^2}{2} \left[ f \left( \frac{L}{D} + 8 \right) + 1 \right]$$

To manually iterate, we solve for  $\bar{V}_2$  and obtain

$$\bar{V}_2 = \left[ \frac{2g(z_1 - z_2)}{f(L/D + 8) + 1} \right]^{1/2} \quad (2)$$

To be conservative, assume the standpipe is the same diameter as the horizontal pipe. Then

$$\frac{L}{D} = \frac{600 \text{ ft} + 80 \text{ ft}}{4 \text{ in.}} \times \frac{12 \text{ in.}}{\text{ft}} = 2040$$

Also

$$z_1 - z_2 = h = 80 \text{ ft}$$

To solve Eq. 2 manually we need to iterate. To start, we make an estimate for  $f$  by assuming the flow is fully turbulent (where  $f$  is constant). This value can be obtained from solving Eq. 8.37 using a calculator or from Fig. 8.13. For a large value of  $Re$  (e.g.,  $10^8$ ), and a roughness ratio  $e/D \approx 0.005$  ( $e = 0.00085 \text{ ft}$  for cast iron is obtained from Table 8.1, and doubled to allow for the fact that the pipe is old), we find that  $f \approx 0.03$ . Thus a first iteration for  $\bar{V}_2$  from Eq. 2 is

$$\bar{V}_2 = \left[ 2 \times 32.2 \frac{\text{ft}}{\text{s}^2} \times 80 \text{ ft} \times \frac{1}{0.03(2040 + 8) + 1} \right]^{1/2} = 9.08 \text{ ft/s}$$

Now obtain a new value for  $f$ :

$$Re = \frac{\rho \bar{V} D}{\mu} = \frac{\bar{V} D}{\nu} = 9.08 \frac{\text{ft}}{\text{s}} \times \frac{\text{ft}}{3} \times \frac{\text{s}}{1.21 \times 10^{-5} \text{ ft}^2} = 2.50 \times 10^5$$

For  $e/D = 0.005$ ,  $f = 0.0308$  from Eq. 8.37. Thus we obtain


$$\bar{V}_2 = \left[ 2 \times 32.2 \frac{\text{ft}}{\text{s}^2} \times 80 \text{ ft} \times \frac{1}{0.0308(2040 + 8) + 1} \right]^{1/2} = 8.97 \text{ ft/s}$$

The values we have obtained for  $\bar{V}_2$  (9.08 ft/s and 8.97 ft/s) differ by less than 2%—an acceptable level of accuracy. If this accuracy had not been achieved we would continue iterating until this, or any other accuracy we desired, was achieved (usually only one or two more iterations at most are necessary for reasonable accuracy). Note that instead of starting with a fully rough value for  $f$ , we could have started with a guess value for  $\bar{V}_2$  of, say, 1 ft/s or 10 ft/s. The volume flow rate is

$$Q = \bar{V}_2 A = \bar{V}_2 \frac{\pi D^2}{4} = 8.97 \frac{\text{ft}}{\text{s}} \times \frac{\pi}{4} \left( \frac{1}{3} \right)^2 \text{ ft}^2 \times 7.48 \frac{\text{gal}}{\text{ft}^3} \times 60 \frac{\text{s}}{\text{min}}$$

$$Q = 351 \text{ gpm} \longleftarrow \underline{\hspace{10em}} Q$$

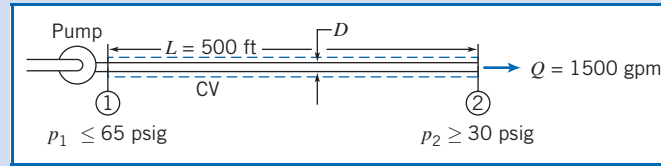
This problem illustrates the method for manually iterating to calculate flow rate.

 The Excel workbook for this problem automatically iterates to solve for the flow rate  $Q$ . It solves Eq. 1 without having to obtain the explicit equation (Eq. 2) for  $\bar{V}_2$  (or  $Q$ ) first. The workbook can be easily used to perform numerous “what-ifs” that would be extremely time-consuming to do manually, e.g., to see how  $Q$  is affected by changing the roughness  $e/D$ . For example, it shows that replacing the old cast-iron pipe with a new pipe ( $e/D \approx 0.0025$ ) would increase the flow rate from 351 gpm to about 386 gpm, a 10% increase! The workbook can be modified to solve other case (c) type problems.

## Example 8.8 FLOW IN AN IRRIGATION SYSTEM: DIAMETER UNKNOWN

Spray heads in an agricultural spraying system are to be supplied with water through 500 ft of drawn aluminum tubing from an engine-driven pump. In its most efficient operating range, the pump output is 1500 gpm at a discharge pressure not exceeding 65 psig. For satisfactory operation, the sprinklers must operate at 30 psig or higher pressure. Minor losses and elevation changes may be neglected. Determine the smallest standard pipe size that can be used.

**Given:** Water supply system, as shown.



**Find:** Smallest standard  $D$ .

**Solution:**

$\Delta p$ ,  $L$ , and  $Q$  are known.  $D$  is unknown, so iteration is needed to determine the minimum standard diameter that satisfies the pressure drop constraint at the given flow rate. The maximum allowable pressure drop over the length,  $L$ , is

$$\Delta p_{\max} = p_{1_{\max}} - p_{2_{\min}} = (65 - 30) \text{ psi} = 35 \text{ psi}$$

**Governing equations:**

$$\begin{aligned} \left( \frac{p_1}{\rho} + \alpha_1 \frac{\bar{V}_1^2}{2} + g z_1 \right) - \left( \frac{p_2}{\rho} + \alpha_2 \frac{\bar{V}_2^2}{2} + g z_2 \right) &= h_{l_T} \\ &= 0(3) \\ h_{l_T} &= h_l + h_{l_m} = f \frac{L}{D} \frac{\bar{V}_2^2}{2} \end{aligned} \quad (8.29)$$

- Assumptions:**
- (1) Steady flow.
  - (2) Incompressible flow.
  - (3)  $h_{l_T} = h_l$ , i.e.,  $h_{l_m} = 0$ .
  - (4)  $z_1 = z_2$ .
  - (5)  $\bar{V}_1 = \bar{V}_2 = \bar{V}$ ;  $\alpha_1 \simeq \alpha_2$ .

Then

$$\Delta p = p_1 - p_2 = f \frac{L}{D} \frac{\rho \bar{V}^2}{2} \quad (1)$$

Equation 1 is difficult to solve for  $D$  because both  $\bar{V}$  and  $f$  depend on  $D$ ! The best approach is to use a computer application such as *Excel* to automatically solve for  $D$ . For completeness here we show the manual iteration procedure. The first step is to express Eq. 1 and the Reynolds number in terms of  $Q$  instead of  $\bar{V}$  ( $Q$  is constant but  $\bar{V}$  varies with  $D$ ). We have  $\bar{V} = Q/A = 4Q/\pi D^2$  so that

$$\Delta p = f \frac{L}{D} \frac{\rho}{2} \left( \frac{4Q}{\pi D^2} \right)^2 = \frac{8fL\rho Q^2}{\pi^2 D^5} \quad (2)$$

The Reynolds number in terms of  $Q$  is

$$Re = \frac{\rho \bar{V} D}{\mu} = \frac{\bar{V} D}{\nu} = \frac{4Q}{\pi D^2} \frac{D}{\nu} = \frac{4Q}{\pi \nu D}$$

Finally,  $Q$  must be converted to cubic feet per second.

$$Q = 1500 \frac{\text{gal}}{\text{min}} \times \frac{\text{min}}{60 \text{ s}} \times \frac{\text{ft}^3}{7.48 \text{ gal}} = 3.34 \text{ ft}^3/\text{s}$$

For an initial guess, take nominal 4 in. (4.026 in. i.d.) pipe:

$$Re = \frac{4Q}{\pi \nu D} = \frac{4}{\pi} \times 3.34 \frac{\text{ft}^3}{\text{s}} \times \frac{\text{s}}{1.21 \times 10^{-5} \text{ft}^2} \times \frac{1}{4.026 \text{ in.}} \times 12 \frac{\text{in.}}{\text{ft}} = 1.06 \times 10^6$$

For drawn tubing,  $e = 5 \times 10^{-6}$  ft (Table 8.1) and hence  $e/D = 1.5 \times 10^{-5}$ , so  $f \simeq 0.012$  (Eq. 8.37), and

$$\begin{aligned} \Delta p &= \frac{8fL\rho Q^2}{\pi^2 D^5} = \frac{8}{\pi^2} \times 0.012 \times 500 \text{ ft} \times 1.94 \frac{\text{slug}}{\text{ft}^3} \times (3.34)^2 \frac{\text{ft}^6}{\text{s}^2} \\ &\quad \times \frac{1}{(4.026)^5 \text{ in.}^5} \times 1728 \frac{\text{in.}^3}{\text{ft}^3} \times \frac{\text{lbf} \cdot \text{s}^2}{\text{slug} \cdot \text{ft}} \\ \Delta p &= 172 \text{ lbf/in.}^2 > \Delta p_{\max} \end{aligned}$$

Since this pressure drop is too large, try  $D = 6$  in. (actually 6.065 in. i.d.):

$$Re = \frac{4}{\pi} \times 3.34 \frac{\text{ft}^3}{\text{s}} \times \frac{\text{s}}{1.21 \times 10^{-5} \text{ft}^2} \times \frac{1}{6.065 \text{ in.}} \times 12 \frac{\text{in.}}{\text{ft}} = 6.95 \times 10^5$$

For drawn tubing with  $D = 6$  in.,  $e/D = 1.0 \times 10^{-5}$ , so  $f \simeq 0.013$  (Eq. 8.37), and

$$\begin{aligned} \Delta p &= \frac{8}{\pi^2} \times 0.013 \times 500 \text{ ft} \times 1.94 \frac{\text{slug}}{\text{ft}^3} \times (3.34)^2 \frac{\text{ft}^6}{\text{s}^2} \\ &\quad \times \frac{1}{(6.065)^5 \text{ in.}^5} \times (12)^3 \frac{\text{in.}^3}{\text{ft}^3} \times \frac{\text{lbf} \cdot \text{s}^2}{\text{slug} \cdot \text{ft}} \\ \Delta p &= 24.0 \text{ lbf/in.}^2 < \Delta p_{\max} \end{aligned}$$

Since this is less than the allowable pressure drop, we should check a 5 in. (nominal) pipe. With an actual i.d. of 5.047 in.,


$$Re = \frac{4}{\pi} \times 3.34 \frac{\text{ft}^3}{\text{s}} \times \frac{\text{s}}{1.21 \times 10^{-5} \text{ft}^2} \times \frac{1}{5.047 \text{ in.}} \times 12 \frac{\text{in.}}{\text{ft}} = 8.36 \times 10^5$$

For drawn tubing with  $D = 5$  in.,  $e/D = 1.2 \times 10^{-5}$ , so  $f \simeq 0.0122$  (Eq. 8.37), and

$$\begin{aligned} \Delta p &= \frac{8}{\pi^2} \times 0.0122 \times 500 \text{ ft} \times 1.94 \frac{\text{slug}}{\text{ft}^3} \times (3.34)^2 \frac{\text{ft}^6}{\text{s}^2} \\ &\quad \times \frac{1}{(5.047)^5 \text{ in.}^5} \times (12)^3 \frac{\text{in.}^3}{\text{ft}^3} \times \frac{\text{lbf} \cdot \text{s}^2}{\text{slug} \cdot \text{ft}} \\ \Delta p &= 56.4 \text{ lbf/in.}^2 > \Delta p_{\max} \end{aligned}$$

Thus the criterion for pressure drop is satisfied for a minimum nominal diameter of 6 in. pipe.  $\longleftarrow D$

This problem illustrates the method for manually iterating to calculate pipe diameter.

 The Excel workbook for this problem automatically iterates to solve for the exact pipe diameter  $D$  that satisfies Eq. 1, without having to obtain the explicit equation (Eq. 2) for  $D$  first. Then all that needs to be done is to select the smallest standard pipe size that is equal to or greater than this value. For the given data,  $D = 5.58$  in., so the appropriate pipe size is 6 in. The workbook can be used to perform numerous “what-ifs” that would be extremely time-consuming to do manually, e.g., to see how the required  $D$  is affected by changing the pipe length  $L$ . For example, it shows that reducing  $L$  to 250 ft would allow 5 in. (nominal) pipe to be used. The workbook can be modified for solving other case (d) type problems.

We have solved Examples 8.7 and 8.8 by iteration (manual, or using *Excel*). Several specialized forms of friction factor versus Reynolds number diagrams have been introduced to solve problems of this type without the need for iteration. For examples of these specialized diagrams, see Daily and Harleman [20] and White [21].

Examples 8.9 and 8.10 illustrate the evaluation of minor loss coefficients and the application of a diffuser to reduce exit kinetic energy from a flow system.

### Example 8.9 CALCULATION OF ENTRANCE LOSS COEFFICIENT

Hamilton [22] reports results of measurements made to determine entrance losses for flow from a reservoir to a pipe with various degrees of entrance rounding. A copper pipe 10 ft long, with 1.5 in. i.d., was used for the tests. The pipe discharged to atmosphere. For a square-edged entrance, a discharge of  $0.566 \text{ ft}^3/\text{s}$  was measured when the reservoir level was 85.1 ft above the pipe centerline. From these data, evaluate the loss coefficient for a square-edged entrance.

**Given:** Pipe with square-edged entrance discharging from reservoir as shown.

**Find:**  $K_{\text{entrance}}$ .

**Solution:**

Apply the energy equation for steady, incompressible pipe flow.

**Governing equations:**

$$\frac{p_1}{\rho} + \alpha_1 \frac{\bar{V}_1^2}{2} + gz_1 = \frac{p_2}{\rho} + \alpha_2 \frac{\bar{V}_2^2}{2} + gz_2 + h_{l_T} \quad \begin{matrix} \approx 0(2) \\ = 0 \end{matrix}$$

$$h_{l_T} = f \frac{L}{D} \frac{\bar{V}_2^2}{2} + K_{\text{entrance}} \frac{\bar{V}_2^2}{2}$$

**Assumptions:** (1)  $p_1 = p_2 = p_{\text{atm}}$ .

(2)  $\bar{V}_1 \approx 0$ .

Substituting for  $h_{l_T}$  and dividing by  $g$  gives  $z_1 = h = \alpha_2 \frac{\bar{V}_2^2}{2g} + f \frac{L}{D} \frac{\bar{V}_2^2}{2g} + K_{\text{entrance}} \frac{\bar{V}_2^2}{2g}$

or

$$K_{\text{entrance}} = \frac{2gh}{\bar{V}_2^2} - f \frac{L}{D} - \alpha_2 \quad (1)$$

The average velocity is

$$\bar{V}_2 = \frac{Q}{A} = \frac{4Q}{\pi D^2}$$

$$\bar{V}_2 = \frac{4}{\pi} \times 0.566 \frac{\text{ft}^3}{\text{s}} \times \frac{1}{(1.5)^2 \text{ in.}^2} \times 1.44 \frac{\text{in.}^2}{\text{ft}^2} = 46.1 \text{ ft/s}$$

Assume  $T = 70^\circ\text{F}$ , so  $\nu = 1.05 \times 10^{-5} \text{ ft}^2/\text{s}$  (Table A.7). Then

$$Re = \frac{\bar{V}D}{\nu} = 46.1 \frac{\text{ft}}{\text{s}} \times 1.5 \text{ in.} \times \frac{\text{s}}{1.05 \times 10^{-5} \text{ ft}^2} \times \frac{\text{ft}}{12 \text{ in.}} = 5.49 \times 10^5$$

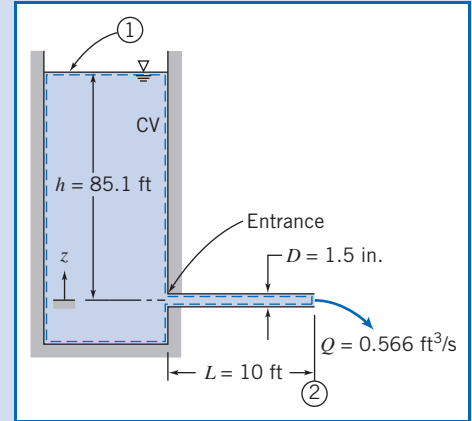
For drawn tubing,  $e = 5 \times 10^{-6} \text{ ft}$  (Table 8.1), so  $e/D = 0.000,04$  and  $f = 0.0135$  (Eq. 8.37).

In this problem we need to be careful in evaluating the kinetic energy correction factor  $\alpha_2$ , as it is a significant factor in computing  $K_{\text{entrance}}$  from Eq. 1. We recall from Section 8.6 and previous Examples that we have usually assumed  $\alpha \approx 1$ , but here we will compute a value from Eq. 8.27:

$$\alpha = \left( \frac{U}{\bar{V}} \right)^3 \frac{2n^2}{(3+n)(3+2n)} \quad (8.27)$$

To use this equation we need values for the turbulent power-law coefficient  $n$  and the ratio of centerline to mean velocity  $U/\bar{V}$ . For  $n$ , from Section 8.5

$$n = -1.7 + 1.8 \log(Re_U) \approx 8.63 \quad (8.23)$$



where we have used the approximation  $Re_U \approx Re_{\bar{V}}$ . For  $\bar{V}/U$ , we have

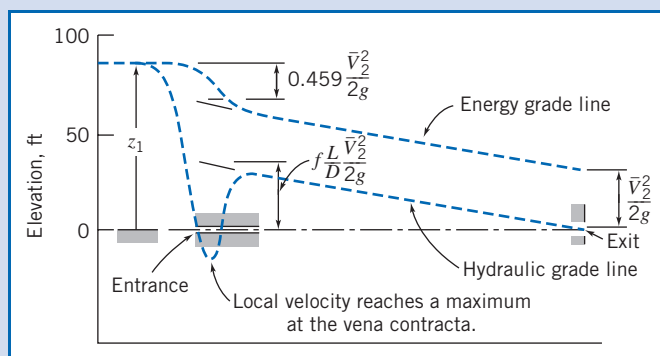
$$\frac{\bar{V}}{U} = \frac{2n^2}{(n+1)(2n+1)} = 0.847 \quad (8.24)$$

Using these results in Eq. 8.27 we find  $\alpha = 1.04$ . Substituting into Eq. 1, we obtain

$$K_{\text{entrance}} = 2 \times 32.2 \frac{\text{ft}}{\text{s}^2} \times 85.1 \text{ ft} \times \frac{\text{s}^2}{(46.1)^2 \text{ ft}^2} - (0.0135) \frac{10 \text{ ft}}{1.5 \text{ in.}} \times 12 \frac{\text{in.}}{\text{ft}} - 1.04$$

$$K_{\text{entrance}} = 0.459 \leftarrow K_{\text{entrance}}$$

This coefficient compares favorably with that shown in Table 8.2. The hydraulic and energy grade lines are shown below. The large head loss in a square-edged entrance is due primarily to separation at the sharp inlet corner and formation of a vena contracta immediately downstream from the corner. The effective flow area reaches a minimum at the vena contracta, so the flow velocity is a maximum there. The flow expands again following the vena contracta to fill the pipe. The uncontrolled expansion following the vena contracta is responsible for most of the head loss. (See Example 8.12.)



Rounding the inlet corner reduces the extent of separation significantly. This reduces the velocity increase through the vena contracta and consequently reduces the head loss caused by the entrance. A “well-rounded” inlet almost eliminates flow separation; the flow pattern approaches that shown in Fig. 8.1. The added head loss in a well-rounded inlet compared with fully developed flow is the result of higher wall shear stresses in the entrance length.

**This problem:**

- ✓ Illustrates a method for obtaining the value of a minor loss coefficient from experimental data.
- ✓ Shows how the EGL and HGL lines first introduced in Section 6.5 for inviscid flow are modified by the presence of major and minor losses. The EGL line continuously drops as mechanical energy is consumed—quite sharply when, for example, we have a square-edged entrance loss; the HGL at each location is lower than the EGL by an amount equal to the local dynamic head  $\bar{V}^2/2g$ —at the vena contracta, for example, the HGL experiences a large drop, then recovers.

### Example 8.10 USE OF DIFFUSER TO INCREASE FLOW RATE

Water rights granted to each citizen by the Emperor of Rome gave permission to attach to the public water main a calibrated, circular, tubular bronze nozzle [23]. Some citizens were clever enough to take unfair advantage of a law that regulated flow rate by such an indirect method. They installed diffusers on the outlets of the nozzles to increase their discharge. Assume the static head available from the main is  $z_0 = 1.5 \text{ m}$  and the nozzle exit diameter is  $D = 25 \text{ mm}$ . (The discharge is to atmospheric pressure.) Determine the increase in flow rate when a diffuser with  $N/R_1 = 3.0$  and  $AR = 2.0$  is attached to the end of the nozzle.

**Given:** Nozzle attached to water main as shown.

**Find:** Increase in discharge when diffuser with  $N/R_1 = 3.0$  and  $AR = 2.0$  is installed.

**Solution:** Apply the energy equation for steady, incompressible pipe flow.

**Governing equation:** 
$$\frac{p_0}{\rho} + \alpha_0 \frac{\bar{V}_0^2}{2} + gz_0 = \frac{p_1}{\rho} + \alpha_1 \frac{\bar{V}_1^2}{2} + gz_1 + h_{l_T} \quad (8.29)$$

**Assumptions:** (1)  $\bar{V}_0 \approx 0$ .  
(2)  $\alpha_1 \approx 1$ .

For the nozzle alone,

$$\begin{aligned} \frac{p_0}{\rho} + \alpha_0 \frac{\bar{V}_0^2}{2} + gz_0 &= \frac{p_1}{\rho} + \alpha_1 \frac{\bar{V}_1^2}{2} + gz_1 + h_{l_T} \\ \frac{p_0}{\rho} + \alpha_0 \frac{\bar{V}_0^2}{2} + gz_0 &\approx \frac{p_1}{\rho} + \alpha_1 \frac{\bar{V}_1^2}{2} + gz_1 + h_{l_T} \\ h_{l_T} &= K_{\text{entrance}} \frac{\bar{V}_1^2}{2} \end{aligned}$$

Thus

$$gz_0 = \frac{\bar{V}_1^2}{2} + K_{\text{entrance}} \frac{\bar{V}_1^2}{2} = (1 + K_{\text{entrance}}) \frac{\bar{V}_1^2}{2} \quad (1)$$

Solving for the velocity and substituting the value of  $K_{\text{entrance}} \approx 0.04$  (from Table 8.2),

$$\bar{V}_1 = \sqrt{\frac{2gz_0}{1.04}} = \sqrt{\frac{2}{1.04} \times 9.81 \frac{\text{m}}{\text{s}^2} \times 1.5 \text{ m}} = 5.32 \text{ m/s}$$

$$Q = \bar{V}_1 A_1 = \bar{V}_1 \frac{\pi D_1^2}{4} = 5.32 \frac{\text{m}}{\text{s}} \times \frac{\pi}{4} \times (0.025)^2 \text{ m}^2 = 0.00261 \text{ m}^3/\text{s} \quad \leftarrow Q$$

For the nozzle with diffuser attached,

$$\begin{aligned} \frac{p_0}{\rho} + \alpha_0 \frac{\bar{V}_0^2}{2} + gz_0 &= \frac{p_1}{\rho} + \alpha_1 \frac{\bar{V}_1^2}{2} + gz_1 + h_{l_T} \\ \frac{p_0}{\rho} + \alpha_0 \frac{\bar{V}_0^2}{2} + gz_0 &\approx \frac{p_1}{\rho} + \alpha_1 \frac{\bar{V}_1^2}{2} + gz_1 + h_{l_T} \\ h_{l_T} &= K_{\text{entrance}} \frac{\bar{V}_1^2}{2} + K_{\text{diffuser}} \frac{\bar{V}_1^2}{2} \end{aligned}$$

or

$$gz_0 = \frac{\bar{V}_1^2}{2} + (K_{\text{entrance}} + K_{\text{diffuser}}) \frac{\bar{V}_1^2}{2} \quad (2)$$

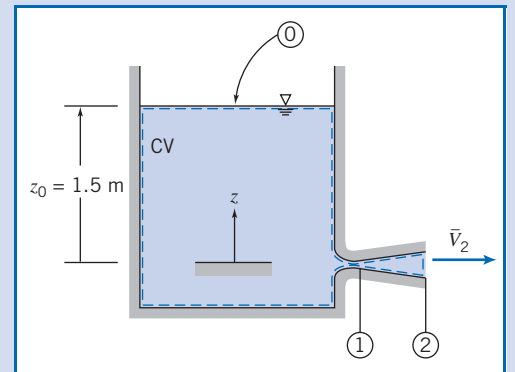
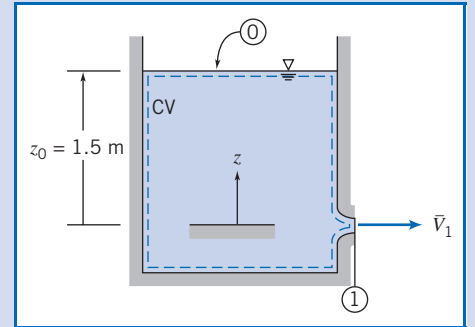
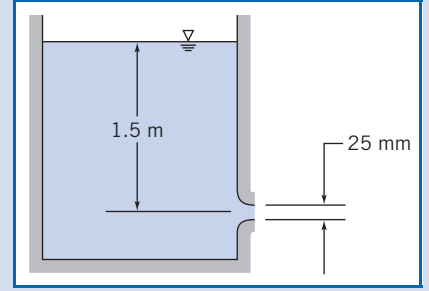
From continuity  $\bar{V}_1 A_1 = \bar{V}_2 A_2$ , so

$$\bar{V}_2 = \bar{V}_1 \frac{A_1}{A_2} = \bar{V}_1 \frac{1}{AR}$$

and Eq. 2 becomes

$$gz_0 = \left[ \frac{1}{(AR)^2} + K_{\text{entrance}} + K_{\text{diffuser}} \right] \frac{\bar{V}_1^2}{2} \quad (3)$$

Figure 8.16 gives data for  $C_p = \frac{p_2 - p_1}{\frac{1}{2} \rho \bar{V}_1^2}$  for diffusers.



To obtain  $K_{\text{diffuser}}$ , apply the energy equation from ① to ②.

$$\frac{p_1}{\rho} + \alpha_1 \frac{\bar{V}_1^2}{2} + g z_1 = \frac{p_2}{\rho} + \alpha_2 \frac{\bar{V}_2^2}{2} + g z_2 + K_{\text{diffuser}} \frac{\bar{V}_1^2}{2}$$

Solving, with  $\alpha_2 \approx 1$ , we obtain

$$K_{\text{diffuser}} = 1 - \frac{\bar{V}_2^2}{\bar{V}_1^2} - \frac{p_2 - p_1}{\frac{1}{2}\rho\bar{V}_1^2} = 1 - \left(\frac{A_1}{A_2}\right)^2 - C_p = 1 - \frac{1}{(AR)^2} - C_p$$

From Fig. 8.16,  $C_p = 0.45$ , so

$$K_{\text{diffuser}} = 1 - \frac{1}{(2.0)^2} - 0.45 = 0.75 - 0.45 = 0.3$$

Solving Eq. 3 for the velocity and substituting the values of  $K_{\text{entrance}}$  and  $K_{\text{diffuser}}$ , we obtain

$$\bar{V}_1^2 = \frac{2gz_0}{0.25 + 0.04 + 0.3}$$

so

$$\bar{V}_1 = \sqrt{\frac{2gz_0}{0.59}} = \sqrt{\frac{2}{0.59} \times 9.81 \frac{\text{m}}{\text{s}^2} \times 1.5 \text{ m}} = 7.06 \text{ m/s}$$

and

$$Q_d = \bar{V}_1 A_1 = \bar{V}_1 \frac{\pi D_1^2}{4} = 7.06 \frac{\text{m}}{\text{s}} \times \frac{\pi}{4} \times (0.025)^2 \text{ m}^2 = 0.00347 \text{ m}^3/\text{s} \longleftarrow Q_d$$

The flow rate increase that results from adding the diffuser is

$$\frac{\Delta Q}{Q} = \frac{Q_d - Q}{Q} = \frac{Q_d}{Q} - 1 = \frac{0.00347}{0.00261} - 1 = 0.330 \quad \text{or} \quad 33 \text{ percent} \longleftarrow \frac{\Delta Q}{Q}$$

Addition of the diffuser significantly increases the flow rate! There are two ways to explain this.

First, we can sketch the EGL and HGL curves—approximately to scale—as shown below. We can see that, as required, the HGL at the exit is zero for both flows (recall that the HGL is the sum of static pressure and potential heads). However, the pressure rises through the diffuser, so the pressure at the diffuser inlet will be, as shown, quite low (below atmospheric). Hence, with the diffuser, the  $\Delta p$  driving force for the nozzle is much larger than that for the bare nozzle, leading to a much greater velocity, and flow rate, at the nozzle exit plane—it is as if the diffuser acted as a suction device on the nozzle.

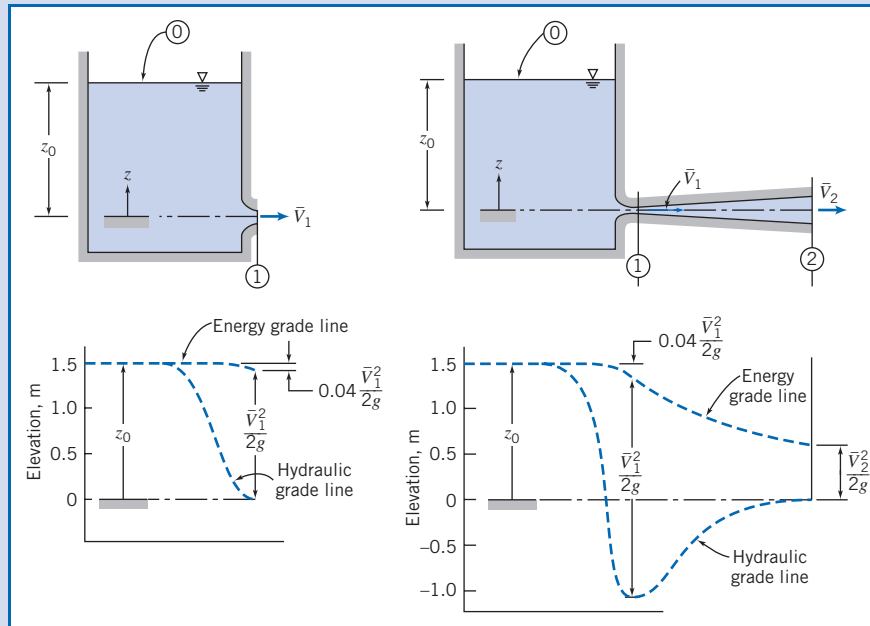
Second, we can examine the energy equations for the two flows (for the bare nozzle Eq. 1, and for the nozzle with diffuser Eq. 3). These equations can be rearranged to yield equations for the velocity at the nozzle exit,

$$\bar{V}_1 = \sqrt{\frac{2gz_0}{1 + K_{\text{entrance}}}} \quad (\text{bare nozzle}) \quad \bar{V}_1 = \sqrt{\frac{2gz_0}{\frac{1}{(AR)^2} + K_{\text{diffuser}} + K_{\text{entrance}}}} \quad (\text{nozzle + diffuser})$$

Comparing these two expressions, we see that the diffuser introduces an extra term (its loss coefficient  $K_{\text{diffuser}} = 0.3$ ) to the denominator, tending to reduce the nozzle velocity, but on the other hand we replace the term 1 (representing loss of the bare nozzle exit plane kinetic energy) with  $1/(AR)^2 = 0.25$  (representing a smaller loss, of the diffuser exit plane kinetic energy). The net effect is that we replace 1 in the denominator with  $0.25 + 0.3 = 0.55$ , leading to a net



increase in the nozzle velocity. The resistance to flow introduced by adding the diffuser is more than made up by the fact that we “throw away” much less kinetic energy at the exit of the device (the exit velocity for the bare nozzle is 5.32 m/s, whereas for the diffuser it is 1.77 m/s).



Water Commissioner Frontinus standardized conditions for all Romans in 97 A.D. He required that the tube attached to the nozzle of each customer’s pipe be the same diameter for at least 50 lineal feet from the public water main (see Problem 8.157).

### \*Multiple-Path Systems

Many real-world pipe systems (e.g., the pipe network that supplies water to the apartments in a large building) consist of a network of pipes of various diameters assembled in a complicated configuration that may contain parallel and series connections. As an example, consider part of a system as shown in Fig. 8.18. Water is supplied at some pressure from a manifold at point 1, and flows through the components shown to the drain at point 5. Some water flows through pipes *A*, *B*, *C*, and *D*, constituting a *series* of pipes (and pipe *B* has a lower flow rate than the others); some flows through *A*, *E*, *F* or *G*, *H*, *C*, and *D* (*F* and *G* are *parallel*), and these two main branches are in *parallel*. We analyze this type of problem in a similar way to how we analyze DC resistor circuits in electrical theory: by applying a few basic rules to the system. The electrical potential at each point in the circuit is analogous to the HGL (or static pressure head if we neglect gravity) at corresponding points in the system. The current in each resistor is analogous to the flow rate in each pipe section. We have the additional difficulty in pipe systems that the resistance to flow in each pipe is a function of the flow rate (electrical resistors are usually considered constant).

The simple rules for analyzing networks can be expressed in various ways. We will express them as follows:

1. The net flow out of any node (junction) is zero.
2. Each node has a unique pressure head (HGL).

\*This section may be omitted without loss of continuity in the text material.

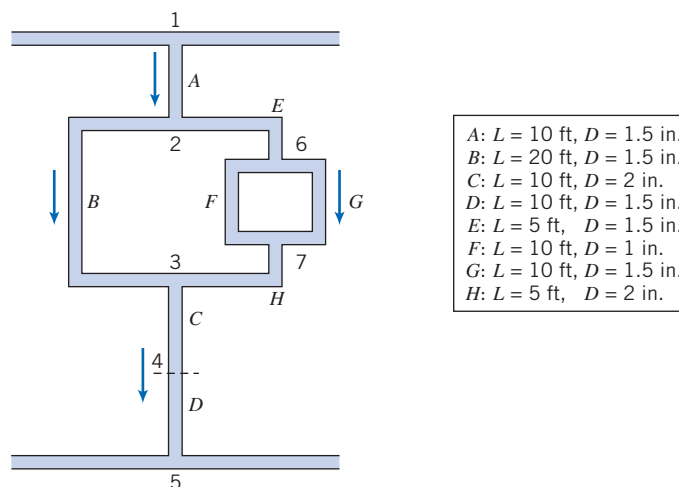


Fig. 8.18 Schematic of part of a pipe network.

For example, in Fig. 8.18 rule 1 means that the flow into node 2 from pipe A must equal the sum of outflows to pipes B and E. Rule 2 means that the pressure head at node 7 must be equal to the head at node 6 less the losses through pipe F or pipe G, as well as equal to the head at node 3 plus the loss in pipe H.

These rules apply in addition to all the pipe-flow constraints we have discussed (e.g., for  $Re \geq 2300$  the flow will be turbulent, and the fact that we may have significant minor losses from features such as sudden expansions). We can anticipate that the flow in pipe F (diameter 1 in.) will be a good deal less than the flow in pipe G (diameter 1.5 in.), and the flow through branch E will be larger than that through branch B (why?).

The problems that arise with pipe networks can be as varied as those we discussed when studying single-path systems, but the most common involve finding the flow delivered to each pipe, given an applied pressure difference. We examine this case in Example 8.11. Obviously, pipe networks are much more difficult and time-consuming to analyze than single-path problems, almost always requiring iterative solution methods, and in practice are usually only solved using the computer. A number of computer schemes for analyzing networks have been developed [24], and many engineering consulting companies use proprietary software applications for such analysis. A spreadsheet such as *Excel* is also very useful for setting up and solving such problems.

### Example 8.11 FLOW RATES IN A PIPE NETWORK

In the section of a cast-iron water pipe network shown in Fig. 8.18, the static pressure head (gage) available at point 1 is 100 ft of water, and point 5 is a drain (atmospheric pressure). Find the flow rates (gpm) in each pipe.

**Given:** Pressure head  $h_{1-5}$  of 100 ft across pipe network.

**Find:** The flow rate in each pipe.

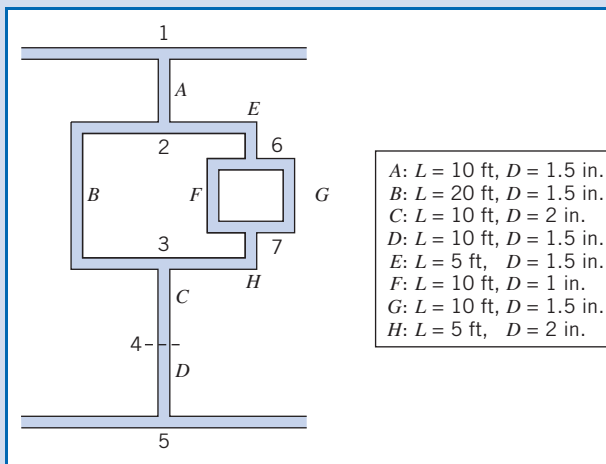
**Solution:**

**Governing equations:**

For each pipe section,

$$\left( \frac{p_1}{\rho} + \alpha_1 \frac{\bar{V}_1^2}{2} + g z_1 \right) - \left( \frac{p_2}{\rho} + \alpha_2 \frac{\bar{V}_2^2}{2} + g z_2 \right) = h_{l_T} = h_l + \sum h_{l_m} \quad (8.29)$$

$\begin{matrix} = 0(1) & & = 0(1) & & = 0(2) \\ \nearrow & & \nearrow & & \nearrow \end{matrix}$



where

$$h_f = f \frac{L}{D} \frac{\bar{V}^2}{2} \quad (8.34)$$

and  $f$  is obtained from either Eq. 8.36 (laminar) or Eq. 8.37 (turbulent). For the cast-iron pipe, Table 8.1 gives a roughness for cast iron of  $e = 0.00085$  ft.

**Assumptions:** (1) Ignore gravity effects.  
(2) Ignore minor losses.

(Assumption 2 is applied to make the analysis clearer—minor losses can be incorporated easily later.)

In addition we have mathematical expressions for the basic rules

1. The net flow out of any node (junction) is zero.
2. Each node has a unique pressure head (HGL).

We can apply basic rule 1 to nodes 2 and 6:

$$\text{Node 2: } Q_A = Q_B + Q_E \quad (1)$$

$$\text{Node 6: } Q_E = Q_F + Q_G \quad (2)$$

and we also have the obvious constraints

$$Q_A = Q_C \quad (3)$$

$$Q_A = Q_D \quad (4)$$

$$Q_E = Q_H \quad (5)$$

We can apply basic rule 2 to obtain the following pressure drop constraints:

$$h_{1-5}: h = h_A + h_B + h_C + h_D \quad (6) \quad h_{2-3}: h_B = h_E + h_F + h_H \quad (7) \quad h_{6-7}: h_F = h_G \quad (8)$$

This set of eight equations (as well as Eqs. 8.29 and 8.34 for each pipe section!) must be solved iteratively. If we were to manually iterate, we would use Eqs. 3, 4, and 5 to immediately reduce the number of unknowns and equations to five ( $Q_A$ ,  $Q_B$ ,  $Q_E$ ,  $Q_F$ ,  $Q_G$ ). There are several approaches to the iteration, one of which is:

1. Make a guess for  $Q_A$ ,  $Q_B$ , and  $Q_F$ .
2. Eqs. 1 and 2 then lead to values for  $Q_E$  and  $Q_G$ .
3. Eqs. 6, 7, and 8 are finally used as a check to see if rule 2 (for unique pressure heads at the nodes) is satisfied.
4. If any of Eqs. 6, 7, or 8 are not satisfied, use knowledge of pipe flow to adjust the values of  $Q_A$ ,  $Q_B$ , or  $Q_F$ .
5. Repeat steps 2 through 5 until convergence occurs.

An example of applying step 4 would be if Eq. 8 were not satisfied. Suppose  $h_F > h_G$ ; then we would have selected too large a value for  $Q_F$ , and would reduce this slightly, and recompute all flow rates and heads.

This iterative process is obviously quite unrealistic for manual calculation (remember that obtaining each head loss  $h$  from each  $Q$  involves a good amount of calculation). Fortunately, we can use a spreadsheet such as *Excel* to automate all these calculations—it will simultaneously solve for all eight unknowns automatically! The first step is to set up one worksheet for each pipe section for computing the pipe head  $h$  given the flow rate  $Q$ . A typical such worksheet is shown below:

Pipe Data			Flow Rate	Computations				
$L$ (ft)	$D$ (in)	$e$ (ft)	$Q$ (ft³/s)	$V$ (ft/s)	$Re$	$e/D$	$f$	$h$ (ft²/s²)
10	1.5	8.50E-04	0.100	8.1	97009	6.80E-03	0.0342	91

In these worksheets, knowing  $L$ ,  $D$ , and  $e$ , a given flow rate  $Q$  is used to compute  $\bar{V}$ ,  $Re$ ,  $f$ , and finally  $h$  from  $L$ ,  $D$ , and  $e$ .

The next step is to set up a calculation page that collects together the flow rates and corresponding head losses for all of the pipe sections, and then use these to check whether Eqs. 1 through 8 are satisfied. Shown below is this page with initial guess values of  $0.1 \text{ ft}^3/\text{s}$  for each of the flow rates. The logic of the workbook is that the eight values entered for  $Q_A$  through  $Q_H$  determine all the other values—that is,  $h_A$  through  $h_H$ , and the values of the constraint equations. The absolute errors for each of the constraint equations are shown, as well as their sum. We can then use *Excel's Solver* feature (repeatedly as necessary) to minimize the total error (currently 735%) by varying  $Q_A$  through  $Q_H$ .

Microsoft Excel - Example 8.11

Available Head:

$h = 100 \text{ ft}$

Flows:

$Q_A (\text{ft}^3/\text{s})$	$Q_B (\text{ft}^3/\text{s})$	$Q_C (\text{ft}^3/\text{s})$	$Q_D (\text{ft}^3/\text{s})$	$Q_E (\text{ft}^3/\text{s})$	$Q_F (\text{ft}^3/\text{s})$	$Q_G (\text{ft}^3/\text{s})$	$Q_H (\text{ft}^3/\text{s})$
0.100	0.100	0.100	0.100	0.100	0.100	0.100	0.100

$Q_A (\text{gpm})$	$Q_B (\text{gpm})$	$Q_C (\text{gpm})$	$Q_D (\text{gpm})$	$Q_E (\text{gpm})$	$Q_F (\text{gpm})$	$Q_G (\text{gpm})$	$Q_H (\text{gpm})$
45	45	45	45	45	45	45	45

Heads:

$h_A (\text{ft}^2/\text{s}^2)$	$h_B (\text{ft}^2/\text{s}^2)$	$h_C (\text{ft}^2/\text{s}^2)$	$h_D (\text{ft}^2/\text{s}^2)$	$h_E (\text{ft}^2/\text{s}^2)$	$h_F (\text{ft}^2/\text{s}^2)$	$h_G (\text{ft}^2/\text{s}^2)$	$h_H (\text{ft}^2/\text{s}^2)$
91	182	20	91	45	778	91	10

$h_A (\text{ft})$	$h_B (\text{ft})$	$h_C (\text{ft})$	$h_D (\text{ft})$	$h_E (\text{ft})$	$h_F (\text{ft})$	$h_G (\text{ft})$	$h_H (\text{ft})$
3	6	1	3	1	24	3	0

Constraints:

$Q_A = Q_C$	$Q_A = Q_D$	$Q_A = Q_B + Q_E$	$Q_E = Q_H$	$Q_E = Q_F + Q_G$
0.0%	0.0%	100.0%	0.0%	100.0%

$h = h_A + h_B + h_C + h_D$  88.1%

$h_B = h_E + h_F + h_H$  358.7%

$h_F = h_G$  88.3%

Error: 735.2%

The final results obtained by *Excel* are:

Microsoft Excel - Example 8.11

Available Head:

$h = 100 \text{ ft}$

Flows:

$Q_A (\text{ft}^3/\text{s})$	$Q_B (\text{ft}^3/\text{s})$	$Q_C (\text{ft}^3/\text{s})$	$Q_D (\text{ft}^3/\text{s})$	$Q_E (\text{ft}^3/\text{s})$	$Q_F (\text{ft}^3/\text{s})$	$Q_G (\text{ft}^3/\text{s})$	$Q_H (\text{ft}^3/\text{s})$
0.373	0.161	0.373	0.373	0.211	0.053	0.158	0.211

$Q_A (\text{gpm})$	$Q_B (\text{gpm})$	$Q_C (\text{gpm})$	$Q_D (\text{gpm})$	$Q_E (\text{gpm})$	$Q_F (\text{gpm})$	$Q_G (\text{gpm})$	$Q_H (\text{gpm})$
167	72	167	167	95	24	71	95

Heads:

$h_A (\text{ft}^2/\text{s}^2)$	$h_B (\text{ft}^2/\text{s}^2)$	$h_C (\text{ft}^2/\text{s}^2)$	$h_D (\text{ft}^2/\text{s}^2)$	$h_E (\text{ft}^2/\text{s}^2)$	$h_F (\text{ft}^2/\text{s}^2)$	$h_G (\text{ft}^2/\text{s}^2)$	$h_H (\text{ft}^2/\text{s}^2)$
1240	469	271	1240	200	224	224	44

$h_A (\text{ft})$	$h_B (\text{ft})$	$h_C (\text{ft})$	$h_D (\text{ft})$	$h_E (\text{ft})$	$h_F (\text{ft})$	$h_G (\text{ft})$	$h_H (\text{ft})$
39	15	8	39	6	7	7	1

Constraints:

$Q_A = Q_C$	$Q_A = Q_D$	$Q_A = Q_B + Q_E$	$Q_E = Q_H$	$Q_E = Q_F + Q_G$
0.0%	0.0%	0.0%	0.0%	0.0%

$h = h_A + h_B + h_C + h_D$  0.0%

$h_B = h_E + h_F + h_H$  0.0%

$h_F = h_G$  0.0%

Error: 0.0%

The flow rates are:

$$\begin{aligned}Q_A &= Q_C = Q_D = 167 \text{ gpm} \\Q_B(\text{gpm}) &= 72 \text{ gpm} \\Q_E(\text{gpm}) &= Q_H(\text{gpm}) = 95 \text{ gpm} \\Q_F(\text{gpm}) &= 24 \text{ gpm} \\Q_G(\text{gpm}) &= 71 \text{ gpm}\end{aligned}$$

This problem illustrates use of *Excel* to solve a set of coupled, nonlinear equations for unknown flow rates. The *Excel* workbook for this problem can be modified for solving a variety of other multiple-path systems.

## PART C Flow Measurement

Throughout this text we have referred to the flow rate  $Q$  or average velocity  $\bar{V}$  in a pipe. The question arises: How does one measure these quantities? We will address this question by discussing the various types of flow meters available.

The choice of a flow meter is influenced by the accuracy required, range, cost, complication, ease of reading or data reduction, and service life. The simplest and cheapest device that gives the desired accuracy should be chosen.

### Direct Methods 8.9

The most obvious way to measure flow rate in a pipe is the *direct method*—simply measure the amount of fluid that accumulates in a container over a fixed time period! Tanks can be used to determine flow rate for steady liquid flows by measuring the volume or mass of liquid collected during a known time interval. If the time interval is long enough to be measured accurately, flow rates may be determined precisely in this way.

Compressibility must be considered in volume measurements for gas flows. The densities of gases generally are too small to permit accurate direct measurement of mass flow rate. However, a volume sample often can be collected by displacing a “bell,” or inverted jar over water (if the pressure is held constant by counterweights). If volume or mass measurements are set up carefully, no calibration is required; this is a great advantage of direct methods.

In specialized applications, particularly for remote or recording uses, *positive displacement* flow meters may be specified, in which the fluid moves a component such as a reciprocating piston or oscillating disk as it passes through the device. Common examples include household water and natural gas meters, which are calibrated to read directly in units of product, or gasoline metering pumps, which measure total flow and automatically compute the cost. Many positive-displacement meters are available commercially. Consult manufacturers’ literature or References (e.g., [25]) for design and installation details.

### Restriction Flow Meters for Internal Flows 8.10

Most restriction flow meters for internal flow (except the laminar flow element, discussed shortly) are based on acceleration of a fluid stream through some form of nozzle, as shown schematically in Fig. 8.19. The idea is that the change in velocity

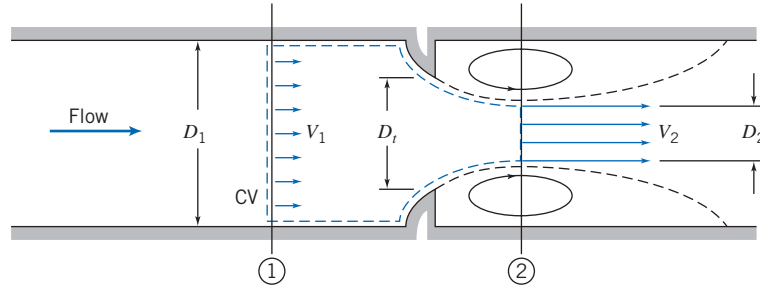


**Fig. 8.19** Internal flow through a generalized nozzle, showing control volume used for analysis.

leads to a change in pressure. This  $\Delta p$  can be measured using a pressure gage (electronic or mechanical) or a manometer, and the flow rate inferred using either a theoretical analysis or an experimental correlation for the device. Flow separation at the sharp edge of the nozzle throat causes a recirculation zone to form, as shown by the dashed lines downstream from the nozzle. The mainstream flow continues to accelerate from the nozzle throat to form a *vena contracta* at section ② and then decelerates again to fill the duct. At the vena contracta, the flow area is a minimum, the flow streamlines are essentially straight, and the pressure is uniform across the channel section.

The theoretical flow rate may be related to the pressure differential between sections ① and ② by applying the continuity and Bernoulli equations. Then empirical correction factors may be applied to obtain the actual flow rate.

Basic equations:

We will need mass-conservation,

$$\sum_{CS} \vec{V} \cdot \vec{A} = 0 \quad (4.13b)$$

[we can use this instead of Eq. 4.12, because of assumption (5) below] and the Bernoulli equation,

$$\frac{p_1}{\rho} + \frac{V_1^2}{2} + g z_1 = \frac{p_2}{\rho} + \frac{V_2^2}{2} + g z_2 \quad (6.8)$$

which we can use if assumption (4) is valid. For the short section of pipe considered, this is reasonable.

- Assumptions:
- (1) Steady flow.
  - (2) Incompressible flow.
  - (3) Flow along a streamline.
  - (4) No friction.
  - (5) Uniform velocity at sections ① and ②.
  - (6) No streamline curvature at sections ① or ②, so pressure is uniform across those sections.
  - (7)  $z_1 = z_2$ .

Then, from the Bernoulli equation,

$$p_1 - p_2 = \frac{\rho}{2} (V_2^2 - V_1^2) = \frac{\rho V_2^2}{2} \left[ 1 - \left( \frac{V_1}{V_2} \right)^2 \right]$$

and from continuity

$$(-\rho V_1 A_1) + (\rho V_2 A_2) = 0$$

or

$$V_1 A_1 = V_2 A_2 \quad \text{so} \quad \left( \frac{V_1}{V_2} \right)^2 = \left( \frac{A_2}{A_1} \right)^2$$

Substituting gives

$$p_1 - p_2 = \frac{\rho V_2^2}{2} \left[ 1 - \left( \frac{A_2}{A_1} \right)^2 \right]$$

Solving for the theoretical velocity,  $V_2$ ,

$$V_2 = \sqrt{\frac{2(p_1 - p_2)}{\rho[1 - (A_2/A_1)^2]}} \quad (8.51)$$

The theoretical mass flow rate is then given by

$$\begin{aligned} \dot{m}_{\text{theoretical}} &= \rho V_2 A_2 \\ &= \rho \sqrt{\frac{2(p_1 - p_2)}{\rho[1 - (A_2/A_1)^2]}} A_2 \end{aligned}$$

or

$$\dot{m}_{\text{theoretical}} = \frac{A_2}{\sqrt{1 - (A_2/A_1)^2}} \sqrt{2\rho(p_1 - p_2)} \quad (8.52)$$

Equation 8.52 shows that, under our set of assumptions, for a given fluid ( $\rho$ ) and flow meter geometry ( $A_1$  and  $A_2$ ), the flow rate is directly proportional to the square root of the pressure drop across the meter taps,

$$\dot{m}_{\text{theoretical}} \propto \sqrt{\Delta p}$$

which is the basic idea of these devices. This relationship limits the flow rates that can be measured accurately to approximately a 4:1 range.

Several factors limit the utility of Eq. 8.52 for calculating the actual mass flow rate through a meter. The actual flow area at section ② is unknown when the vena contracta is pronounced (e.g., for orifice plates when  $D_t$  is a small fraction of  $D_1$ ). The velocity profiles approach uniform flow only at large Reynolds numbers. Frictional effects can become important (especially downstream from the meter) when the meter contours are abrupt. Finally, the location of pressure taps influences the differential pressure reading.

The theoretical equation is adjusted for Reynolds number and diameter ratio  $D_t/D_1$  by defining an empirical *discharge coefficient*  $C$  such that, replacing Eq. 8.52, we have

$$\dot{m}_{\text{actual}} = \frac{CA_t}{\sqrt{1 - (A_t/A_1)^2}} \sqrt{2\rho(p_1 - p_2)} \quad (8.53)$$

Letting  $\beta = D_t/D_1$ , then  $(A_t/A_1)^2 = (D_t/D_1)^4 = \beta^4$ , so

$$\dot{m}_{\text{actual}} = \frac{CA_t}{\sqrt{1 - \beta^4}} \sqrt{2\rho(p_1 - p_2)} \quad (8.54)$$

In Eq. 8.54,  $1/\sqrt{1 - \beta^4}$  is the *velocity-of-approach factor*. The discharge coefficient and velocity-of-approach factor frequently are combined into a single *flow coefficient*,

$$K \equiv \frac{C}{\sqrt{1 - \beta^4}} \quad (8.55)$$

In terms of this flow coefficient, the actual mass flow rate is expressed as

$$\dot{m}_{\text{actual}} = KA_t \sqrt{2\rho(p_1 - p_2)} \quad (8.56)$$



For standardized metering elements, test data [25, 26] have been used to develop empirical equations that predict discharge and flow coefficients from meter bore, pipe diameter, and Reynolds number. The accuracy of the equations (within specified ranges) usually is adequate so that the meter can be used without calibration. If the Reynolds number, pipe size, or bore diameter fall outside the specified range of the equation, the coefficients must be measured experimentally.

For the turbulent flow regime (pipe Reynolds number greater than 4000) the discharge coefficient may be expressed by an equation of the form [25]

$$C = C_{\infty} + \frac{b}{Re_{D_1}^n} \quad (8.57)$$

The corresponding form for the flow-coefficient equation is

$$K = K_{\infty} + \frac{1}{\sqrt{1 - \beta^4}} \frac{b}{Re_{D_1}^n} \quad (8.58)$$

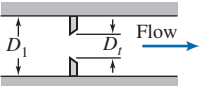
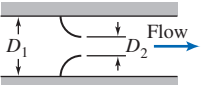
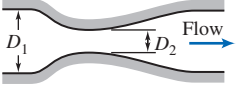
In Eqs. 8.57 and 8.58, subscript  $\infty$  denotes the coefficient at infinite Reynolds number; constants  $b$  and  $n$  allow for scaling to finite Reynolds numbers. Correlating equations and curves of coefficients versus Reynolds number are given in the next three subsections, following a general comparison of the characteristics of specific metering elements.

As we have noted, selection of a flow meter depends on factors such as cost, accuracy, need for calibration, and ease of installation and maintenance. Some of these factors are compared for *orifice plate*, *flow nozzle*, and *venturi* meters in Table 8.6. Note that a high head loss means that the running cost of the device is high—it will consume a lot of the fluid energy. A high initial cost must be amortized over the life of the device. This is an example of a common cost calculation for a company (and an individual!)—between a high initial but low running cost, or low initial but high running cost.

Flow meter coefficients reported in the literature have been measured with fully developed turbulent velocity distributions at the meter inlet (Section ①). If a flow meter is to be installed downstream from a valve, elbow, or other disturbance, a straight section of pipe must be placed in front of the meter. Approximately 10 diameters of straight pipe are required for venturi meters, and up to 40 diameters for orifice plate or flow nozzle meters. When a meter has been properly installed, the flow rate may be computed from Eq. 8.54 or 8.56, after choosing an appropriate value for the empirical discharge coefficient,  $C$ , or flow coefficient,  $K$ , defined in Eqs. 8.53 and 8.55, respectively. Some design data for incompressible flow are given in the next few sections. The same basic methods can be extended to compressible flows, but these will not be treated here. For complete details, see Miller [25] or Bean [26].

Table 8.6

Characteristics of Orifice, Flow Nozzle, and Venturi Flow Meters

Flow Meter Type	Diagram	Head Loss	Initial Cost
Orifice		High	Low
Flow Nozzle		Intermediate	Intermediate
Venturi		Low	High



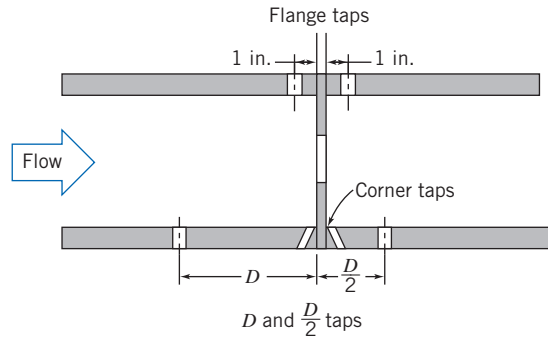


Fig. 8.20 Orifice geometry and pressure tap locations [25].

## The Orifice Plate

The orifice plate (Fig. 8.20) is a thin plate that may be clamped between pipe flanges. Since its geometry is simple, it is low in cost and easy to install or replace. The sharp edge of the orifice will not foul with scale or suspended matter. However, suspended matter can build up at the inlet side of a concentric orifice in a horizontal pipe; an eccentric orifice may be placed flush with the bottom of the pipe to avoid this difficulty. The primary disadvantages of the orifice are its limited capacity and the high permanent head loss caused by the uncontrolled expansion downstream from the metering element.

Pressure taps for orifices may be placed in several locations, as shown in Fig. 8.20 (see [25] or [26] for additional details). Since the location of the pressure taps influences the empirically determined flow coefficient, one must select handbook values of  $C$  or  $K$  consistent with the location of pressure taps.

The correlating equation recommended for a concentric orifice with corner taps [25] is

$$C = 0.5959 + 0.0312\beta^{2.1} - 0.184\beta^8 + \frac{91.71\beta^{2.5}}{Re_{D_1}^{0.75}} \quad (8.59)$$

Equation 8.59 is the form of Eq. 8.57 for the discharge coefficient  $C$  for the orifice plate; it predicts orifice discharge coefficients within  $\pm 0.6$  percent for  $0.2 < \beta < 0.75$  and for  $10^4 < Re_{D_1} < 10^7$ . Some flow coefficients calculated from Eq. 8.59 and 8.55 are presented in Fig. 8.21.

A similar correlating equation is available for orifice plates with  $D$  and  $D/2$  taps. Flange taps require a different correlation for every line size. Pipe taps, located at  $2\frac{1}{2}$  and  $8D$ , no longer are recommended for accurate work.

Example 8.12, which appears later in this section, illustrates the application of flow coefficient data to orifice sizing.

## The Flow Nozzle

Flow nozzles may be used as metering elements in either plenums or ducts, as shown in Fig. 8.22; the nozzle section is approximately a quarter ellipse. Design details and recommended locations for pressure taps are given in [26].

The correlating equation recommended for an ASME long-radius flow nozzle [25] is

$$C = 0.9975 - \frac{6.53\beta^{0.5}}{Re_{D_1}^{0.5}} \quad (8.60)$$

Equation 8.60 is the form of Eq. 8.57 for the discharge coefficient  $C$  for the flow nozzle; it predicts discharge coefficients for flow nozzles within  $\pm 2.0$  percent for

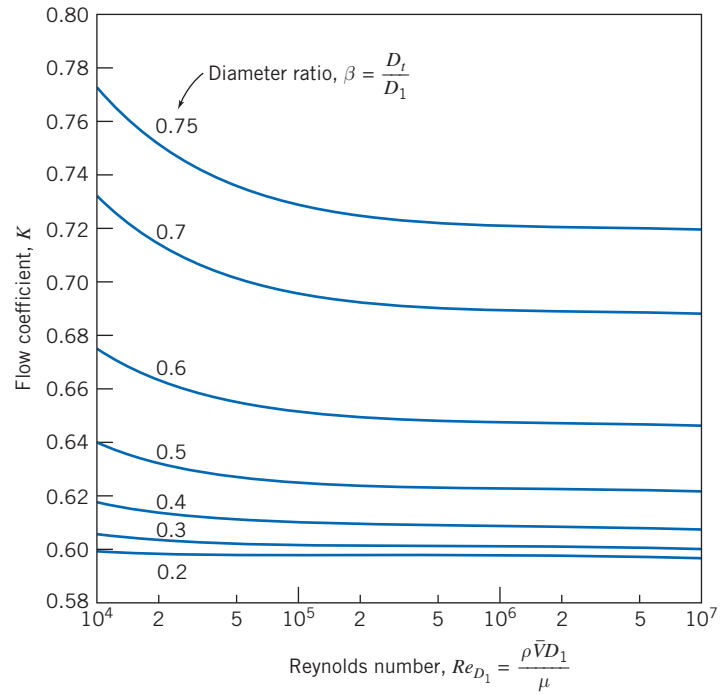


**Fig. 8.21** Flow coefficients for concentric orifices with corner taps.

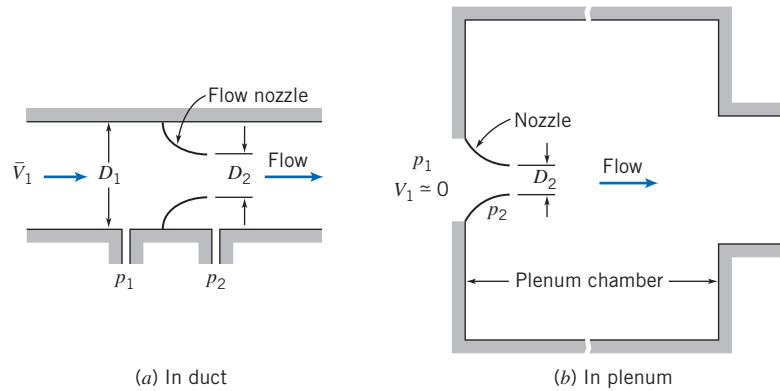


**Fig. 8.22** Typical installations of nozzle flow meters.

$0.25 < \beta < 0.75$  for  $10^4 < Re_{D_1} < 10^7$ . Some flow coefficients calculated from Eq. 8.60 and Eq. 8.55 are presented in Fig. 8.23. ( $K$  can be greater than one when the velocity-of-approach factor exceeds one.)

### a. Pipe Installation

For pipe installation,  $K$  is a function of  $\beta$  and  $Re_{D_1}$ . Figure 8.23 shows that  $K$  is essentially independent of Reynolds number for  $Re_{D_1} > 10^6$ . Thus at high flow rates, the flow rate may be computed directly using Eq. 8.56. At lower flow rates, where  $K$  is a weak function of Reynolds number, iteration may be required.

### b. Plenum Installation

For plenum installation, nozzles may be fabricated from spun aluminum, molded fiberglass, or other inexpensive materials. Thus they are simple and cheap to make

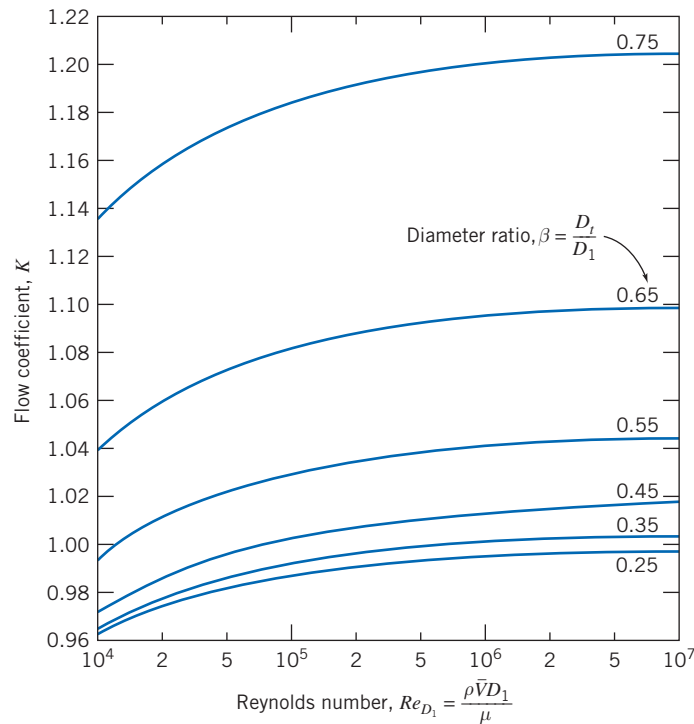


Fig. 8.23 Flow coefficients for ASME long-radius flow nozzles.

and install. Since the plenum pressure is equal to  $p_2$ , the location of the downstream pressure tap is not critical. Meters suitable for a wide range of flow rates may be made by installing several nozzles in a plenum. At low flow rates, most of them may be plugged. For higher flow rates, more nozzles may be used.

For plenum nozzles  $\beta = 0$ , which is outside the range of applicability of Eq. 8.58. Typical flow coefficients are in the range,  $0.95 < K < 0.99$ ; the larger values apply at high Reynolds numbers. Thus the mass rate of flow can be computed within approximately  $\pm 2$  percent using Eq. 8.56 with  $K = 0.97$ .

## The Venturi

Venturi meters, as sketched in Table 8.6, are generally made from castings and machined to close tolerances to duplicate the performance of the standard design. As a result, venturi meters are heavy, bulky, and expensive. The conical diffuser section downstream from the throat gives excellent pressure recovery; therefore, overall head loss is low. Venturi meters are also self-cleaning because of their smooth internal contours.

Experimental data show that discharge coefficients for venturi meters range from 0.980 to 0.995 at high Reynolds numbers ( $Re_{D_1} > 2 \times 10^5$ ). Thus  $C = 0.99$  can be used to measure mass flow rate within about  $\pm 1$  percent at high Reynolds number [25]. Consult manufacturers' literature for specific information at Reynolds numbers below  $10^5$ .

The orifice plate, flow nozzle, and venturi all produce pressure differentials proportional to the square of the flow rate, according to Eq. 8.56. In practice, a meter size must be chosen to accommodate the highest flow rate expected. Because the relationship of pressure drop to flow rate is nonlinear, the range of flow rate that can be measured accurately is limited. Flow meters with single throats usually are considered only for flow rates over a 4:1 range [25].

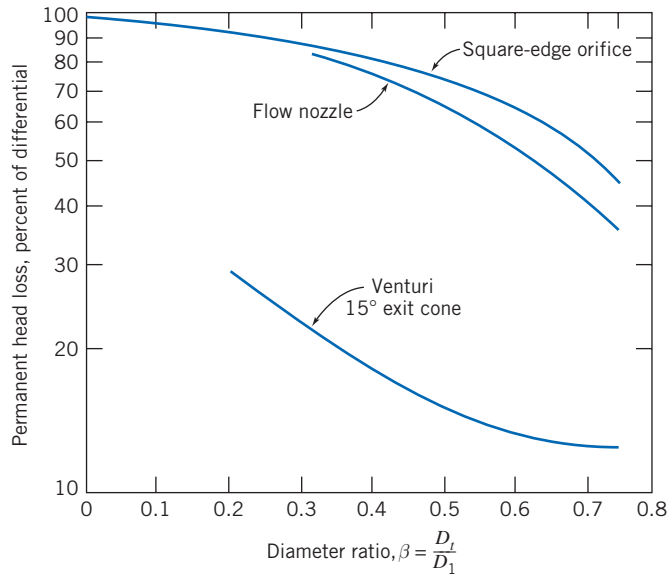


**Fig. 8.24** Permanent head loss produced by various flow metering elements [25].

The unrecoverable loss in head across a metering element may be expressed as a fraction of the differential pressure,  $\Delta p$ , across the element. Pressure losses are displayed as functions of diameter ratio in Fig. 8.24 [25]. Note that the venturi meter has a much lower permanent head loss than the orifice (which has the highest loss) or nozzle, confirming the trends we summarized in Table 8.6.

### The Laminar Flow Element

The *laminar flow element*<sup>3</sup> is designed to produce a pressure differential directly proportional to flow rate. The idea is that the laminar flow element (LFE) contains a metering section in which the flow passes through a large number of tubes or passages (these often look like a bunch of straws) that are each narrow enough that the flow through them is laminar, regardless of the flow conditions in the main pipe (recall that  $Re_{\text{tube}} = \rho V_{\text{tube}} D_{\text{tube}} / \mu$ , so if  $D_{\text{tube}}$  is made small enough we can ensure that  $Re_{\text{tube}} < Re_{\text{crit}} \approx 2300$ ). For each laminar flow tube we can apply the results of Section 8.3, specifically

$$Q_{\text{tube}} = \frac{\pi D_{\text{tube}}^4}{128 \mu L_{\text{tube}}} \Delta p \propto \Delta p \quad (8.13c)$$

so the flow rate in each tube is a linear function of the pressure drop across the device. The flow rate in the whole pipe will be the sum of each of these tube flows, and so will also be a linear function of pressure drop. Usually this linear relation is provided in a calibration from the manufacturer, and the LFE can be used over a 10:1 range of flow rates. The relationship between pressure drop and flow rate for laminar flow also depends on viscosity, which is a strong function of temperature. Therefore, the fluid temperature must be known to obtain accurate metering with an LFE.

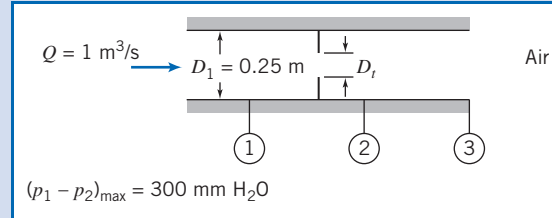
A laminar flow element costs approximately as much as a venturi, but it is much lighter and smaller. Thus the LFE is becoming widely used in applications where compactness and extended range are important.

<sup>3</sup>Patented and manufactured by Meriam Instrument Co., 10920 Madison Ave., Cleveland, Ohio 44102.

### Example 8.12 FLOW THROUGH AN ORIFICE METER

An air flow rate of  $1 \text{ m}^3/\text{s}$  at standard conditions is expected in a  $0.25\text{-m}$  diameter duct. An orifice meter is used to measure the rate of flow. The manometer available to make the measurement has a maximum range of  $300 \text{ mm}$  of water. What diameter orifice plate should be used with corner taps? Analyze the head loss if the flow area at the vena contracta is  $A_2 = 0.65 A_t$ . Compare with data from Fig. 8.24.

**Given:** Flow through duct and orifice as shown.



- Find:** (a)  $D_t$ .  
 (b) Head loss between sections ① and ②.  
 (c) Degree of agreement with data from Fig. 8.24.

**Solution:**

The orifice plate may be designed using Eq. 8.56 and data from Fig. 8.21.

**Governing equation:**

$$\dot{m}_{\text{actual}} = K A_t \sqrt{2\rho(p_1 - p_2)} \quad (8.56)$$

- Assumptions:** (1) Steady flow.  
 (2) Incompressible flow.

Since  $A_t/A_1 = (D_t/D_1)^2 = \beta^2$ ,

$$\dot{m}_{\text{actual}} = K \beta^2 A_1 \sqrt{2\rho(p_1 - p_2)}$$

or

$$\begin{aligned} K \beta^2 &= \frac{\dot{m}_{\text{actual}}}{A_1 \sqrt{2\rho(p_1 - p_2)}} = \frac{\rho Q}{A_1 \sqrt{2\rho(p_1 - p_2)}} = \frac{Q}{A_1} \sqrt{\frac{\rho}{2(p_1 - p_2)}} \\ &= \frac{Q}{A_1} \sqrt{\frac{\rho}{2g\rho_{\text{H}_2\text{O}}\Delta h}} \\ &= 1 \frac{\text{m}^3}{\text{s}} \times \frac{4}{\pi} \frac{1}{(0.25)^2 \text{ m}^2} \left[ \frac{1}{2} \times 1.23 \frac{\text{kg}}{\text{m}^3} \times \frac{\text{s}^2}{9.81 \text{ m}} \times \frac{\text{m}^3}{999 \text{ kg}} \times \frac{1}{0.30 \text{ m}} \right]^{1/2} \\ K \beta^2 &= 0.295 \quad \text{or} \quad K = \frac{0.295}{\beta^2} \quad (1) \end{aligned}$$

Since  $K$  is a function of both  $\beta$  (Eq. 1) and  $Re_{D_1}$  (Fig. 8.21), we must iterate to find  $\beta$ . The duct Reynolds number is

$$\begin{aligned} Re_{D_1} &= \frac{\rho \bar{V}_1 D_1}{\mu} = \frac{\rho (Q/A_1) D_1}{\mu} = \frac{4Q}{\pi \nu D_1} \\ Re_{D_1} &= \frac{4}{\pi} \times 1 \frac{\text{m}^3}{\text{s}} \times \frac{\text{s}}{1.46 \times 10^{-5} \text{ m}^2} \times \frac{1}{0.25 \text{ m}} = 3.49 \times 10^5 \end{aligned}$$

Guess  $\beta = 0.75$ . From Fig. 8.21,  $K$  should be 0.72. From Eq. 1,

$$K = \frac{0.295}{(0.75)^2} = 0.524$$

Thus our guess for  $\beta$  is too large. Guess  $\beta = 0.70$ . From Fig. 8.21,  $K$  should be 0.69. From Eq. 1,

$$K = \frac{0.295}{(0.70)^2} = 0.602$$

Thus our guess for  $\beta$  is still too large. Guess  $\beta = 0.65$ . From Fig. 8.21,  $K$  should be 0.67. From Eq. 1,

$$K = \frac{0.295}{(0.65)^2} = 0.698$$

There is satisfactory agreement with  $\beta \simeq 0.66$  and

$$D_t = \beta D_1 = 0.66(0.25 \text{ m}) = 0.165 \text{ m} \quad \leftarrow \overbrace{\hspace{10em}}^{D_t}$$

To find the permanent head loss for this device, we could simply use the diameter ratio  $\beta \approx 0.66$  in Fig. 8.24; but instead we will find it from the given data. To evaluate the permanent head loss, apply Eq. 8.29 between sections ① and ③.

**Governing equation:**

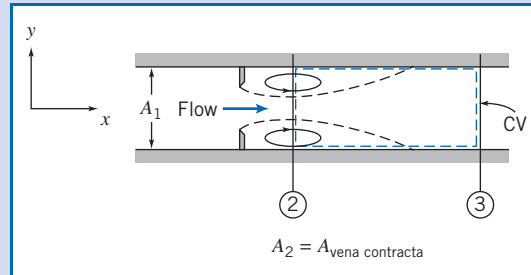
$$\left( \frac{p_1}{\rho} + \alpha_1 \frac{\bar{V}_1^2}{2} + g z_1 \right) - \left( \frac{p_3}{\rho} + \alpha_3 \frac{\bar{V}_3^2}{2} + g z_3 \right) = h_{lr} \quad (8.29)$$

**Assumptions:** (3)  $\alpha_1 \bar{V}_1^2 = \alpha_3 \bar{V}_3^2$ .  
(4) Neglect  $\Delta z$ .

Then

$$h_{lr} = \frac{p_1 - p_3}{\rho} = \frac{p_1 - p_2 - (p_3 - p_2)}{\rho} \quad (2)$$

Equation 2 indicates our approach: We will find  $p_1 - p_3$  by using  $p_1 - p_2 = 300 \text{ mm H}_2\text{O}$ , and obtain a value for  $p_3 - p_2$  by applying the  $x$  component of the momentum equation to a control volume between sections ② and ③.



$$= 0(5) = 0(1)$$

**Governing equation:**

$$F_{S_x} + F_{B_x} = \frac{\partial}{\partial t} \int_{CV} u \rho dV + \int_{CS} u \rho \vec{V} \cdot d\vec{A} \quad (4.18a)$$

**Assumptions:** (5)  $F_{B_x} = 0$   
(6) Uniform flow at sections ② and ③.  
(7) Pressure uniform across duct at sections ② and ③.  
(8) Neglect friction force on CV.

Then, simplifying and rearranging,

$$(p_2 - p_3) A_1 = u_2(-\rho \bar{V}_2 A_2) + u_3(\rho \bar{V}_3 A_3) = (u_3 - u_2) \rho Q = (\bar{V}_3 - \bar{V}_2) \rho Q$$

or

$$p_3 - p_2 = (\bar{V}_2 - \bar{V}_3) \frac{\rho Q}{A_1}$$

Now  $\bar{V}_3 = Q/A_1$ , and

$$\bar{V}_2 = \frac{Q}{A_2} = \frac{Q}{0.65 A_t} = \frac{Q}{0.65 \beta^2 A_1}$$

Thus,

$$\begin{aligned} p_3 - p_2 &= \frac{\rho Q^2}{A_1^2} \left[ \frac{1}{0.65 \beta^2} - 1 \right] \\ p_3 - p_2 &= 1.23 \frac{\text{kg}}{\text{m}^3} \times (1)^2 \frac{\text{m}^6}{\text{s}^2} \times \frac{4^2}{\pi^2} \frac{1}{(0.25)^4 \text{m}^4} \left[ \frac{1}{0.65(0.66)^2} - 1 \right] \frac{\text{N} \cdot \text{s}^2}{\text{kg} \cdot \text{m}} \\ p_3 - p_2 &= 1290 \text{ N/m}^2 \end{aligned}$$

The diameter ratio,  $\beta$ , was selected to give maximum manometer deflection at maximum flow rate. Thus

$$p_1 - p_2 = \rho_{\text{H}_2\text{O}} g \Delta h = 999 \frac{\text{kg}}{\text{m}^3} \times 9.81 \frac{\text{m}}{\text{s}^2} \times 0.30 \text{ m} \times \frac{\text{N} \cdot \text{s}^2}{\text{kg} \cdot \text{m}} = 2940 \text{ N/m}^2$$

Substituting into Eq. 2 gives

$$\begin{aligned} h_{tr} &= \frac{p_1 - p_3}{\rho} = \frac{p_1 - p_2 - (p_3 - p_2)}{\rho} \\ h_{tr} &= (2940 - 1290) \frac{\text{N}}{\text{m}^2} \times \frac{\text{m}^3}{1.23 \text{ kg}} = 1340 \text{ N} \cdot \text{m/kg} \leftarrow h_{tr} \end{aligned}$$

To compare with Fig. 8.24, express the permanent pressure loss as a fraction of the meter differential

$$\frac{p_1 - p_3}{p_1 - p_2} = \frac{(2940 - 1290) \text{ N/m}^2}{2940 \text{ N/m}^2} = 0.561$$

The fraction from Fig. 8.24 is about 0.57. This is satisfactory agreement!

This problem illustrates flow meter calculations and shows use of the momentum equation to compute the pressure rise in a sudden expansion.

## Linear Flow Meters 8.11

The disadvantage of restriction flow meters (except the LFE) is that the measured output ( $\Delta p$ ) is not linear with the flow rate  $Q$ . Several flow meter types produce outputs that are directly proportional to flow rate. These meters produce signals without the need to measure differential pressure. The most common linear flow meters are discussed briefly in the following paragraphs.

*Float meters* may be used to indicate flow rate directly for liquids or gases. An example is shown in Fig. 8.25. In operation, the ball or float is carried upward in the tapered clear tube by the flowing fluid until the drag force and float weight are in equilibrium. Such meters (often called *rotameters*) are available with factory calibration for a number of common fluids and flow rate ranges.

A free-running vaned impeller may be mounted in a cylindrical section of tube (Fig. 8.26) to make a *turbine flow meter*. With proper design, the rate of rotation of the impeller may be made closely proportional to volume flow rate over a wide range.

Rotational speed of the turbine element can be sensed using a magnetic or modulated carrier pickup external to the meter. This sensing method therefore requires no penetrations or seals in the duct. Thus turbine flow meters can be used

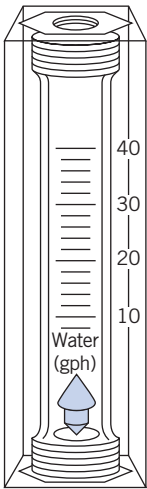


**Fig. 8.25** Float-type variable-area flow meter. (Courtesy of Dwyer Instrument Co., Michigan City, Indiana.)

safely to measure flow rates in corrosive or toxic fluids. The electrical signal can be displayed, recorded, or integrated to provide total flow information.

An interesting device is the *vortex flow meter*. This device takes advantage of the fact that a uniform flow will generate a vortex street when it encounters a bluff body such as a cylinder perpendicular to the flow. A vortex street is a series of alternating vortices shed from the rear of the body; the alternation generates an oscillating sideways force on, and therefore oscillation of, the cylinder (the classic example of this being the “singing” of telephone wires in a high wind). It turns out that the dimensionless group characterizing this phenomenon is the Strouhal number,  $St = fL/V$  ( $f$  is the vortex shedding frequency,  $L$  is the cylinder diameter, and  $V$  is the freestream velocity), and it is approximately constant ( $St \approx 0.21$ ). Hence we have a device for which  $V \propto f$ . Measurement of  $f$  thus directly indicates the velocity  $\bar{V}$  (however, the velocity profile does affect the shedding frequency so calibration is required). The cylinder used in a flow meter is usually quite short in length—10 mm or less—and placed perpendicular to the flow (and for some devices is not a cylinder at all but some other small bluff object). The oscillation can be measured using a strain gage or other sensor. Vortex flow meters can be used over a 20:1 range of flow rates [25].

The *electromagnetic flow meter* uses the principle of magnetic induction. A magnetic field is created across a pipe. When a conductive fluid passes through the field, a voltage is generated at right angles to the field and velocity vectors. Electrodes placed on a pipe diameter are used to detect the resulting signal voltage. The signal voltage is proportional to the average axial velocity when the profile is axisymmetric.

*Magnetic flow meters* may be used with liquids that have electrical conductivities above 100 microsiemens per meter (1 siemen = 1 ampere per volt). The minimum flow speed should be above about 0.3 m/s, but there are no restrictions on Reynolds number. The flow rate range normally quoted is 10:1 [25].

*Ultrasonic flow meters* also respond to average velocity at a pipe cross section. Two principal types of ultrasonic meters are common: Propagation time is measured for clean liquids, and reflection frequency shift (Doppler effect) is measured for flows carrying particulates. The speed of an acoustic wave increases in the flow direction and decreases when transmitted against the flow. For clean liquids, an acoustic path inclined to the pipe axis is used to infer flow velocity. Multiple paths are used to estimate the volume flow rate accurately.

Doppler effect ultrasonic flow meters depend on reflection of sonic waves (in the MHz range) from scattering particles in the fluid. When the particles move at flow speed, the frequency shift is proportional to flow speed; for a suitably chosen path, output is proportional to volume flow rate. One or two transducers may be used; the meter may be clamped to the outside of the pipe. Ultrasonic meters may require calibration in place. Flow rate range is 10:1 [25].

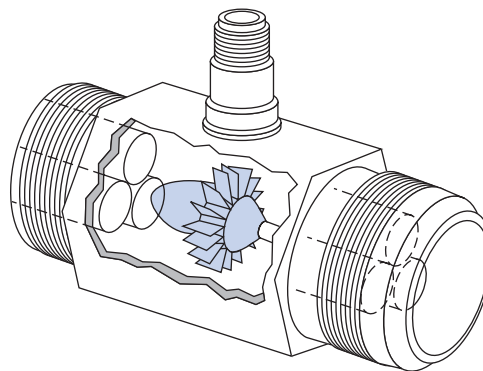


**Fig. 8.26** Turbine flow meter. (Courtesy of Potter Aeronautical Corp., Union, New Jersey.)



## Traversing Methods 8.12

In situations such as in air handling or refrigeration equipment, it may be impractical or impossible to install fixed flow meters. In such cases it may be possible to obtain flow rate data using traversing techniques.

To make a flow rate measurement by traverse, the duct cross section is conceptually subdivided into segments of equal area. The velocity is measured at the center of each area segment using a pitot tube, a total head tube, or a suitable anemometer. The volume flow rate for each segment is approximated by the product of the measured velocity and the segment area. The flow rate through the entire duct is the sum of these segmental flow rates. Details of recommended procedures for flow rate measurements by the traverse method are given in [27].

Use of *pitot* or *pitot-static tubes* for traverse measurements requires direct access to the flow field. Pitot tubes give uncertain results when pressure gradients or streamline curvature are present, and their response times are slow. Two types of anemometers—*thermal anemometers* and *laser Doppler anemometers* (LDAs)—overcome these difficulties partially, although they introduce new complications.

Thermal anemometers use tiny elements (either hot-wire or hot-film elements) that are heated electrically. Sophisticated electronic feedback circuits are used to maintain the temperature of the element constant and to sense the input heating rate needed to do this. The heating rate is related to the local flow velocity by calibration (a higher velocity leads to more heat transfer). The primary advantage of thermal anemometers is the small size of the sensing element. Sensors as small as 0.002 mm in diameter and 0.1 mm long are available commercially. Because the thermal mass of such tiny elements is extremely small, their response to fluctuations in flow velocity is rapid. Frequency responses to the 50 kHz range have been quoted [28]. Thus thermal anemometers are ideal for measuring turbulence quantities. Insulating coatings may be applied to permit their use in conductive or corrosive gases or liquids.

Because of their fast response and small size, thermal anemometers are used extensively for research. Numerous schemes have been published for treating the resulting data [29]. Digital processing techniques, including fast Fourier transforms, can be applied to the signals to obtain mean values and moments, and to analyze frequency content and correlations.

### VIDEO

*Flow Visualization: Laser Induced Fluorescence.*

### VIDEO

*Laser Doppler Anemometry (Animation).*

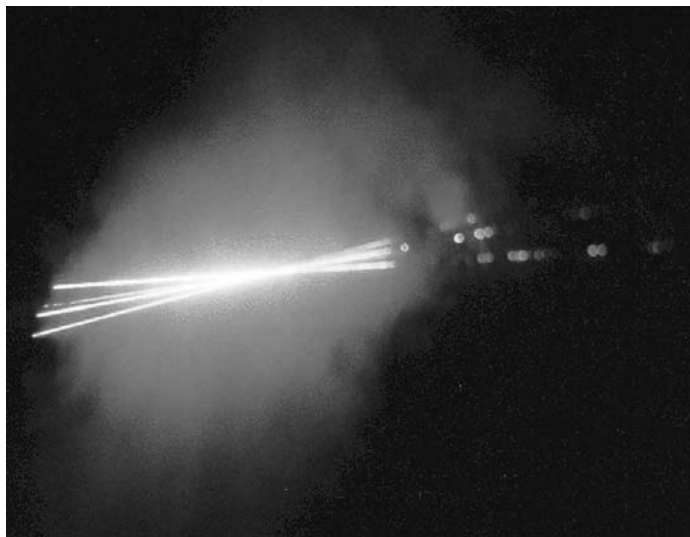


**Fig. 8.27** A 2-component Laser Doppler Anemometer Probe Volume. (Courtesy Dr. Frank W. Chambers, Oklahoma State University)

Laser Doppler anemometers are becoming widely used for specialized applications where direct physical access to the flow field is difficult or impossible. One or more laser beams are focused to a small volume in the flow at the location of interest (as shown in Fig 8.27). Laser light is scattered from particles that are present in the flow (dust or particulates) or introduced for this purpose. A frequency shift is caused by the local flow speed (Doppler effect). Scattered light and a reference beam are collected by receiving optics. The frequency shift is proportional to the flow speed; this relationship may be calculated, so there is no need for calibration. Since velocity is measured directly, the signal is unaffected by changes in temperature, density, or composition in the flow field. The primary disadvantages of LDAs are that the optical equipment is expensive and fragile, and that extremely careful alignment is needed (as the authors can attest).

## 8.13 Summary and Useful Equations

In this chapter we have:

- ✓ Defined many terms used in the study of internal incompressible viscous flow, such as: the entrance length, fully developed flow, the friction velocity, Reynolds stress, the kinetic energy coefficient, the friction factor, major and minor head losses, and hydraulic diameter.
- ✓ Analyzed laminar flow between parallel plates and in pipes and observed that we can obtain the velocity distribution analytically, and from this derive: the average velocity, the maximum velocity and its location, the flow rate, the wall shear stress, and the shear stress distribution.
- ✓ Studied turbulent flow in pipes and ducts and learned that semi-empirical approaches are needed, e.g., the power-law velocity profile.
- ✓ Written the energy equation in a form useful for analyzing pipe flows.
- ✓ Discussed how to incorporate pumps, fans, and blowers into a pipe flow analysis.
- ✓ Described various flow measurement devices: direct measurement, restriction devices (orifice plate, nozzle, and venturi), linear flow meters (rotameters, various electromagnetic or acoustic devices, and the vortex flow meter), and traversing devices (pitot tubes and laser-Doppler anemometers).

We have learned that pipe and duct flow problems often need iterative solution—the flow rate  $Q$  is not a linear function of the driving force (usually  $\Delta p$ ), except for laminar flows (which are not common in practice). \*We have also seen that pipe networks can be analyzed using the same techniques as a single-pipe system, with the addition of a few basic rules, and that in practice a computer application such as *Excel* is needed to solve all but the simplest networks.

**Note:** Most of the Useful Equations in the table below have a number of constraints or limitations—*be sure to refer to their page numbers for details!*

### Useful Equations

Velocity profile for pressure-driven laminar flow between stationary parallel plates:	$u = \frac{a^2}{2\mu} \left( \frac{\partial p}{\partial x} \right) \left[ \left( \frac{y}{a} \right)^2 - \left( \frac{y}{a} \right) \right]$	(8.5)	Page 335
Flow rate for pressure-driven laminar flow between stationary parallel plates:	$\frac{Q}{l} = -\frac{1}{12\mu} \left[ \frac{-\Delta p}{L} \right] a^3 = \frac{a^3 \Delta p}{12\mu L}$	(8.6c)	Page 336

\*This topic applies to a section that may be omitted without loss of continuity in the text material.

Velocity profile for pressure-driven laminar flow between stationary parallel plates (centered coordinates):	$u = \frac{a^2}{2\mu} \left( \frac{\partial p}{\partial x} \right) \left[ \left( \frac{y'}{a} \right)^2 - \frac{1}{4} \right]$	(8.7)	Page 337
Velocity profile for pressure-driven laminar flow between parallel plates (upper plate moving):	$u = \frac{Uy}{a} + \frac{a^2}{2\mu} \left( \frac{\partial p}{\partial x} \right) \left[ \left( \frac{y}{a} \right)^2 - \left( \frac{y}{a} \right) \right]$	(8.8)	Page 339
Flow rate for pressure-driven laminar flow between parallel plates (upper plate moving):	$\frac{Q}{l} = \frac{Ua}{2} - \frac{1}{12\mu} \left( \frac{\partial p}{\partial x} \right) a^3$	(8.9b)	Page 340
Velocity profile for laminar flow in a pipe:	$u = -\frac{R^2}{4\mu} \left( \frac{\partial p}{\partial x} \right) \left[ 1 - \left( \frac{r}{R} \right)^2 \right]$	(8.12)	Page 346
Flow rate for laminar flow in a pipe:	$Q = -\frac{\pi R^4}{8\mu} \left[ \frac{-\Delta p}{L} \right] = \frac{\pi \Delta p R^4}{8\mu L} = \frac{\pi \Delta p D^4}{128\mu L}$	(8.13c)	Page 347
Velocity profile for laminar flow in a pipe (normalized form):	$\frac{u}{U} = 1 - \left( \frac{r}{R} \right)^2$	(8.14)	Page 347
Velocity profile for turbulent flow in a smooth pipe (power-law equation):	$\frac{\bar{u}}{U} = \left( \frac{y}{R} \right)^{1/n} = \left( 1 - \frac{r}{R} \right)^{1/n}$	(8.22)	Page 352
Head loss equation:	$\left( \frac{p_1}{\rho} + \alpha_1 \frac{\bar{V}_1^2}{2} + gz_1 \right) - \left( \frac{p_2}{\rho} + \alpha_2 \frac{\bar{V}_2^2}{2} + gz_2 \right) = h_{l_T}$	(8.29)	Page 356
Major head loss equation:	$h_l = f \frac{L}{D} \frac{\bar{V}^2}{2}$	(8.34)	Page 358
Friction factor (laminar flow):	$f_{\text{laminar}} = \frac{64}{Re}$	(8.36)	Page 360
Friction factor (turbulent flow—Colebrook equation):	$\frac{1}{\sqrt{f}} = -2.0 \log \left( \frac{e/D}{3.7} + \frac{2.51}{Re\sqrt{f}} \right)$	(8.37)	Page 360
Minor loss using loss coefficient $K$ :	$h_{l_m} = K \frac{\bar{V}^2}{2}$	(8.40a)	Page 361
Minor loss using equivalent length $L_e$ :	$h_{l_m} = f \frac{L_e}{D} \frac{\bar{V}^2}{2}$	(8.40b)	Page 362
Diffuser pressure recovery coefficient:	$C_p \equiv \frac{p_2 - p_1}{\frac{1}{2} \rho \bar{V}_1^2}$	(8.41)	Page 363
Ideal diffuser pressure recovery coefficient:	$C_{p_i} = 1 - \frac{1}{AR^2}$	(8.42)	Page 364
Head loss in diffuser in terms of pressure recovery coefficients:	$h_{l_m} = (C_{p_i} - C_p) \frac{\bar{V}_1^2}{2}$	(8.44)	Page 365
Pump work:	$\dot{W}_{\text{pump}} = Q \Delta p_{\text{pump}}$	(8.47)	Page 368

Pump efficiency:	$\eta = \frac{\dot{W}_{\text{pump}}}{\dot{W}_{\text{in}}}$	(8.48)	Page 368
Hydraulic diameter:	$D_h \equiv \frac{4A}{P}$	(8.50)	Page 368
Mass flow rate equation for a flow meter (in terms of discharge coefficient $C$ ):	$\dot{m}_{\text{actual}} = \frac{CA_t}{\sqrt{1-\beta^4}} \sqrt{2\rho(p_1 - p_2)}$	(8.54)	Page 389
Mass flow rate equation for a flow meter (in terms of flow coefficient $K$ ):	$\dot{m}_{\text{actual}} = KA_t \sqrt{2\rho(p_1 - p_2)}$	(8.56)	Page 389
Discharge coefficient (as a function of $Re$ ):	$C = C_\infty + \frac{b}{Re_{D_1}^n}$	(8.57)	Page 390
Flow coefficient (as a function of $Re$ ):	$K = K_\infty + \frac{1}{\sqrt{1-\beta^4}} \frac{b}{Re_{D_1}^n}$	(8.58)	Page 390

## References

- Streeter, V. L., ed., *Handbook of Fluid Dynamics*. New York: McGraw-Hill, 1961.
- Rouse, H., and S. Ince, *History of Hydraulics*. New York: Dover, 1957.
- Moin, P., and J. Kim, "Tackling Turbulence with Supercomputers," *Scientific American*, 276, 1, January 1997, pp. 62–68.
- Panton, R. L., *Incompressible Flow*, 2nd ed. New York: Wiley, 1996.
- Laufer, J., "The Structure of Turbulence in Fully Developed Pipe Flow," U.S. National Advisory Committee for Aeronautics (NACA), Technical Report 1174, 1954.
- Tennekes, H., and J. L. Lumley, *A First Course in Turbulence*. Cambridge, MA: The MIT Press, 1972.
- Hinze, J. O., *Turbulence*, 2nd ed. New York: McGraw-Hill, 1975.
- Moody, L. F., "Friction Factors for Pipe Flow," *Transactions of the ASME*, 66, 8, November 1944, pp. 671–684.
- Colebrook, C. F., "Turbulent Flow in Pipes, with Particular Reference to the Transition Region between the Smooth and Rough Pipe Laws," *Journal of the Institution of Civil Engineers, London*, 11, 1938–39, pp. 133–156.
- Haaland, S. E., "Simple and Explicit Formulas for the Friction Factor in Turbulent Flow," *Transactions of ASME, Journal of Fluids Engineering*, 103, 1983, pp. 89–90.
- "Flow of Fluids Through Valves, Fittings, and Pipe," New York: Crane Company, Technical Paper No. 410, 1982.
- ASHRAE Handbook—Fundamentals*. Atlanta, GA: American Society of Heating, Refrigerating, and Air Conditioning Engineers, Inc., 1981.
- Cockrell, D. J., and C. I. Bradley, "The Response of Diffusers to Flow Conditions at Their Inlet," Paper No. 5, *Symposium on Internal Flows*, University of Salford, Salford, England, April 1971, pp. A32–A41.
- Sovran, G., and E. D. Klomp, "Experimentally Determined Optimum Geometries for Rectilinear Diffusers with Rectangular, Conical, or Annular Cross-Sections," in *Fluid Mechanics of Internal Flows*, G. Sovran, ed. Amsterdam: Elsevier, 1967.
- Feiereisen, W. J., R. W. Fox, and A. T. McDonald, "An Experimental Investigation of Incompressible Flow Without Swirl in R-Radial Diffusers," *Proceedings, Second International Japan Society of Mechanical Engineers Symposium on Fluid Machinery and Fluidics*, Tokyo, Japan, September 4–9, 1972, pp. 81–90.
- McDonald, A. T., and R. W. Fox, "An Experimental Investigation of Incompressible Flow in Conical Diffusers," *International Journal of Mechanical Sciences*, 8, 2, February 1966, pp. 125–139.
- Runstadler, P. W., Jr., "Diffuser Data Book," Hanover, NH: Creare, Inc., Technical Note 186, 1975.
- Reneau, L. R., J. P. Johnston, and S. J. Kline, "Performance and Design of Straight, Two-Dimensional Diffusers," *Transactions of the ASME, Journal of Basic Engineering*, 89D, 1, March 1967, pp. 141–150.
- Aerospace Applied Thermodynamics Manual*. New York: Society of Automotive Engineers, 1969.
- Daily, J. W., and D. R. F. Harleman, *Fluid Dynamics*. Reading, MA: Addison-Wesley, 1966.
- White, F. M., *Fluid Mechanics*, 6th ed. New York: McGraw-Hill, 2007.
- Hamilton, J. B., "The Suppression of Intake Losses by Various Degrees of Rounding," University of Washington, Seattle, WA, Experiment Station Bulletin 51, 1929.
- Herschel, C., *The Two Books on the Water Supply of the City of Rome, from Sextus Julius Frontinus (ca. 40–103 A.D.)*. Boston, 1899.

24. Lam, C. F., and M. L. Wolla, "Computer Analysis of Water Distribution Systems: Part 1, Formulation of Equations," *Proceedings of the ASCE, Journal of the Hydraulics Division*, 98, HY2, February 1972. pp. 335–344.
25. Miller, R. W., *Flow Measurement Engineering Handbook*. 3rd ed. New York: McGraw Hill, 1996.
26. Bean, H. S., ed., *Fluid Meters, Their Theory and Application*. New York: American Society of Mechanical Engineers, 1971.
27. ISO 7145, *Determination of Flowrate of Fluids in Closed Conduits or Circular Cross Sections—Method of Velocity Determination at One Point in the Cross Section*, ISO UDC 532.57.082.25:532.542, 1st ed. Geneva: International Standards Organization, 1982.
28. Goldstein, R. J., ed., *Fluid Mechanics Measurements*, 2nd ed. Washington, D.C.: Taylor & Francis, 1996.
29. Bruun, H. H., *Hot-Wire Anemometry—Principles and Signal Analysis*. New York: Oxford University Press, 1995.
30. Bruus, H., *Theoretical Microfluidics* (Oxford University Press, 2007).
31. Swamee, P. K., and A. K. Jain, "Explicit Equations for Pipe-Flow Problems," *Proceedings of the ASCE, Journal of the Hydraulics Division*, 102, HY5, May 1976. pp. 657–664.
32. Potter, M. C., and J. F. Foss, *Fluid Mechanics*. New York: Ronald, 1975.

## Case Study

### The Fountains at the Bellagio in Las Vegas



The fountains at the Bellagio in Las Vegas.

Any visitor to Las Vegas will be familiar with the water fountains at the Bellagio hotel. These are a set of high-powered water jets designed and built by the WET Design Company that are choreographed to vary in their strength and direction to selected pieces of music.

WET developed many innovations to make the fountains. Traditional fountains use pumps and pipes,

which must be matched for optimum flow (one of the topics we discussed in this chapter). Many of WET's designs use compressed air instead of water pumps, which allows energy to be continuously generated and accumulated, ready for instant output. This innovative use of compressed air allowed the fountains to become a reality—with the traditional systems of pipes or pumps, a fountain such as the Bellagio's would be impractical and expensive. For example, it would be difficult to obtain the 240-foot heights the fountains achieve without expensive, large, and noisy water pumps. The "Shooter" that WET developed works on the principle of introducing a large bubble of compressed air into the piping, which forces trapped water through a nozzle at high pressure. The ones installed at the Bellagio are able to shoot about 75 gallons per second of water over 240 feet in the air. In addition to providing a spectacular effect, they require only about 1/10th the energy of traditional water pumps to produce the same effect. Other air-powered devices produce pulsing water jets, achieving a maximum height of 125 feet. In addition to their power, these innovations lead to a saving of 80 percent or more in energy costs and have project construction costs that are about 50 percent less than traditional pipe-pump fountains.

## Problems

### Laminar versus Turbulent Flow

**8.1** Air at 100°C enters a 125-mm-diameter duct. Find the volume flow rate at which the flow becomes turbulent. At this flow rate, estimate the entrance length required to establish fully developed flow.

**8.2** Consider incompressible flow in a circular channel. Derive general expressions for Reynolds number in terms of (a) volume flow rate and tube diameter and (b) mass flow rate and tube diameter. The Reynolds number is 1800 in a section where the tube diameter is 10 mm. Find the Reynolds number for the same flow rate in a section where the tube diameter is 6 mm.